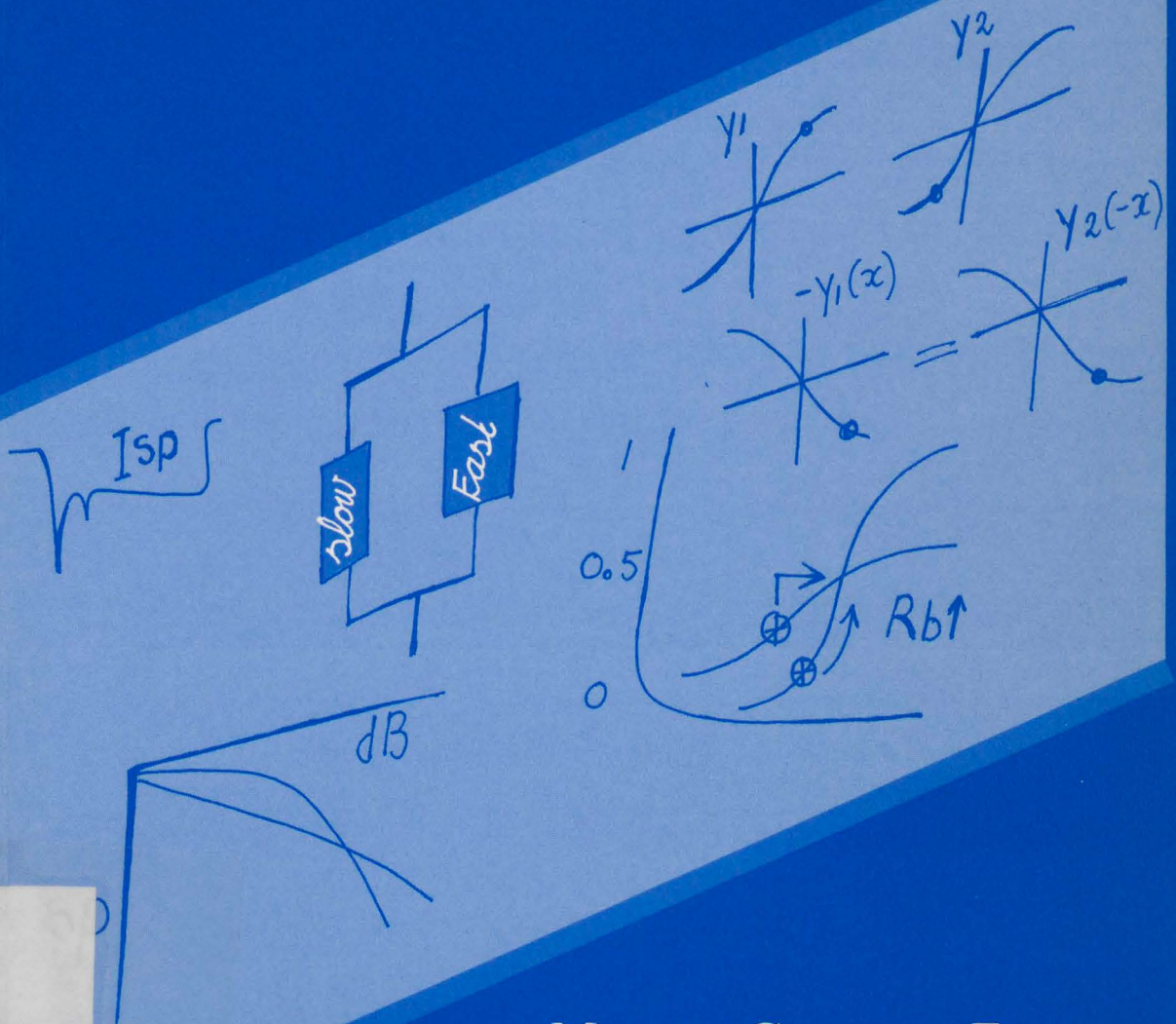


# Origin of the cochlear summing potential in the guinea pig



Maarten Geert van Emst

RIJKSUNIVERSITEIT TE UTRECHT



2643 174 6

AS @ 9553

# Origin of the cochlear summing potential in the guinea pig

Oorsprong van de cochleaire sommatiepotentiaal  
in de cavia

(met een samenvatting in het Nederlands)

## Proefschrift

ter verkrijging van de graad van doctor  
aan de Universiteit Utrecht  
op gezag van de Rector Magnificus, Prof. Dr. J.A. van Ginkel  
ingevolge het besluit van het College van Decanen  
in het openbaar te verdedigen  
op dinsdag 10 december 1996 des middags te 2.30 uur

door

**Maarten Geert van Emst**

geboren op 12 september 1967, te Utrecht

BIBLIOTHEEK DER  
RIJKSUNIVERSITEIT  
UTRECHT

Promotor:

Prof. Dr. G.F. Smoorenburg  
Verbonden aan de Faculteit der Geneeskunde van  
de Universiteit Utrecht

Co-promotor:

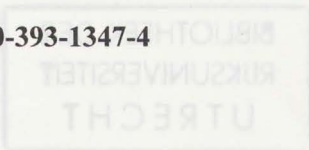
Dr. S.F.L. Klis  
Verbonden aan de Faculteit der Geneeskunde van  
de Universiteit Utrecht

### Proefschrift

The work presented in this thesis was performed at the Department of Otorhinolaryngology, Utrecht University, as a part of the research programme "Analysis of Inner Ear Disorders" and supported by The Heinsius-Houbolt Fund.

Publication of this study was funded by the ORLU Foundation, GN Danavox Nederland BV, Oticon Nederland BV, A.C.M. Ooms Allergie BV, Veenhuis Medical Audio BV and Glaxo Wellcome.

ISBN 90-393-1347-4



# Chapter 1

## General introduction

### Contents

<b>Chapter 1</b> General introduction	1
<b>Chapter 2</b> Tetraethylammonium effects on cochlear potentials in the guinea pig	14
<b>Chapter 3</b> 4-Aminopyridine effects on summing potentials in the guinea pig	35
<b>Chapter 4</b> Identification of the nonlinearity governing even-order distortion products in cochlear potentials	54
<b>Chapter 5</b> Generation of DC receptor potentials in a computational model of the organ of Corti with voltage-dependent $K^+$ channels in the basolateral membrane of inner hair cells	74
<b>Chapter 6</b> Summary	112
Samenvatting	118
Een woord van dank	123
Curriculum Vitae	124



# Chapter 1

## General introduction

### Transduction and the anatomy of the cochlea

In the field of sensory physiology, transduction is the term reserved for the conversion of stimuli from the environment into bio-electric signals. The electric signals travel along afferent nerve fibres to be processed by the central nervous system. In mammalian hearing, transduction takes place in the cochlea. Seen from the outside, the cochlea resembles a snail's shell which has several turns. Two windows in the cochlea, the oval window and the round window, serve as interfaces to the outside world. Sound waves, which are actually pressure waves in the medium surrounding the animal, are led through the outer ear and middle ear, where some crude filtering and impedance matching takes place and enter the cochlea through the oval window. Inside, the cochlea can be described as a coiled tube. The tube is divided by two membranes, Reissner's membrane and the basilar membrane, which run along the length of the tube. This results in a division of the tube in three compartments. A cross section of the cochlear tube (Fig. 1) shows the three compartments. The two outer compartments, which are called scala vestibuli (SV) and scala tympani (ST), are filled with perilymph. In its ionic composition perilymph resembles extracellular fluid (Sterkers et al., 1988). The main cation in this fluid is  $\text{Na}^+$  and it contains little  $\text{K}^+$ . In between Reissner's membrane and the basilar membrane lies the scala media (SM), which is filled with endolymph, a fluid resembling intracellular fluid with  $\text{K}^+$  as the main cation and little  $\text{Na}^+$ .

When the oval window starts to vibrate, pressure differences occur over the whole length of the basilar membrane. The response of this membrane to sinusoidal stimulation takes the form of a travelling wave which moves from the base of the cochlea, where the oval window is located, to its apex. The vibrations reach a maximum amplitude at a place along the length of the basilar membrane that depends on stimulus frequency (Von Békésy, 1947). While high-frequency pressure waves most effectively drive a stretch of basilar membrane that is near the oval window, low-frequency pressure waves produce maximum displacement of the basilar membrane near the apex of the cochlea. The frequency at which maximum displacement is found, the characteristic frequency, is arranged in a monotonic order along the basilar membrane. Thus, the basilar membrane acts as a kind of spectrum analyzer (Pickles, 1988).

The information about frequency, which is carried in the vibration patterns of the basilar membrane, has yet to be coded into neural signals in the auditory nerve. This conversion is carried out by a complicated structure, the organ of Corti. In this organ, which lies on the basilar membrane, the mechanical stimuli are finally transduced into electric signals. The stimulus transduction is carried out by the hair cells in the organ of Corti (Fig. 1). These cells respond to the movement of the basilar membrane by changing the electric potential across their membrane. A cross-section of the organ of Corti contains 3 outer hair cells (OHCs) and 1 inner hair cell (IHC). These cells owe their name to a bundle of hair-like structures on top of the cell. Although electric signals are generated in both the inner and outer hair cells, only the electric signals in the IHCs appear to be transmitted to afferent nerve fibres. The OHCs are thought to operate in a feedback loop. After the forward transduction of mechanical stimuli into electric signals, the electric signals appear to induce changes in the length of the OHC (Santos-Sacchi, 1991). The latter process is called reverse transduction and is thought to feed energy back into basilar membrane motion (Hubbard and Mountain, 1990). This electro-mechanical process is held responsible for the high frequency resolving power which the cochlea displays under normal physiological conditions (Murugasu and Russell, 1996).

### **Gross potentials from the cochlea**

To understand cochlear transduction it is first of all necessary to determine the relation between the stimulus and the electric response of the transducer. This can be done by recording the gross electric responses from the cochlea to sound. When a click or a short tone burst is delivered to the cochlea, an electrode placed either on the cochlea or in the extracellular fluids inside the cochlea can pick up an electric response consisting of three components (Figure 2):

1) The cochlear microphonics (CM), an alternating current (AC) response which directly follows the sound-induced displacements of the basilar membrane (Sellick et al., 1982). The frequency of the CM is the same as that of the stimulus.

2) The summing potential (SP). This is a positive or negative direct current (DC) response. Its polarity and magnitude depend on the position of the recording electrode, and the frequency and sound pressure level (SPL) of the stimulus (Dallos et al., 1972; Van Deelen and Smoorenburg, 1986).



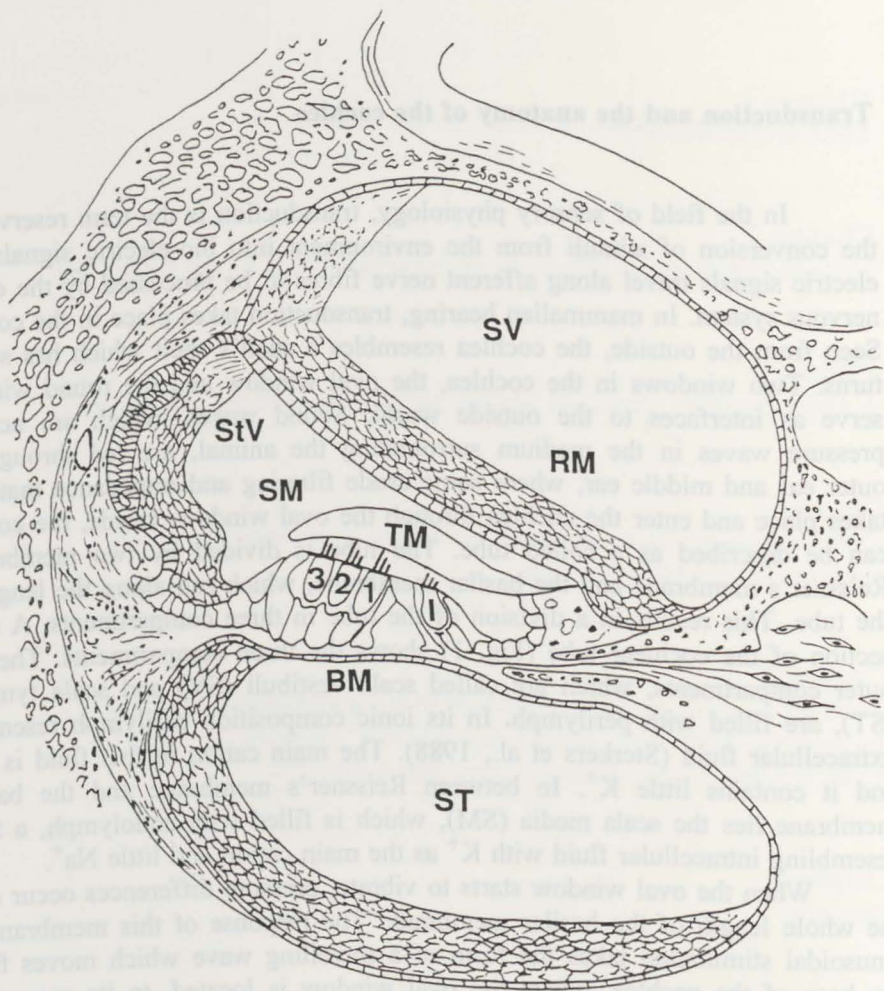


Figure 1. Schematic drawing of a cross section of the cochlea.  
 SM- Scala media; SV- Scala vestibuli; ST- Scala tympani; RM- Reissner's membrane; BM- basilar membrane; StV- stria vascularis; TM- tectorial membrane; 1- Inner hair cell; 1, 2, 3- Outer hair cells.

3) The compound action potential (CAP), which is a signal predominantly present at stimulus onset. It is produced by a number of afferent nerve fibres responding synchronously to transients in the stimulus (Goldstein and Kiang, 1958).

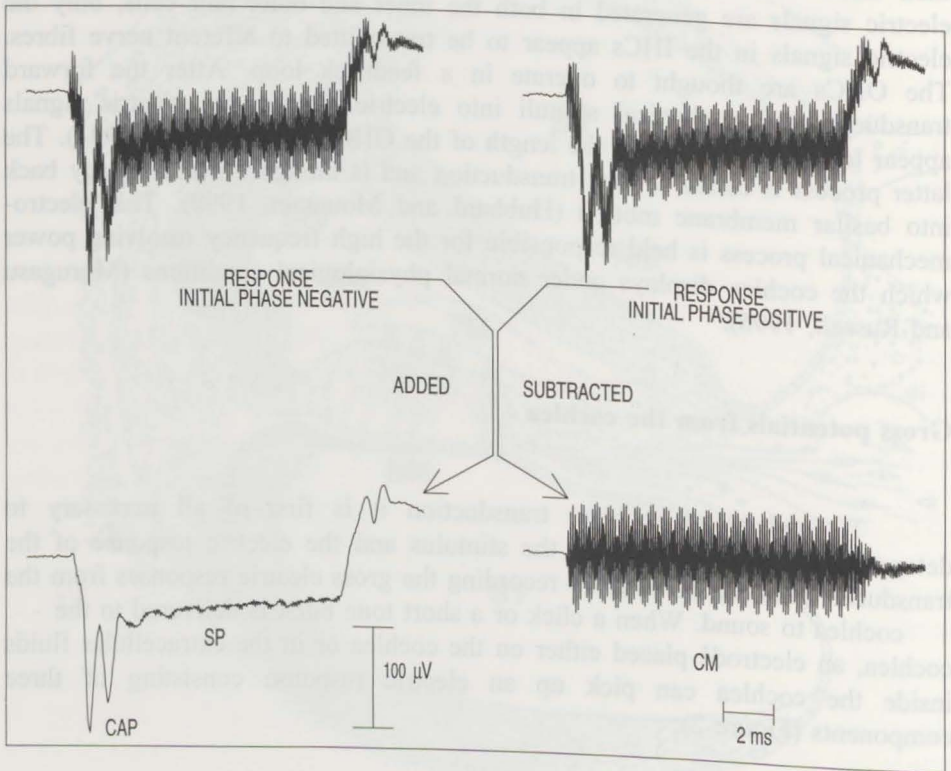


Figure 2. An example of the three potentials, recorded in the guinea pig's cochlea, with the electrode in the first turn of SV and with a 12 kHz stimulus presented at 60 dB SPL. Tone bursts were presented with alternating polarity (180° difference). The averaged responses to the tone bursts of opposite polarity are shown at the top of the figure. The SP and CAP were obtained by addition of the responses to the opposite polarity tone bursts, the CM by subtraction.

The complex relation between stimulus and SP makes this potential the least understood component amongst the cochlear potentials. Where does the SP originate? What does or can it tell us about cochlear transduction? These questions made us decide to take a closer look at the SP. Knowledge about its origin will also improve our understanding of Ménière's disease. People suffering from this disease display an increased SP (Goin et al., 1982; Mori et al., 1987), a finding that was replicated in several animal models of the disease (Klis and Smoorenburg, 1985; Van Deelen et al., 1987; Klis and Smoorenburg, 1994; Van Benthem et al., 1994).

Since it became possible to record intracellularly from cochlear hair cells (Russell and Sellick, 1978; Dallos et al., 1982) it has been established that the SP is connected to DC potentials that are generated inside the hair cells during stimulation (Cheatham and Dallos, 1994). Thus, knowledge about hair cell electrophysiology is essential in a study concerning the origin of the SP.

### **Hair cell electrophysiology**

The generation of electric signals in a hair cell is made possible by the presence of a large potential difference across the apical membrane of the hair cell (Russell, 1983). The apical membrane faces two opposing potentials; one of approximately +80 mV in the SM, and one of approximately -70 mV inside the cell (Fig. 3). The positive potential in SM is called the endocochlear potential. It is actively generated by the stria vascularis. The negative potential inside the cell is close to the  $K^+$  equilibrium potential because the basolateral membrane of the hair cell separates fluids with different concentrations of potassium ions ( $K^+$ ) and possesses channels which are selectively conductive to  $K^+$  ions. These basolateral channels belong to a family of voltage and time-dependent  $K^+$  channels.

The hairs of the cell possess a channel which conducts several types of ions (Hudspeth, 1989). The  $\pm 150$  mV potential difference across the apical membrane, together with the non-selective apical conductance allow current to flow into the hair cell. The current is carried predominantly by  $K^+$  ions. When the basilar membrane is displaced towards SV, each hair bundle bridging the gap between haircell and tectorial membrane is deflected in the direction of the tallest hair in the bundle (fig. 1). This deflection is sensed by the channels in the hairs, which respond with an increase in conductance (Hudspeth, 1989). Consequently, the current flow into the hair cell increases and the potential of the cell becomes less negative, i.e. the hair cell depolarizes. Reversely, displacement of the basilar membrane towards ST displaces the tuft of hairs in the opposite direction, and the conductance associated with the apical channels decreases. Consequently, the hair cell hyperpolarizes. Thus, mechanical vibra-

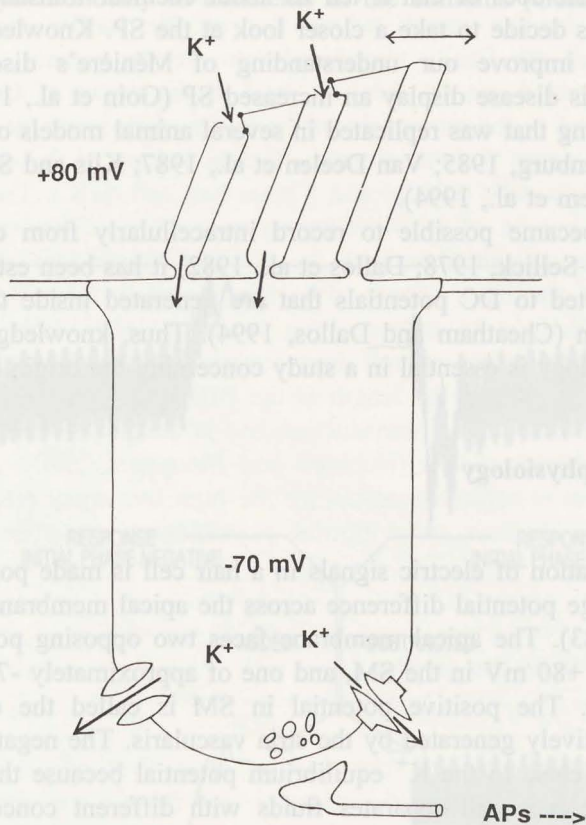


Figure 3. Current model of mechano-electrical transduction by cochlear hair cells. At rest,  $K^+$  ions enter the hair cell through the mechano-sensitive channels in the apical membrane of the hair cell along an electrical gradient formed by the endocochlear potential (+80 mV) and the basolateral membrane potential (-70 mV). The  $K^+$  ions leave the hair cell through  $K^+$ -selective channels in the basolateral membrane according to their chemical gradient (Russell, 1983). The motion of the hair bundle during acoustic stimulation is indicated by the horizontal bidirectional arrow on top of the tallest hair. The links between the tips of the hairs are assumed to translate the bundle-movement into apical conductance changes (Hudspeth, 1989). The modulation of the apical conductance modulates the standing  $K^+$  current and, thereby, the potential in the hair cell. Depolarization of the membrane potential causes a release of transmitter from the synaptic vesicles and the generation of action potentials (APs) in the afferent nerve fibres.

tions are transduced into alternating potentials by the apical mechano-electrical transduction channel. The sound-evoked alternating potential is called the AC receptor potential. The CM is directly related to the intracellular AC receptor potential.

Recordings from the IHC have shown that there is always an asymmetry in the response waveform (Cody and Russell, 1987). The magnitude of the depolarizing phase of the response exceeds that of the hyperpolarizing phase. Thus, a shift of the membrane potential in the positive direction occurs during stimulation. This shift is called the positive DC receptor potential.

DC receptor potentials are also produced by the OHCs. The sign of the DC receptor potential produced by the OHC depends on the frequency and sound pressure level of the stimulus. Since the polarity of the SP can be either positive or negative it is tempting to conclude that the SP is derived mainly from OHC responses. However, dominance of the OHC contribution to the SP is certainly limited to particular locations and specific stimuli. Basal turn OHCs, for example, do not produce a DC receptor potential when stimulated with characteristic high-frequency ( $\geq 12$  kHz) sound (Cody and Russell, 1987). Under these circumstances the SP probably reflects the positive DC receptor potential inside the IHC.

Because it is generally recognized that there is a relation between the SP and the DC responses from the two hair-cell populations (Harvey and Steel, 1992) we will frequently use the knowledge about hair cell responses in the present study concerning the origin of the SP.

### **Nonlinear aspects of stimulus transduction**

Perhaps the most important aspect of the SP is its nonlinear nature. The SP is a continuous DC potential in the cochlear response to sound, although there is no such steady term present in the sound itself. This means that the SP originates with nonlinear aspects of stimulus transduction. For example, if the basilar membrane would move more easily towards SV than towards ST then this asymmetry could eventually cause a flow of stimulus-related DC through the hair cell, which would give rise to an extracellular DC potential. However, it has been shown that substantial changes in the SP can be affected by changing the operating point of the hair cell (Konishi and Slepian, 1971; Gans, 1977). This strongly suggests that the most important nonlinearities contributing to the stimulus-evoked DC potentials are located at the level of the hair cell. Experimental work on isolated hair cells has shown that they have a number of asymmetrical properties which might contribute to the generation of the SP.

## Asymmetrical nonlinearities in hair cell transduction

The nonlinearities described below have been found in hair cells that were isolated from the guinea pig's cochlea:

I. The mechano-electrical transduction conductance in the apical membrane of either IHC or OHC operates asymmetrically. The sigmoidal relation describing the dependence of apical conductance on stereociliar deflection follows the Boltzmann function. *In vitro* experiments have shown that at rest only 9% of the maximum apical conductance is activated. This suggests that during sinusoidal stimulation of the hair-bundle the increase in apical conductance exceeds the decrease. Consequently, a stimulus-evoked DC flows through the hair cell. This will result in a stimulus-related DC potential (Kros et al., 1992).

II. The voltage response of the cochlear transducer also depends on the impedance of the basolateral membrane of the hair cells. The basolateral impedance is probably affected by the active conductances that have been demonstrated in the basolateral membrane of both the IHC and the OHC (Kros and Crawford, 1990; Housley and Ashmore, 1992). The active basolateral conductances are dominated by voltage and time-dependent  $K^+$  channels. The  $K^+$  conductance of these basolateral channels increases when the membrane potential becomes less negative, i.e. the  $K^+$  channels activate with membrane depolarization. The relation between  $K^+$  conductance and membrane potential can be described by an asymmetrical compressive transfer function, the Boltzmann function. In summary, the  $K^+$  channels are responsible for a dynamic basolateral impedance. The nonlinear dynamics of the basolateral impedance will shape the voltage response of the cochlear transducer and, thereby, might be involved in the generation of the stimulus-related DC potential.

## This thesis

### Aim of the present study

The active nonlinear conductances that have been demonstrated in both the apical and basolateral membrane of isolated cochlear hair cells probably contribute to the generation of the SP *in vivo*. The mechano-electrical transducer conductance is believed to be the major nonlinearity underlying the generation of the stimulus-evoked DC potential (Russell, 1983). However, the stimulus-evoked potentials are the result of the interaction between all active conductances. In this thesis we set out to estimate the contribution from the

different active conductances in the hair cells to the generation of the SP.

## Experimental Approach

I. In the first experiments we concentrated on the basolateral  $K^+$  channels. Isolated hair cells express several types of  $K^+$  channels in their basolateral membrane (Kros and Crawford, 1990; Housley and Ashmore, 1992). Most of these channels can be blocked by application of either tetraethylammonium (TEA) or 4-aminopyridine (4-AP) to the fluid surrounding the isolated hair cell. Therefore, we studied the contribution from these channels to the SP by blocking them with the above mentioned drugs.

The results are presented in chapter 2 and 3.

II. Because blocking the apical transduction channel abolishes stimulus transduction we studied the effect of a gradual change in apical conductance on the SP. Russell and Kössl (1991) have shown that the apical conductance of the OHC depends on the membrane potential. Therefore, we chose to examine the contribution from the apical conductance to the SP by means of manipulating electrically the operating point of the apical channel.

The results are presented in chapter 4.

III. An alternative approach to studying the role of the active conductances in generating DC receptor potentials is via mathematical modelling of the organ of Corti and computing the receptor potentials. For this purpose we modified the circuit model of Dallos (1983, 1984). The first modification involved the incorporation of the characteristics of the apical mechano-electrical transducer channel, as determined *in vitro* by Kros et al. (1992). Secondly, the model was extended to account for the voltage and time-dependent properties of basolateral  $K^+$  channels found *in vitro* experiments (Kros and Crawford, 1990; Housley and Ashmore, 1992).

The results are presented in chapter 5.

## References

- Cheatham, M.A. and Dallos, P (1994) Stimulus biasing: a comparison between cochlear hair cell and organ of Corti response patterns. *Hear. Res.* 75, 103-113.
- Cody, A.R. and Russell, I.J. (1987) The responses of hair cells in the basal turn of the guinea pig cochlea to tones. *J.Physiol.* 383, 551-569.
- Dallos, P., Schoeny, Z.G. and Cheatham, M.A. (1972) Cochlear summing potentials. Descriptive aspects. *Acta Otolaryngol. Suppl.* 302, 5-46.
- Dallos, P., Santos-Sacchi, J. and Flock, Å. (1982) Intracellular recordings from cochlear outer hair cells. *Science* 218, 582-584.
- Dallos, P. (1983) Some electrical circuit properties of the organ of Corti. I. Analysis without reactive elements. *Hear. Res.* 12, 89-119.
- Dallos, P. (1984) Some electrical circuit properties of the organ of Corti. II. Analysis including reactive elements. *Hear. Res.* 14, 281-291.
- Gans, D.P. (1977) Effects of crossed olivocochlear bundle stimulation on the cochlear summing potential. *J. Acoust. Soc. Am.* 61, 792-801.
- Goin, D.W., Staller, S.J., Asher, D.L. and Mischke, R.E. (1982) Summing potential in Meniere's disease. *Laryngoscope* 92, 1383-1389.
- Goldstein, M.H. Jr. and Kiang, N.Y.S. (1958) Synchrony of neural activity in electric responses evoked by transient acoustic stimuli. *J. Acoust. Soc. Am.* 30, 107-114.
- Harvey, D. and Steel, K.P. (1992) The development and interpretation of the summing potential response. *Hear. Res.* 61, 137-146.
- Housley, G.D. and Ashmore, J.F. (1992) Ionic currents of outer hair cells isolated from the guinea-pig cochlea. *J. Physiol.* 448, 73-98.
- Hubbard, A.E. and Mountain, D.C. (1990) Haircell forward and reverse transduction: Differential suppression and enhancement. *Hear. Res.*, 43, 269-272.
- Hudspeth, A.J. (1989) How the ear's works work. *Nature*, 341, 397-404.
- Klis, J.F.L. and Smoorenburg, G.F. (1985) Modulation at the guinea pig round window of summing potentials and compound action potentials by low-



frequency sound. *Hear. Res.* 20, 15-23.

Klis, S.F.L. and Smoorenburg, G.F. (1994) Osmotically induced pressure difference in the cochlea and its effect on cochlear potentials. *Hear. Res.* 75, 114-120.

Konishi, T and Slepian, J. (1971) Summating potential with electrical stimulation of crossed olivocochlear bundles. *Science* 172, 483-484.

Kros, C.J. and Crawford, A.C. (1990) Potassium currents in inner hair cells isolated from the guinea-pig cochlea. *J. Physiol.* 421, 263-291.

Kros, C.J., Rüschi, A. and Richardson, G.P. (1992) Mechano-electrical transducer currents in hair cells of the cultured neonatal mouse cochlea. *Proc. R. Soc. Lond. B* 249, 185-193.

Mori, N., Asai, H., Doi, K. and Matsunaga, T. (1987) Diagnostic value of extratympanic electrocochleography in Ménière's disease. *Audiology* 26, 13-110.

Murugasu, E. and Russell, I.J. (1996) The effect of efferent stimulation on basilar membrane displacement in the basal turn of the guinea pig cochlea. *J. Neurosci.* 16, 325-332.

Pickles, J.O. An introduction to the physiology of hearing. London, Academic Press 1988.

Russell, I.J. and Sellick, P.M. (1978) Intracellular studies of hair cells in the mammalian cochlea. *J. Physiol.* 284, 261-290.

Russell, I.J. (1983) Origin of the receptor potential in inner hair cells of the mammalian cochlea - evidence for Davis' theory. *Nature* 301, 334-336.

Russell, I.J. and Kössl, M. (1991) The voltage responses of hair cells in the basal turn of the guinea-pig cochlea. *J. Physiol.* 435, 493-511.

Santos-Sacchi, J. (1991) Reversible inhibition of voltage-dependent outer hair cell motility and capacitance. *J. of Neurosci.* 11, 3096-3110.

Sellick, P.M., Patuzzi, R. and Johnstone, B.M. (1982) Modulation of responses of spiral ganglion cells in the guinea pig cochlea by low-frequency sound. *Hear. Res.* 7, 199-221.

Sterkers, O., Ferrary, E. and Amiel, C. (1988) Production of inner ear fluids.

Physiol. Rev. 68, 1083-1127.

Van Benthem, P.P.G., Klis, S.F.L., Albers, F.W.J., de Wildt, D.J., Veldman, J.E., Huizing, E.H. and Smoorenburg, G.F. (1994) The effect of nimodipine on cochlear potentials and  $\text{Na}^+/\text{K}^+$ -ATPase activity in normal and hydroptic cochleas of the albino guinea pig. *Hear. Res.* 77, 9-18.

Van Deelen, G.W. and Smoorenburg, G.F. (1986) Electrocochleography for different electrode positions in guinea pig. *Acta Otolaryngol.* 101, 207-216.

Van Deelen, G.W., Ruding, P.R.J.W., Veldman, J.E., Huizing, E.H. and Smoorenburg, G.F. (1987) Electrocochleographic study of experimentally induced endolymphatic hydrops. *Arch. Otorhinolaryngol.* 244, 167-173.

Von Békésy, G. (1947) The variations of phase along the basilar membrane with sinusoidal vibrations. *J. Acoust. Soc. Am.* 19, 452-460.

During stimulation with constant DC a DC potential can be recorded (Pettigrew, 1986). The DC potential is recorded from the apical surface of the inner hair cells. The polarity of the DC potential is dependent on the direction of the current flow. The DC potential is recorded from the apical surface of the inner hair cells. The polarity of the DC potential is dependent on the direction of the current flow. The DC potential is recorded from the apical surface of the inner hair cells. The polarity of the DC potential is dependent on the direction of the current flow.

The SP is related to the DC receptor potentials in the hair cells. Inner hair cells in the guinea pig cochlea produce only depolarizing receptor potentials (Russell et al., 1986), whereas outer hair cells produce hyperpolarizing receptor potentials. The DC potential is recorded from the apical surface of the inner hair cells. The polarity of the DC potential is dependent on the direction of the current flow. The DC potential is recorded from the apical surface of the inner hair cells. The polarity of the DC potential is dependent on the direction of the current flow.

The receptor potentials in the IHCs and OHCs are due to mainly  $K^+$  currents. At rest,  $K^+$  ions cross the hair cell apical surface along an electrical gradient. The DC potential is recorded from the apical surface of the inner hair cells. The polarity of the DC potential is dependent on the direction of the current flow.

## Chapter 2

### Tetraethylammonium effects on cochlear potentials in the guinea pig

Maarten G. van Emst, Sjaak F.L. Klis and Guido F. Smoorenburg

*Published in Hear. Res. (1995) 88, 27-35*

#### Abstract

Voltage-dependent  $K^+$  channels in the basolateral membrane of hair cells in the guinea pig cochlea might contribute to the nonlinear current-voltage relationships in these hair cells, and thereby to the generation of the extracellular summing potential (SP). To evaluate the role of  $K^+$  channels in the generation of the SP the perilymphatic perfusion technique was used to introduce the  $K^+$ -channel blocker tetraethylammonium (TEA) into the cochlea. Sound-evoked cochlear potentials were measured subsequently. Without blocking nerve activity TEA induced reversible shifts of the SP in the negative direction, irrespective of whether we recorded from scala vestibuli or scala tympani. The shifts in the negative direction were probably due to TEA acting directly on the afferent fibres, since removal of nerve activity by the potent  $Na^+$  channel blocker tetrodotoxin (TTX) prevented TEA from shifting the SP in the negative direction. Once nerve activity had been removed by TTX, administration of TEA caused a small decrease in the magnitude of the SP, both in scala vestibuli and in scala tympani, irrespective of its polarity. The decrease was significant for the highest test frequencies only (8 - 12 kHz), and completely reversible. The rapidly activated  $K^+$  channel in the inner hair cell (IHC) is probably blocked by TEA and this blocking might be responsible for the small decrease in the magnitude of the SP. The asymmetric contribution from this  $K^+$  channel to the IHC's current-voltage relationship seems to be only partly responsible for the generation of the SP, since blocking of this  $K^+$  channel with TEA caused relatively small decreases in the amplitude of the SP. TEA did not affect the endocochlear potential.

*Keywords:* Summing potential; Tetraethylammonium; Compound action potential; Perilymphatic perfusion

## 1. Introduction

During stimulation with sound a DC potential can be recorded extracellularly in the cochlea which is known as the summing potential (SP). Amongst the cochlear potentials the SP is perhaps the least understood component. Its polarity can be either positive or negative, depending on frequency and intensity of the stimulus and on the location of the recording electrode (Dallos et al., 1972; Van Deelen and Smoorenburg, 1986).

The SP is related to the DC receptor potentials in the hair cells. Inner hair cells (IHCs) in the guinea pig cochlea produce only depolarizing DC receptor potentials (Dallos, 1985; Russell et al., 1986), whereas outer hair cells (OHCs) can produce both hyperpolarizing and depolarizing DC receptor potentials, depending on the frequency and intensity of the stimulus (Dallos et al., 1982; Dallos, 1985; Russell et al., 1986). Since the polarity of the SP can be either positive or negative at one specific location, it is tempting to conclude that the SP is derived mainly from OHC responses. This view is supported by the relation between OHC DC receptor potentials and the extracellular SP, while biasing the cochlear partition (Cheatham and Dallos, 1994). However, dominance of the OHC contribution to the SP seems limited to particular locations and specific stimuli, e.g. to the third turn of the guinea pig cochlea for low-frequency stimulation (Dallos, 1985). OHC dominance is not found in the basal turn where OHCs do not generate DC responses when stimulated with characteristic high-frequency stimuli at low and moderate levels (Russell et al., 1986; Cody and Russell, 1987). Furthermore, Harvey and Steel (1992) present evidence that the negative SP recorded in scala tympani of the basal turn of the mouse cochlea for low-frequency, low-level stimuli does not derive from local, hyperpolarized OHCs. Instead they suggest that this negative SP is the far-field representation of apical, depolarizing hair cells. The positive SP recorded in scala tympani of the basal turn, evoked by high-frequency, high-level stimuli, would be a combination of contributions from basal turn IHCs and OHCs.

Thus, although the relationship between the SP and the DC responses from the two hair cell populations appears complex, there is general agreement that they are related, and therefore, pharmacological manipulation of hair cell membrane processes could give information about the processes underlying SP generation.

The receptor potentials in IHCs and OHCs are due to mainly  $K^+$  currents. At rest,  $K^+$  ions cross the hair cell apical surface along an electrical gradient formed by the endocochlear potential (EP) and the intracellular potential and leave the hair cell at the basolateral membrane according to their chemical gradient (Russell, 1983). Sound-evoked modulation of this standing

$K^+$  current yields the intracellular AC receptor potential. The AC receptor potential shows a strong rectification, which results in a stimulus-related DC receptor potential. A variety of nonlinearities has been suggested to take part in this rectification process: an asymmetry in mechano-electrical transduction (Hudspeth and Corey, 1977; Russell and Sellick, 1978; Corey and Hudspeth, 1983; Russell, 1983), voltage- and time-dependent conductances in the basolateral membrane of the hair cells (Dallos and Cheatham, 1990; Kros and Crawford, 1990) and, in the OHCs, asymmetric voltage-dependent motility (Santos-Sacchi, 1989; Evans et al., 1991) and capacitance (Santos-Sacchi, 1991).

Since  $K^+$  plays such a dominant role in the generation of the receptor potentials, it is plausible that the receptor potential is modulated by voltage- and time-dependent  $K^+$  conductances in the basolateral membrane of the hair cell (Dallos and Cheatham, 1990; Kros and Crawford, 1990). It is known that  $K^+$  channels possess nonlinear properties. An interesting property is that their conductance depends on the membrane potential (Hille, 1984). This voltage dependent conductance seems to be partly responsible for the sensitivity of the IHC DC receptor potential to changes in the transmembrane voltage when polarizing current is passed through the cell (Nuttall, 1985; Russell et al., 1986; Dallos and Cheatham, 1990). The question of this study is whether the voltage-dependent  $K^+$  channels with their nonlinear properties contribute to the asymmetry in the hair cell current-voltage relationships under normal physiological conditions, and whether they are thus involved in the generation of the intracellular DC receptor potential and, consequently, the extracellular SP.

Several types of voltage-dependent  $K^+$  channels have been found in the IHCs and OHCs of the guinea pig cochlea. Inner hair cells possess at least two different voltage-dependent  $K^+$  channels: one is rapidly activated (0.15-0.35 ms) and blocked by tetraethylammonium (TEA), the other is slowly activated (2-10 ms) and blocked by 4-aminopyridine (4-AP). The TEA sensitive  $K^+$  channel shows outward rectification, and contributes considerably to a compressive nonlinear relation between current injected into the hair cell and the voltage response of the hair cell. This channel operates in the range of membrane potentials measured *in vivo*. It does not appear to depend on the influx of  $Ca^{++}$  into the cell (Kros and Crawford, 1990).

Outer hair cells possess at least two  $Ca^{++}$ -activated  $K^+$  channels ( $IK_{(Ca)}$ ). One is a large conductance ( $\sim 230$  pS)  $I_c$  type, showing outward rectification and voltage dependence of the open probability, and it is sensitive to TEA. The other is an intermediate conductance ( $\sim 45$  pS), probably active at relatively negative membrane potentials ( $-80$  mV). It is not sensitive to TEA but blocked by  $Cs^+$  (Ashmore and Meech, 1986; Gitter et al., 1992; Housley

and Ashmore, 1992).

Several studies have addressed the effects of  $K^+$  channel blockers on cochlear potentials. Katsuki et al. (1966) found an irreversible decrease of the compound action potential (CAP) and the cochlear microphonics (CM) after iontophoretic application of TEA to the hair cell region. Salt and Konishi (1982) perfused 10 mM TEA through the perilymphatic compartment and found a reduction in CAP and no change in CM. The SP was not investigated in these studies. Puel et al. (1990) studied the effects of quinine on the cochlear potentials evoked by 10 kHz tone bursts in guinea pig. Quinine reduced the CAP, the CM and the negative SP measured in scala vestibuli. Wang et al. (1993) observed the effects of several  $K^+$ -channel blockers on the cochlear potentials evoked by 2 kHz tone bursts in guinea pig. TEA and quinine reduced the CAP, CM and the negative SP measured in scala tympani, and caused a slight increase of the EP. 4-AP exerted different effects on the SP and the EP: the negative SP measured in scala tympani was increased after perilymphatic perfusion with 4-AP, while no effect on the EP was found.

In this study we shall try to clarify the role that some of the voltage-dependent  $K^+$  channels may play in the generation of the SP. To this end, we affected the  $K^+$  channels by perfusing the perilymphatic spaces of the guinea pig cochlea with the  $K^+$  channel blocker, TEA.

## 2. Materials and methods

Experiments were performed on albino female guinea pigs, Dunkin Hartley strain, which weighed 250-300 g. Pre-operatively the animals were treated with Thalamonal (0.15 ml/100 g body weight, i.m.). Thalamonal is a mixture of 2.5 mg/ml droperidol and 0.05 mg/ml fentanyl. During surgery and experimental procedures the animals were anaesthetized by artificial ventilation through a cannula in the exposed trachea with a gas mixture containing 33%  $O_2$ , 66%  $N_2O$  and 1% halothane. Heart frequency was monitored, and body temperature was kept at 38°C. The care and use of the animals reported on in this paper were approved by the Animal Care and Use Committee of the Faculty of Medicine, Utrecht University, under number FDC-89007, GDL-20008. The cochlea was exposed using a ventrolateral approach. Two 0.2-mm holes were drilled in the cochlea. One hole opened into the scala tympani, and the other one into the scala vestibuli of the basal turn. These holes were used for both perfusion of the cochlea and measurement of sound-evoked intracochlear potentials. For measuring the EP an extra 0.1-mm hole was drilled in the bony wall overlying the scala media of the second turn.

Stimulus generation and data acquisition were controlled by a pc using

a CED 1401-plus laboratory interface. Tone bursts were calculated and stored in a revolving memory consisting of 2,500 points with 12-bit resolution. Tone bursts of 2, 4 and 8 kHz were used, while in some experiments 12 kHz was added. The stimuli were constructed with cosine-shaped rise-and-fall times of 1 ms and a plateau of 14 ms. Consecutive tone bursts were presented with alternating polarity at 99-ms intervals from onset to onset. The stimuli were led through a computer-controlled attenuator to a Beyer DT 48 dynamic transducer, which was connected to a hollow ear bar fitted into the exposed outer ear canal.

Sound-evoked potentials were measured single-endedly with a silver electrode in either the scala vestibuli or the scala tympani. A surgical clamp connected to the neck musculature served as ground electrode. Signals were led through a computer-controlled amplifier and band-pass filtered between 1 Hz and 10 kHz before AD conversion and averaging (max. 500 times). The averaged responses to the tone bursts of opposite polarity were stored separately for off-line analysis. The SP and the compound action potential (CAP) were obtained by addition of the responses to the opposite polarity tone bursts, the cochlear microphonics (CM) by subtraction. The SP was measured as the difference between the pre-stimulus DC level and the DC level approximately 12 ms after the start of the 16 ms tone burst. The CAP was measured relative to the SP, i.e. the distance between the first negative peak ( $N_1$ ) and the steady-state level of the SP was taken as CAP amplitude. This method of measurement of the CAP has the advantage over the more common  $N_1$ - $P_1$  method that it is less sensitive to changes in the waveform of the CAP. CM was determined as the peak-to-peak value of the AC response.

The EP was measured with a glass micropipette filled with 3 M KCl (impedance 5-10 M $\Omega$ ), which was connected to a WPI 705 preamplifier through an Ag-AgCl pellet. The EP was measured relative to a chlorided silver wire in the neck musculature. AD-converted samples of the EP were taken every two seconds.

For perfusion of the cochlea a blunt glass micropipette was positioned in the hole drilled in scala tympani. The perfusate was introduced at a rate of 1.25  $\mu$ l/min for 1 min, maintained at a steady level of 2.5  $\mu$ l/min for 13 min, and reduced to 1.25  $\mu$ l/min for 1 min. The fluid flowing out of the hole drilled in scala vestibuli was removed by suction with a paper wick.

All test agents were dissolved in normal artificial perilymph (ArP). ArP contained (mM): 137 NaCl, 3 KCl, 2 CaCl<sub>2</sub>, 1 MgCl<sub>2</sub>, 11 glucose, 1 NaH<sub>2</sub>PO<sub>4</sub> and 12 NaHCO<sub>3</sub>; pH 7.2-7.3. TEA (*Sigma*) was prepared in concentrations of 5, 15, and 30 mM, keeping osmolality constant by reducing the Na<sup>+</sup> concentration (checked on a Knauer osmometer). It was verified that reducing



the  $\text{Na}^+$  concentration of the ArP did not by itself affect cochlear potentials (Klis and Smoorenburg, 1994). Tetrodotoxin ((TTX), *Sigma*), a blocker of  $\text{Na}^+$  channels, was dissolved at a concentration of 10  $\mu\text{M}$ .

The experiments with TEA consisted of a control perfusion with ArP, perfusion with ArP containing TEA at one of the three concentrations, and another perfusion with ArP to test the reversibility of the effects of TEA. After each perfusion sound-evoked potentials were recorded from scala vestibuli. For scala tympani, sound-evoked potentials were recorded for 15 mM TEA only, in separate experiments.

During the first TEA experiments it became clear that the waveform of the CAP changed profoundly after perfusion of the cochlea with TEA. This change could influence the measurement of the SP. To check for the possibility of TEA affecting afferent fibre activity TTX was perfused into the cochlea preceding and during perfusion with TEA (see Discussion). In the experiments thus performed perfusions were conducted in the following order: 1) Perfusion with ArP, 2) Perfusion with ArP containing 10  $\mu\text{M}$  TTX, 3) Perfusion with ArP containing 10  $\mu\text{M}$  TTX and 15 mM TEA, 4) Perfusion with ArP containing 10  $\mu\text{M}$  TTX.

In additional experiments the EP was monitored during perfusion of the perilymphatic compartments with ArP and ArP containing 15 mM TEA. Only those preparations where a stable recording of the EP of initially more than 70 mV for 10 min had been achieved were used to study the effect of perfusion.

Statistical evaluation of the data was based on analysis of variance (ANOVA) for repeated measurements. Stimulus frequency, stimulus level and test agent were all within-subject factors, concentration a between-subject factor.

### 3. Results

In control experiments it was established that repeated perfusions of the cochlea with ArP did not change the cochlear potentials appreciably (results not shown here). Threshold variations of the CAP during repeated perfusions were within 10 dB. This finding justifies our model in which we compared the SP measured after TEA perfusion with the SP measured after the first perfusion with plain ArP.

Fig. 1 shows a typical example of the effects of 15 mM TEA on the CAP and the SP, which were measured in scala vestibuli and evoked by 4 kHz tone bursts at 65 dB SPL. Perfusion with TEA caused an increase in the CAP and radically changed the waveform of this potential. The normal waveform of the CAP composed of several distinct negative peaks is no longer visible, but

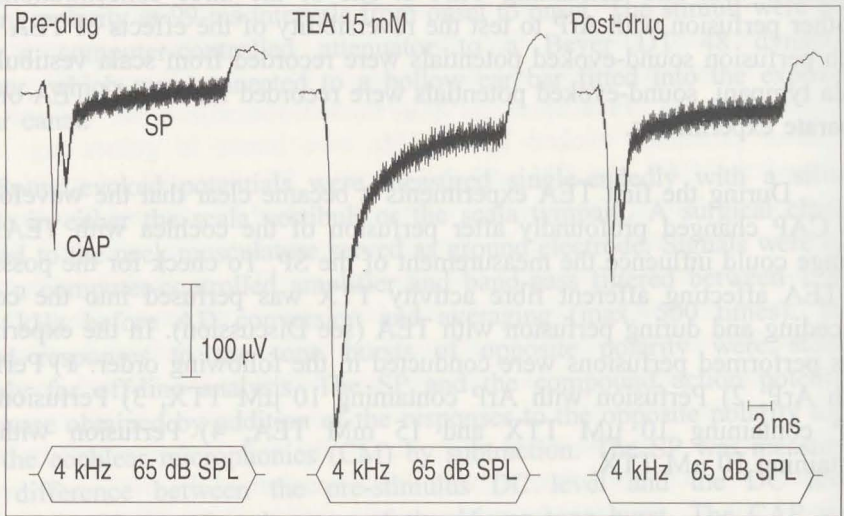


Fig. 1. Example of the effects of 15 mM TEA on the SP and the CAP measured in scala vestibuli. The responses were recorded, after the pre-drug perfusion with ArP, after the perfusion with 15 mM TEA, and after the post-drug perfusion with ArP. Some CM can still be observed in the responses due to imperfect cancellation of the CM in the addition of the original responses to the tone bursts of opposite polarity.

one broader negative peak with a larger amplitude appears instead. In this example CAP amplitude increased from 170  $\mu$ V in the pre-drug condition to 330  $\mu$ V after TEA perfusion. The increase in amplitude was found for each of the 3 frequencies tested, and was completely reversed after rinsing with ArP. The latency of the CAP after TEA treatment was equal to or slightly longer (0 - 0.4 ms) than the one measured after perfusion with plain ArP.

A shift of the SP in the negative direction was observed concomitantly. The TEA-evoked shift in the SP was reversible as the recording after a subsequent ArP perfusion shows (Fig. 1; Post-drug). The input-output functions presented in Fig. 2 provide a more complete description of the effects of one TEA concentration (15 mM) on the SP and their reversibility (n=4). The pola-

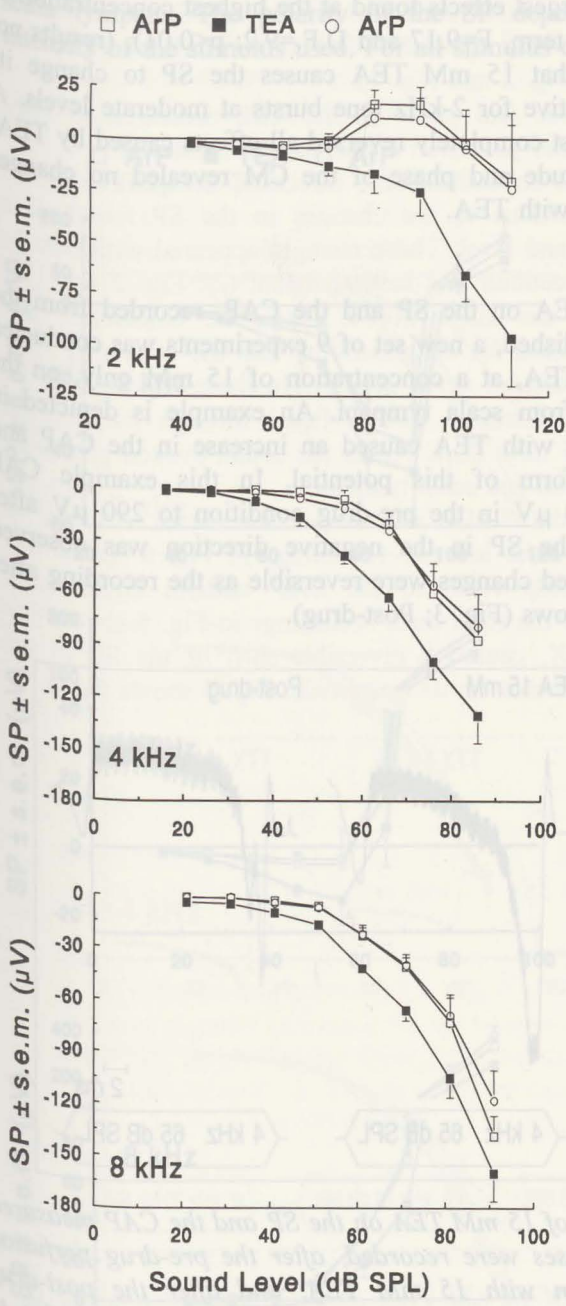


Fig. 2. Effects of 15 mM TEA on the SP input-output curves, which were recorded from scala vestibuli, and evoked by 2, 4, and 8 kHz stimuli. Each graph shows the input-output functions recorded after the pre-drug ArP perfusion (□), after the perfusion with 15 mM TEA (■), and after the post-drug perfusion with ArP (○). For the 3 frequencies tested 15 mM TEA caused a reversible shift of the SP in the negative direction. Number of animals: 4.

ity of the SP depended upon the frequency and intensity of the stimulus used. TEA significantly shifted the SP in the negative direction at each concentration that was tested (ANOVA, 5 mM TEA -  $F=11.52$  and  $D.F.=3,1$ ;  $p<0.05$ ; 15

mM TEA -  $F=31.35$  and  $D.F.=3,1$ :  $p<0.05$ ; 30 mM TEA -  $F=53.91$  and  $D.F.=3,1$ :  $p<0.01$ ), with the largest effects found at the highest concentration of 30 mM (ANOVA, interaction term,  $F=9.17$  and  $D.F.=9,2$ :  $p<0.01$ ), (results not shown here). Fig 2. shows that 15 mM TEA causes the SP to change its polarity from positive to negative for 2-kHz tone bursts at moderate levels. A final perfusion with ArP almost completely reversed all effects caused by TEA.

Analysis of the amplitude and phase of the CM revealed no changes after perfusion of the cochlea with TEA.

After the effects of TEA on the SP and the CAP, recorded from the scala vestibuli, had been established, a new set of 9 experiments was conducted to investigate the effects of TEA, at a concentration of 15 mM only, on the cochlear potentials recorded from scala tympani. An example is depicted in Fig. 3. Once again, perfusion with TEA caused an increase in the CAP and radically changed the waveform of this potential. In this example CAP amplitude increased from 230  $\mu\text{V}$  in the pre-drug condition to 290  $\mu\text{V}$  after TEA perfusion. A shift of the SP in the negative direction was observed concomitantly. The TEA-evoked changes were reversible as the recording after a subsequent ArP perfusion shows (Fig. 3; Post-drug).

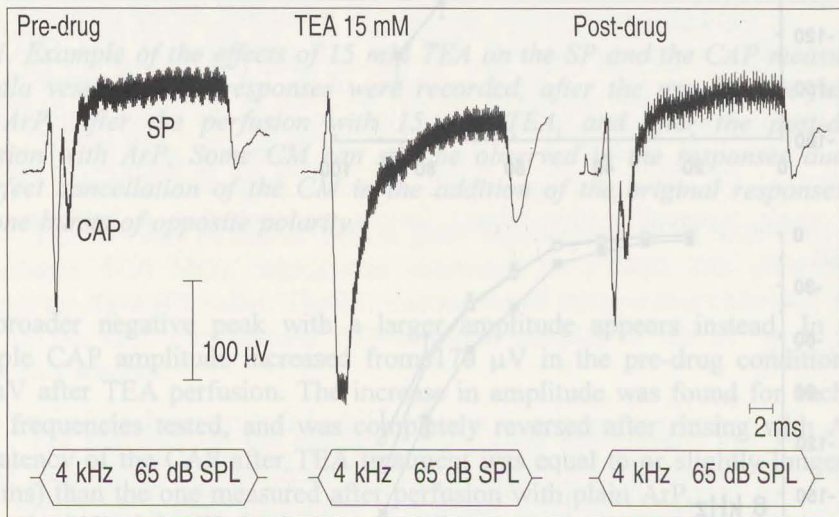


Fig. 3. Example of the effects of 15 mM TEA on the SP and the CAP measured in scala tympani. The responses were recorded, after the pre-drug perfusion with ArP, after the perfusion with 15 mM TEA, and after the post-drug perfusion with ArP. Some CM can still be observed in the responses due to imperfect cancellation of the CM in the addition of the original responses to the tone bursts of opposite polarity.

Fig. 4 shows the SP as a function of stimulus frequency and level in scala tympani. The polarity of the SP depended upon the frequency and intensity of the stimulus used. For all stimulus conditions TEA shifted the SP

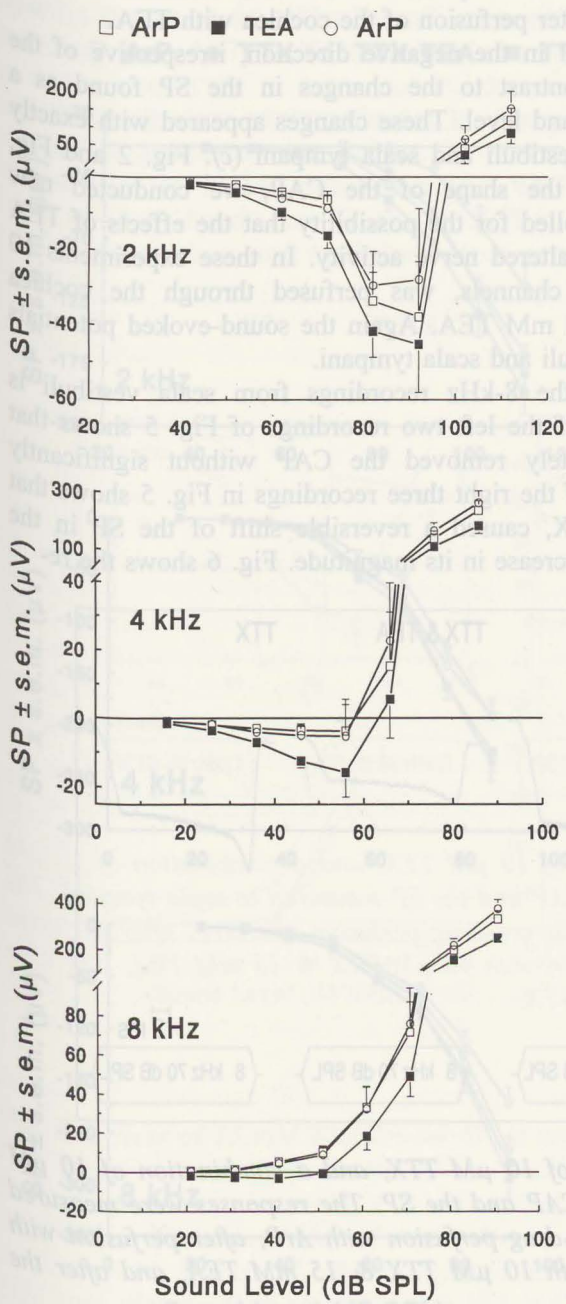


Fig. 4. Effects of 15 mM TEA on the SP, which was recorded from scala tympani, and evoked by 2, 4, and 8 kHz stimuli. The input-output functions recorded after the pre-drug perfusion with ArP (□), after the perfusion with 15 mM TEA (■), and after the post-drug perfusion with ArP (○) are shown. For the 3 frequencies tested TEA caused a reversible shift of the SP in the negative direction. Number of animals: 9.

in the negative direction (ANOVA,  $F=10.77$  and  $D.F.=8,1$ :  $p<0.05$ ). A final perfusion with ArP completely reversed the effect caused by TEA. The shift of the SP in scala tympani was in the same direction as the shift of the SP in scala vestibuli, but smaller (*cf.* Fig. 2 and Fig. 4).

Analysis of the amplitude and phase of the CM, measured in scala tympani, revealed no changes after perfusion of the cochlea with TEA.

TEA thus shifted the SP in the negative direction, irrespective of the recording site. This was in contrast to the changes in the SP found as a function of stimulus frequency and level. These changes appeared with exactly the opposite polarity in scala vestibuli and scala tympani (*cf.* Fig. 2 and Fig. 4). Since TEA also affected the shape of the CAP, we conducted new experiments in which we controlled for the possibility that the effects of TEA on the SP might be related to altered nerve activity. In these experiments  $10\ \mu\text{M}$  TTX, a blocker of  $\text{Na}^+$  channels, was perfused through the cochlea preceding the perfusion with  $15\ \text{mM}$  TEA. Again the sound-evoked potentials were recorded from scala vestibuli and scala tympani.

A typical example of the 8-kHz recordings from scala vestibuli is shown in Fig. 5. Comparison of the left two recordings of Fig. 5 shows that TTX by itself almost completely removed the CAP without significantly affecting the SP. Comparison of the right three recordings in Fig. 5 shows that TEA, in combination with TTX, caused a reversible shift of the SP in the positive direction, implying a decrease in its magnitude. Fig. 6 shows the re-

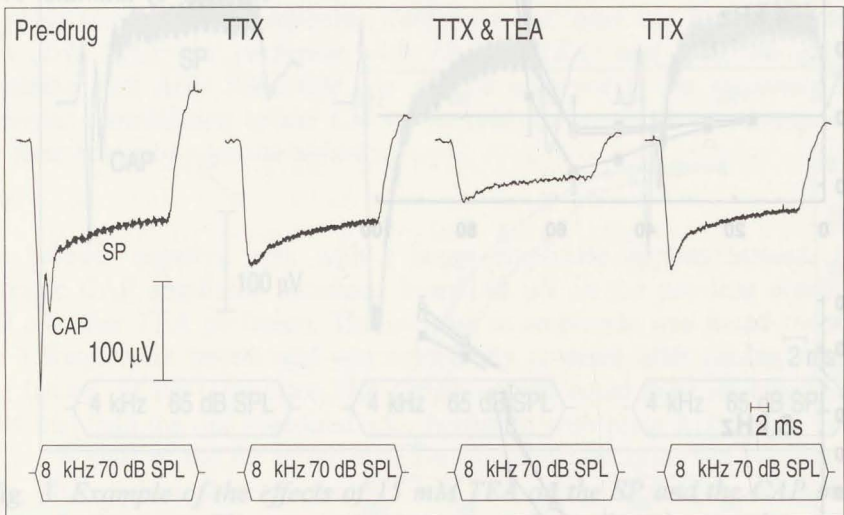


Fig. 5. Example of the effects of  $10\ \mu\text{M}$  TTX, and a combination of  $10\ \mu\text{M}$  TTX and  $15\ \text{mM}$  TEA, on the CAP and the SP. The responses were measured in scala vestibuli, after the pre-drug perfusion with ArP, after perfusion with  $10\ \mu\text{M}$  TTX, after perfusion with  $10\ \mu\text{M}$  TTX &  $15\ \text{mM}$  TEA, and after the final perfusion with  $10\ \mu\text{M}$  TTX.

sults of the group as a function of stimulus frequency and level for all 9 experiments performed. The reversible effect of TEA was significant at 8 kHz only. At 8 kHz both the difference in the SP found between the perfusion with

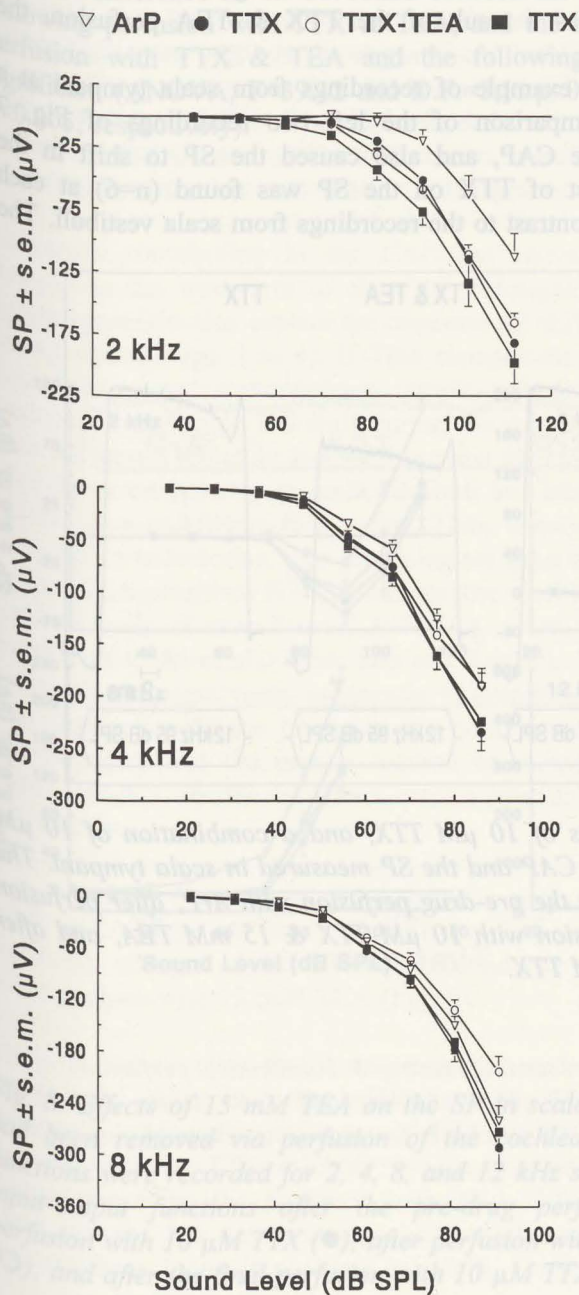


Fig. 6. Effects of 15 mM TEA on the SP in scala vestibuli after nerve activity had been removed by perfusion of the cochlea with TTX. SP input-output functions were recorded for 2, 4, and 8 kHz stimuli. Each graph shows the input-output functions after the pre-drug perfusion with ArP (▽), after perfusion with 10 µM TTX (●), after perfusion with 10 µM TTX & 15 mM TEA (○), and after the final perfusion with 10 µM TTX (■). Number of animals: 9.

TTX and the following perfusion with TTX & TEA, and the difference found between the perfusion with TTX & TEA and the following perfusion with TTX were significant (ANOVA,  $F=39.31$  and  $D.F.=8,1$ :  $p<0.001$ ;  $F=49.95$  and  $D.F.=8,1$ :  $p<0.001$ , respectively). At the lower frequencies (4 and 2 kHz) the results were different (Fig. 6). First of all, TTX perfusion caused a marked shift of the SP in the negative direction. Second, although there was a trend toward reduction of the SP as a result of the TTX & TEA perfusion, the reduction was not significant.

Fig. 7 gives a typical example of recordings from scala tympani at a high stimulus frequency. Comparison of the left two recordings of Fig. 7 shows that TTX removed the CAP, and also caused the SP to shift in the negative direction. This effect of TTX on the SP was found ( $n=6$ ) at each frequency tested (Fig. 8), in contrast to the recordings from scala vestibuli. The

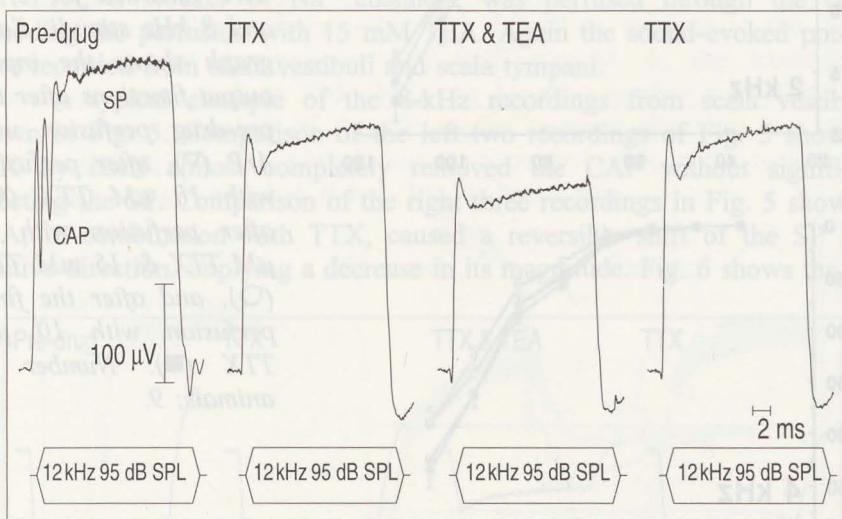


Fig. 7. Example of the effects of  $10 \mu\text{M}$  TTX, and a combination of  $10 \mu\text{M}$  TTX and  $15 \text{ mM}$  TEA, on the CAP and the SP measured in scala tympani. The responses were recorded after the pre-drug perfusion with ArP, after perfusion with  $10 \mu\text{M}$  TTX, after perfusion with  $10 \mu\text{M}$  TTX &  $15 \text{ mM}$  TEA, and after the final perfusion with  $10 \mu\text{M}$  TTX.



right three recordings of Fig. 7 show that TEA, in combination with TTX, reduced the amplitude of the positive SP in a reversible manner, with respect to the amplitude found for TTX alone. However, this reversible effect of TEA was statistically significant for only the highest test frequency of 12 kHz. There was no significant shift in SP at 8, 4 and 2 kHz (Fig. 8). At 12 kHz, both the difference in the SP found between the perfusion with TTX and the following perfusion with TTX & TEA, and the difference found between the following perfusion with TTX & TEA and the following perfusion with TTX were significant (ANOVA,  $F=39.12$  and D.F.=5,1:  $p<0.005$ ;  $F=52.96$  and D.F.=5,1:  $p<0.005$ , respectively).

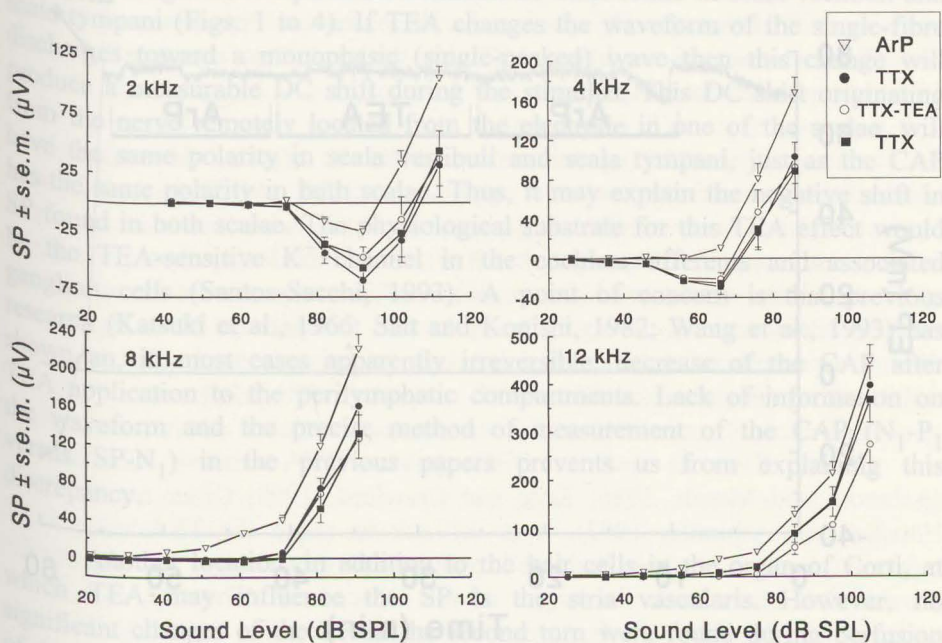


Fig. 8. Effects of 15 mM TEA on the SP in scala tympani after nerve activity had been removed via perfusion of the cochlea with TTX. SP input-output functions were recorded for 2, 4, 8, and 12 kHz stimuli. Each graph shows the input-output functions after the pre-drug perfusion with ArP ( $\nabla$ ), after perfusion with 10  $\mu$ M TTX ( $\bullet$ ), after perfusion with 10  $\mu$ M TTX & 15 mM TEA ( $\circ$ ), and after the final perfusion with 10  $\mu$ M TTX ( $\blacksquare$ ). Number of animals: 6.

In summary, TEA caused a reduction in the amplitude of the SP evoked by the higher test frequencies once nerve activity had been removed by TTX. This effect was found for both the negative SP recorded in scala vestibuli and the positive SP recorded in scala tympani.

In order to examine the possibility that changes in the EP would be responsible for the effects of TEA on the SP, the EP in the second turn was measured during perfusion of the cochlea with 15 mM TEA. In the four experiments that were completed no changes in the EP were found. The average level of the EP during perfusion with ArP was around 75 mV, and remained at that level during the subsequent perfusion with 15 mM TEA. Fig. 9 shows an example of the absence of an effect of TEA on the EP. At the end of the experiment anoxia was applied to check for the occurrence of the negative diffusion potential.

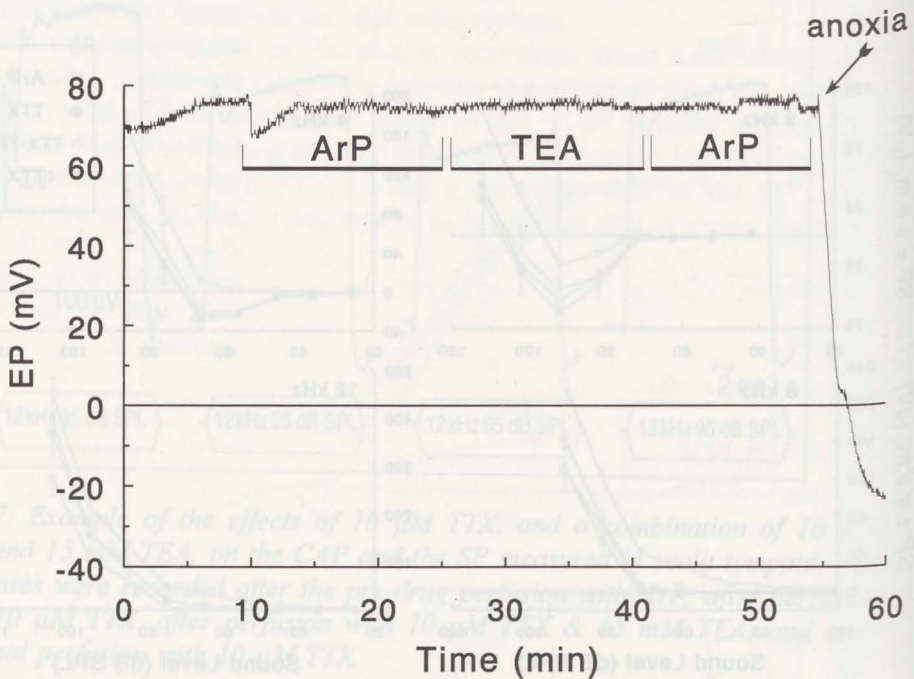


Fig. 9. Example of an EP recording during 3 consecutive perfusions of the perilymphatic spaces with ArP, 15 mM TEA, and ArP. At the end of the experiment anoxia was applied to check for the occurrence of the negative diffusion potential.

#### 4. Discussion

Although our main objective was to study the contribution from TEA-sensitive  $K^+$  channels in the membrane of the hair cells to the SP, we were confronted with large TEA effects on the CAP (Fig. 1 and Fig. 3). The waveform of the CAP became monophasic (single-peaked) and the CAP amplitude ( $SP-N_1$ ) became larger. In both scala vestibuli and scala tympani the SP shifted in the negative direction (Fig. 2 and Fig. 4). If the SP is the result of a rectification process which leads to a net  $K^+$  current through the hair cells (Johnstone et al., 1989), then TEA effects on the hair cells should shift the SP in scala vestibuli and scala tympani in opposite directions. Therefore, we suspected a relation between the uniform shifts of the SP and the alteration in CAP waveform. Apparently, the shape and/or timing of single afferent-fibre discharges contributing to the CAP has altered, leading to rather drastic changes in the waveform of the CAP. Changes in the shape of single-fibre discharges might also explain the common SP shift found in scala vestibuli and scala tympani (Figs. 1 to 4). If TEA changes the waveform of the single-fibre discharges toward a monophasic (single-peaked) wave then this change will produce a measurable DC shift during the stimulus. This DC shift originating from the nerve remotely located from the electrode in one of the scalae, will have the same polarity in scala vestibuli and scala tympani, just as the CAP has the same polarity in both scalae. Thus, it may explain the negative shift in SP found in both scalae. The physiological substrate for this TEA effect would be the TEA-sensitive  $K^+$  channel in the cochlear afferents and associated ganglion cells (Santos-Sacchi, 1993). A point of concern is that previous research (Katsuki et al., 1966; Salt and Konishi, 1982; Wang et al., 1993) has shown an, in most cases apparently irreversible, decrease of the CAP after TEA application to the perilymphatic compartments. Lack of information on the waveform and the precise method of measurement of the CAP ( $N_1-P_1$  versus  $SP-N_1$ ) in the previous papers prevents us from explaining this discrepancy.

Another location, in addition to the hair cells in the organ of Corti, at which TEA may influence the SP is the stria vascularis. However, no significant changes of the EP in the second turn were found during perfusion of the cochlea with 15 mM TEA (Fig. 9).

It became clear that if we wanted to study the contribution from TEA-sensitive  $K^+$  channels in the hair cells to the SP we first had to remove the apparently confounding influence of TEA on afferent nerve activity. This was done by perfusing TTX, a highly specific blocker of  $Na^+$  channels, through the cochlea preceding the perfusion with TEA. TTX was expected to block all nerve activity, but not to change hair cell functioning because  $Na^+$  channels have not been found in cochlear hair cells. However, perfusion of the cochlea

with TTX not only removed afferent and possibly also efferent nerve activity, as was indicated by the removal of the CAP, but also shifted the SP in the negative direction both in scala vestibuli and scala tympani (Fig. 6 and Fig. 8), be it in a frequency-dependent way in scala vestibuli (at 8 kHz TTX hardly affected the SP). It is not obvious how removal of nerve activity by the  $\text{Na}^+$  channel blocker TTX can cause these shifts of the SP, but a shift of the SP in the negative direction in both scalae indicates that this TTX effect is related to changes at a remote location with respect to the electrode position.

When the TTX perfusion was followed by one with TTX & TEA, TEA reduced, significantly and reversibly, the amplitude of the SP at the highest test-frequencies; both the negative SP evoked by 8 kHz stimuli in scala vestibuli and the positive SP evoked by 12 kHz stimuli in scala tympani decreased in magnitude (Fig. 6 and Fig. 8, respectively). This reduction indicates that the source of the shift has to be found in between scala vestibuli and scala tympani, i.e. at the hair cell level. Thus, it is probably related to blocking of TEA-sensitive  $\text{K}^+$  channels in the basolateral membrane of the hair cell. The positions of the electrodes were well suited to measure this local effect at high stimulus frequencies.

Wang et al. (1993) found a decrease of the negative SP evoked by 2 kHz stimuli in scala tympani after application of 30 mM TEA. At the same location and the same stimulus frequency, we found, while not blocking nerve activity, an increase of the negative SP (Fig. 4) which we attributed to altered afferent activity as discussed above. Since in their experiments nerve activity was apparently reduced during TEA application, it is perhaps better to compare their results with our results after blocking nerve activity. In that case, the results are roughly comparable.

Since IHCs as well as OHCs possess TEA-sensitive  $\text{K}^+$  channels (Ashmore and Meech, 1986; Kros and Crawford, 1990; Gitter et al., 1992; Housley and Ashmore, 1992), it is difficult to relate the TEA-induced SP reduction to one of these hair cell populations specifically, but the results provide two clues as to the origin of the reduced SP. The first clue is the undisturbed CM. The CM is normally dominated by the OHCs (Sellick and Russell, 1980; Dallos, 1983). The finding that TEA did not change the CM indicates that OHC function was not substantially affected and, thus, that the decrease in SP amplitude was related to an effect of TEA on IHC function. The second clue is that the decrease of the SP was frequency-dependent which also points into the direction of the IHCs being responsible for the decrease in SP. The SP in the basal turn of the cochlea is dominated by contributions from OHCs for frequencies up to about 4 kHz, but for higher frequencies the output becomes increasingly dependent on contributions from the IHC's DC receptor potential (Cheatham and Dallos, 1994). In our experiments a significantly

reduced SP, after perfusion with a combination of TTX and TEA, was found for only the highest test frequencies (8 kHz and 12 kHz). This suggests that the present effect of TEA on the SP derives from the IHCs. OHCs might either not be affected or their TEA-sensitive,  $\text{Ca}^{++}$ -dependent  $\text{K}^+$  channel is not substantially related to SP generation.

TEA probably blocks the rapidly activated  $\text{K}^+$  channel that is present in the basolateral membrane of the IHC (Kros and Crawford, 1990). The voltage dependence of this channel conductance is responsible for a compressive asymmetry in the relationship between the current injected into the IHC and the IHC voltage response; bathing of the IHC in 25 mM TEA removed this nonlinear behaviour of the membrane (Kros and Crawford, 1990). This voltage dependent property of the TEA-sensitive  $\text{K}^+$  channel might also be effective *in vivo*. Extended depolarizations of the IHC transmembrane voltage during stimulation with high-frequency sound would increase the conductance of the  $\text{K}^+$  channels. This would increase the  $\text{K}^+$  current through the IHCs producing a negative potential shift in scala vestibuli and a positive potential shift in scala tympani. Blocking the  $\text{K}^+$  channel with TEA would prevent activation of these channels during sound stimulation and thus would decrease the magnitude of the DC potential in scala vestibuli and scala tympani. The asymmetry that this  $\text{K}^+$  channel contributes to the IHC's current-voltage relationship seems to be only partly responsible for the generation of the high-frequency SP, since removing this nonlinear behaviour by applying TEA caused relatively small changes in the amplitude of the SP, rather than complete disappearance of the SP. Nonlinearities situated at different locations in the transduction chain, e.g. the apical mechano-electrical transduction process, are probably mainly responsible for the generation of the stimulus related DC receptor potentials and the extracellular SP, whereas TEA-sensitive voltage-dependent  $\text{K}^+$  conductances in the basolateral membrane of the IHC seem to contribute to a lesser extent.

## References

- Ashmore, J.F. and Meech, R.W. (1986) Ionic basis of membrane potential in outer hair cells of guinea pig cochlea. *Nature* 322, 368-371.
- Cheatham, M.A. and Dallos, P. (1994) Stimulus biasing: A comparison between cochlear hair cell and organ of corti response patterns. *Hear. Res.* 75, 103-113.
- Cody, A.R. and Russell, I.J. (1987) The responses of hair cells in the basal turn of the guinea-pig cochlea to tones. *J. Physiol.* 383, 551-569.
- Corey, D.P. and Hudspeth, A.J. (1983) Kinetics of the receptor current in bullfrog saccular hair cells. *J. Neurosci.* 3, 962-976.
- Dallos, P., Schoeny, Z.G. and Cheatham, M.A. (1972) Cochlear summing potentials. Descriptive aspects. *Acta Otolaryngol. Suppl.* 302, 5-46.
- Dallos, P., Santos-Sacchi, J. and Flock, Å. (1982) Intracellular recordings from cochlear outer hair cells. *Science* 218, 582-584.
- Dallos, P. (1983) Some electrical circuit properties of the organ of Corti. I. Analysis without reactive elements. *Hear. Res.* 12, 89-119.
- Dallos, P. (1985) Response characteristics of mammalian cochlear hair cells. *J. Neurosci.* 5, 1591-1608.
- Dallos, P. and Cheatham, M.A. (1990) Effects of electrical polarization on inner hair cell receptor potentials. *J. Acoust. Soc. Am.* 87, 1636-1647.
- Evans, B.N., Hallworth, R. and Dallos, P. (1991) Outer hair cell electromotility: The sensitivity and vulnerability of the DC component. *Hear. Res.* 52, 288-304.
- Gitter, A.H., Frömter, E. and Zenner, H.P. (1992) C-type potassium channels in the lateral cell membrane of guinea-pig outer hair cells. *Hear. Res.* 60, 13-19.
- Harvey, D. and Steel, K.P. (1992) The development and interpretation of the summing potential response. *Hear. Res.* 61, 137-146.
- Hille, B. (1984) Potassium channels and chloride channels. In: B. Hille, *Ionic Channels of Excitable Membranes*. Sinauer Associates, Inc., Sunderland, Mass., pp. 99-116.

- Housley, G.D. and Ashmore, J.F. (1992) Ionic currents of outer hair cells isolated from the guinea-pig cochlea. *J. Physiol.* 448, 73-98.
- Hudspeth, A.J. and Corey, D.P. (1977) Sensitivity, polarity and conductance change in the response of vertebrate hair cells to controlled mechanical stimuli. *Proc. Natl. Acad. Sci. U.S.A.* 74, 2407-2411.
- Johnstone, B.M., Patuzzi, R., Syka, J. and Sykova, E. (1989) Stimulus-related potassium changes in the organ of Corti of guinea-pig. *J. Physiol.* 408, 77-92.
- Katsuki, Y., Yanagisawa, K. and Kanzaki, J. (1966) Tetraethylammonium and tetrodotoxin: effects on cochlear potentials. *Science* 151, 1544-1545.
- Klis, S.F.L. and Smoorenburg, G.F. (1994) Osmotically induced pressure difference in the cochlea and its effect on cochlear potentials. *Hear. Res.* 75, 114-120.
- Kros, C.J. and Crawford, A.C. (1990) Potassium currents in inner hair cells isolated from the guinea-pig cochlea. *J. Physiol.* 421, 263-291.
- Nuttall, A.L. (1985) Influence of direct current on dc receptor potentials from cochlear inner hair cells in the guinea pig. *J. Acoust. Soc. Am.* 77, 165-175.
- Puel, J.-L., Bobbin, R.P. and Fallon, M. (1990) Salicylate, mefenamate, meclofenamate and quinine on cochlear potentials. *Otolaryngol. Head Neck Surg.* 102, 66-73.
- Russell, I.J. and Sellick, P.M. (1978) Intracellular studies of hair cells in the mammalian cochlea. *J. Physiol.* 284, 261-290.
- Russell, I.J. (1983) Origin of the receptor potential in inner hair cells of the mammalian cochlea - evidence for Davis' theory. *Nature* 301, 334-336.
- Russell, I.J., Cody, A.R. and Richardson, G.P. (1986) The responses of inner and outer hair cells in the basal turn of the guinea-pig cochlea and in the mouse cochlea grown in vitro. *Hear. Res.* 22, 199-216.
- Salt, A.N. and Konishi, T. (1982) Functional importance of sodium and potassium in the guinea pig cochlea studied with amiloride and tetraethylammonium. *Jap. J. Physiol.* 32, 219-230.
- Santos-Sacchi, J. (1989) Asymmetry in Voltage-Dependent Movements of Isolated Outer Hair Cells from the Organ of Corti. *J. Neurosci.* 9(8), 2954-2962.

Santos-Sacchi, J. (1991) Reversible inhibition of voltage-dependent outer hair cell motility and capacitance. *J. Neurosci.* 11, 3096-3110.

Santos-Sacchi, J. (1993) Voltage-dependent ionic conductances of type I spiral ganglion cells from the guinea pig inner ear. *J. Neurosci.* 13, 3599-3611.

Sellick, P.M. and Russell, I.J. (1980) The responses of inner hair cells to basilar membrane velocity during low-frequency auditory stimulation in the guinea pig cochlea. *Hear. Res.* 2, 439-445.

Van Deelen, G.W. and Smoorenburg, G.F. (1986) Electrocochleography for different electrode positions in guinea pig. *Acta Otolaryngol.* 101, 207-216.

Wang, J., Li, Q., Dong, W. and Chen, J. (1993) Effects of K<sup>+</sup>-channel blockers on cochlear potentials in the guinea pig. *Hear. Res.* 68, 152-158.



## Chapter 3

### 4-aminopyridine effects on summing potentials in the guinea pig

Maarten G. van Emst, Sjaak F.L. Klis and Guido F. Smoorenburg

*Accepted for publication in Hearing Research (1996)*

#### Abstract

DC receptor potentials measured in hair cells, and the associated extracellular DC potential known as the summing potential (SP), originate with nonlinear elements in the mechanoelectric transduction chain. Nonlinear electric conductance has been demonstrated in the basolateral membrane of the hair cell, and is commonly attributed to the presence of voltage- and time-dependent  $K^+$  conductances in this part of the haircell membrane. To study a possible contribution of these  $K^+$  channels to the SP we perfused the perilymphatic spaces of the guinea pig cochlea with the  $K^+$  channel blocker 4-aminopyridine (4-AP). Since 4-AP might also affect the afferent fibres and, thus, interfere with SP measurement, we added tetrodotoxin (TTX) to the perfusion solutions to block the neuronal discharges (Van Emst et al., 1995). Sound-evoked (2-12 kHz) intracochlear potentials were recorded from the basal turn of both scala vestibuli and scala tympani. The results showed a frequency- and level-dependent effect of 4-AP on the magnitude of the SP. At low and moderate levels of 8 and 12 kHz stimuli 4-AP mostly reduced the SP amplitude, while at high levels of these stimuli and at all levels of 2 and 4 kHz stimuli 4-AP enlarged the SP amplitude. These effects were reversible and occurred in both scala vestibuli and scala tympani. We attribute these bidirectional effects on the SP amplitude to a differential effect of 4-AP on inner hair cell (IHC) and outer hair cell (OHC) physiology. The decrease in SP was found for stimulus conditions where the SP presumably depends mainly on contributions from basal turn IHCs. Blocking the 4-AP sensitive  $K^+$  channel in the IHC membrane should lead to a reduced contribution from the IHCs to the SP, because of an increase in basolateral membrane resistance. The increase in SP was found for stimulus conditions where the SP is assumed to depend mainly on contributions from basal turn OHCs. In this case the OHCs seemed to respond to blocking of the 4-AP sensitive  $K^+$  channel in the basolateral membrane with an increased contribution to the nonlinearity of the transduction chain.

Administration of 4-AP did not effect the endocochlear potential. Lightmicroscopical examination revealed no apparent changes in morphology after 4-AP perfusion.

**Keywords:** Summating potential; 4-Aminopyridine; Perilymphatic perfusion; Guinea pig

## 1. Introduction

During sound stimulation a DC receptor potential can be recorded extracellularly in the cochlea. This potential is known as the summating potential (SP). Its polarity can be either positive or negative, depending on frequency and intensity of the stimulus and on the location of the recording electrode (Dallos et al., 1972; Van Deelen and Smoorenburg, 1986). The SP is thought to reflect the DC receptor potentials measured inside the hair cells.

The DC receptor potential appears to follow the conductance changes in the membrane of the hair cell during sound stimulation (Russell and Sellick, 1978). The membrane conductance changes are probably governed by the asymmetrical saturating conductance in the hair cell apical membrane (Hudspeth and Corey, 1977; Russell and Sellick, 1978; Corey and Hudspeth, 1983; Russell, 1983), but might be modulated by active, i.e. voltage-gated, conductances in the basolateral membrane of the hair cell (Nuttall, 1985; Russell et al., 1986; Dallos and Cheatham, 1990; Kros and Crawford, 1990). The majority of these basolateral membrane conductances is selectively permeable to  $K^+$  ions (Ashmore, 1991).

Several types of voltage- and time-dependent  $K^+$  conductances have been found in the basolateral membrane of IHCs and OHCs of the guinea pig cochlea. They have been characterized *in vitro*. IHCs possess at least two different voltage-dependent  $K^+$  channels: one, having the largest conductance, is rapidly activated (0.15-0.35 ms) and can be blocked by 25 mM tetraethylammonium (TEA), the other is slowly activated (2-10 ms) and can be blocked by 10 mM 4-aminopyridine (4-AP) (Kros and Crawford, 1990). The TEA sensitive  $K^+$  channel is half-activated at -41 mV, the 4-AP sensitive  $K^+$  channel is half-activated at -45 mV. Evidence for the presence of a  $Ca^{++}$ -activated  $K^+$  current has also been presented (Dulon et al., 1995). This current could be blocked by extracellular application of TEA or charybdotoxin.

Ashmore and Meech (1986) identified two main  $Ca^{++}$ - and voltage-dependent  $K^+$  currents in OHCs. One is related to a large conductance ( $\sim 230$  pS)  $I_c$  type  $K^+$  channel (Gitter et al., 1992). It seems to be slowly activated (10-20 ms) when the membrane potential is depolarized to voltages more

positive than  $-35$  mV. It is dependent on  $\text{Ca}^{++}$ , and can be partially blocked by  $30$  mM TEA (Housley and Ashmore, 1992). Mammano et al. (1995) showed that  $100$   $\mu\text{M}$  4-AP, which is a blocker of  $\text{Ca}^{++}$ -independent  $\text{K}^+$  channels, completely blocked the current activated above  $-35$  mV, which argues against it being due exclusively to a  $\text{Ca}^{++}$ -dependent  $\text{K}^+$  channel. In accordance, Lin et al. (1995) provided direct evidence for the activation of a  $\text{Ca}^{++}$ -independent  $\text{K}^+$  current when OHCs were depolarized to voltages more positive than  $-35$  mV. The second current identified by Ashmore and Meech (1986) is related to an intermediate  $\text{K}^+$  conductance ( $\sim 45$  pS). It activates at potentials above  $-100$  mV, which probably makes it fully activated at the normal physiological resting level of the cell. It relaxes with a time constant of  $20$ - $40$  ms on hyperpolarization to  $-120$  mV. It is  $\text{Ca}^{++}$  dependent, and can be blocked by  $\text{Cs}^+$ , but not by 4-AP (Housley and Ashmore, 1992).

In a previous study we investigated to what extent the TEA-sensitive  $\text{K}^+$  channels contribute to the generation of the SP *in vivo* (Van Emst et al., 1995). Perfusion of the perilymphatic spaces with  $15$  mM TEA resulted in small reversible decreases ( $20$ - $30\%$ ) in the magnitude of the SP recorded from scala vestibuli and scala tympani of the basal turn. The small decrease was present only at the highest test frequencies of  $8$  and  $12$  kHz, not at  $2$  and  $4$  kHz. We tentatively concluded that the rapidly-activated  $\text{K}^+$  channel in the IHC is blocked by TEA and that this blocking might be responsible for the small decrease in magnitude of the SP. The small decrease in the magnitude of the SP indicated that the contribution of the TEA-sensitive  $\text{K}^+$  channels in the basolateral membrane of the hair cells to the SP is rather small.

In this study we will try to clarify the role of the voltage-dependent  $\text{K}^+$  channels sensitive to 4-AP, which are found in both IHCs and OHCs, in the generation of the SP. To this end, we perfused the perilymphatic spaces of the guinea pig cochlea with the  $\text{K}^+$  channel blocker 4-AP. The SP was recorded from scala vestibuli and scala tympani at frequencies ranging from  $2$  to  $12$  kHz.

## 2. Materials and methods

Experiments were performed on albino female guinea pigs, Dunkin Hartley strain (Cpb/Hsd DH), which weighed 250-300 g. Pre-operatively the animals were treated with Thalamonal (0.15 ml/100 g body weight, i.m.). Thalamonal is a mixture of 2.5 mg/ml droperidol and 0.05 mg/ml fentanyl. During surgery and measurements the animals were anaesthetized by artificial ventilation through a cannula in the exposed trachea with a gas mixture containing 33% O<sub>2</sub>, 66% N<sub>2</sub>O and 1% halothane. Heart frequency was monitored, and body temperature was kept at  $\pm 37.7^{\circ}\text{C}$ . The cochlea was exposed using a ventrolateral approach. Two 0.2-mm holes were drilled in the cochlea. One hole opened into scala tympani, and the other one into scala vestibuli of the basal turn. These holes were used for both perfusion of the cochlea and measurement of sound-evoked intracochlear potentials. For measuring the endocochlear potential (EP) an extra 0.1-mm hole was drilled in the bony wall overlying the scala media of the second turn. The care and use of the animals in this research were approved by the Animal Care and Use Committee of the Faculty of Medicine, Utrecht University, under number FDC-89007, GDL-20008.

Stimulus generation, data acquisition and data processing have been described in detail by Van Emst et al. (1995). In summary, 16 ms tone bursts of 2, 4, 8 and 12 kHz were used. The stimuli were constructed with cosine-shaped rise-and-fall times of 1 ms to reduce spectral spread of energy. Consecutive tone bursts were presented with alternating polarity. All stimulus levels are given in dB SPL. Sound-evoked potentials were measured single-endedly with a silver electrode in either scala vestibuli or scala tympani. The SP and compound action potential (CAP) responses were separated from the cochlear microphonic (CM) responses by mathematically combining the averaged responses to the alternating tone bursts. The SP was measured as the difference between the pre-stimulus DC level and the DC level approximately 12 ms after the start of the 16 ms tone burst. The CAP was measured relative to the SP, i.e. the distance between the first negative peak (N<sub>1</sub>) and the steady-state level of the SP was taken as CAP amplitude. CM was determined as the peak-to-peak value of the AC response.

The EP was measured through Ag/AgCl electrodes with a conventional glass micropipette, which had been filled with 3 M KCl (impedance 5-10 M $\Omega$ ).

For perfusion of the cochlea a blunt glass micropipette was positioned in the hole drilled in scala tympani. The perfusate was introduced at a rate of 1.25  $\mu\text{l}/\text{min}$  for 1 min, maintained at a steady level of 2.5  $\mu\text{l}/\text{min}$  for 13 min, and reduced to 1.25  $\mu\text{l}/\text{min}$  for 1 min. The fluid flowing out of the hole drilled in scala vestibuli was removed by suction with a paper wick.

All test agents were dissolved in artificial perilymph (ArP). ArP contained (mM): 141.5 NaCl, 3 KCl, 2 CaCl<sub>2</sub>, 1 MgCl<sub>2</sub>, 11 glucose, 10 HEPES and 3.5 NaOH; pH 7.2-7.3. 4-AP (*Sigma*) was prepared in a concentration of 5mM, at which 4-AP could potentially block all the presently known 4-AP-sensitive K<sup>+</sup> channels in hair cells, while the chance of evoking any nonspecific interactions is considered to be small. Because 4-AP is an alkaline compound we left out the NaOH from the ArP. In this way pH was kept constant. The very small change in osmolality and Na<sup>+</sup> concentration resulting from this replacement were previously proven not to change cochlear potentials (Klis and Smoorenburg, 1994). Tetrodotoxin ((TTX), *Sigma*), a blocker of Na<sup>+</sup> channels, was dissolved at a concentration of 10 μM.

The experiments with 4-AP consisted of a control perfusion with ArP, perfusion with ArP containing 5 mM 4-AP, and another perfusion with ArP to test the reversibility of the effects of 4-AP. Sound-evoked potentials were recorded in between perfusions to avoid direct mechanical effects. Different experimental animals were used to record from either scala vestibuli or scala tympani.

During the experiments described above it became clear that the waveform of the CAP changed profoundly after perfusion of the cochlea with 4-AP. This change could influence the measurement of the SP. To control for the possibly interfering effect of 4-AP on afferent fibre activity TTX was perfused into the cochlea preceding and during perfusion with 4-AP. In the experiments thus performed perfusions were conducted in the following order: 1) Perfusion with ArP, 2) Perfusion with ArP containing 10 μM TTX, 3) Perfusion with ArP containing 10 μM TTX and 5 mM 4-AP, 4) Perfusion with ArP containing 10 μM TTX. After each perfusion sound-evoked potentials were recorded. Different experimental animals were used to record from either scala vestibuli or scala tympani.

In additional experiments the EP was monitored during perfusion of the perilymphatic compartments with ArP and ArP containing 5 mM 4-AP. Only those preparations where a stable recording of the EP of initially more than 70 mV for 10 min had been achieved were used to study the effect of perfusion on the EP.

To check for abnormalities in cochlear morphology after 4-AP perfusion a number of cochleas were processed for light-microscopical examination. Fixation and further tissue processing were previously described by De Groot et al (1987).

Statistical evaluation of the data was based on analysis of variance (ANOVA) for repeated measurements. Stimulus frequency, stimulus level and test agent were all within-subject factors.

### 3. Results

In control experiments we established that repeated perfusions of the cochlea with ArP did not change the cochlear potentials appreciably (results not shown here). CAP thresholds (15 dB SPL at 12 kHz) were found to vary within a range of 10 dB during repeated perfusions. This result justifies our experimental approach in which we compared the SP measured after 4-AP perfusion with the SP measured after the preceding perfusion without 4-AP.

Fig. 1 shows a typical example of the effects of 5 mM 4-AP on the CAP and the SP, which were measured in scala vestibuli and evoked by 12 kHz tone bursts at 65 dB SPL. Perfusion with 4-AP radically changed the waveform of the CAP. The normal waveform of the CAP composed of a large negative peak ( $N_1$ ), followed by a smaller negative peak ( $N_2$ ) is no longer evident. Instead, most recordings started with an initial negative peak with a latency which was approximately 0.15 ms longer than that of the pre-drug  $N_1$ . This peak was followed by a larger negative peak. When one compares this latter peak to either the pre-drug  $N_1$  or  $N_2$  then the most salient feature is that it has become much broader. Furthermore, its amplitude, measured relative to the SP, lay mostly in between those of  $N_1$  and  $N_2$ , and its latency was approximately 0.2 ms longer than that of  $N_2$ . This change in waveform was found also for the 2, 4 and 8 kHz stimuli. A shift of the SP in the negative direction was observed concomitantly. A final perfusion with ArP almost completely reversed all effects caused by 4-AP (Fig. 1; Post-drug).

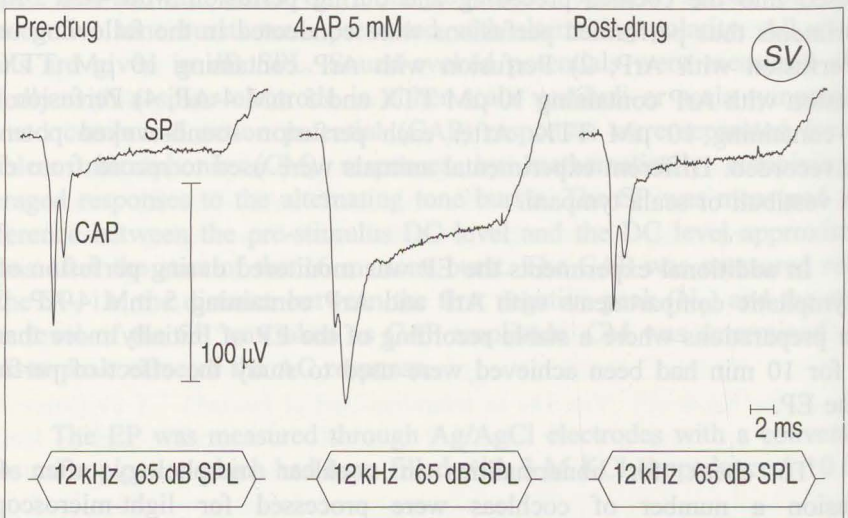


Fig. 1. Typical example of the effects of 5 mM 4-AP on the SP and the CAP measured in scala vestibuli (SV). The responses were recorded, after the pre-drug perfusion with ArP, after the perfusion with 5 mM 4-AP, and after the post-drug perfusion with ArP.

Fig. 2 shows an example of the effects of 5 mM 4-AP on the CAP and the SP, measured in scala tympani and evoked by 12 kHz tone bursts at 65 dB SPL. The 4-AP recording started with a short excursion in the positive direction to a level of the pre-drug SP. The effect of 4-AP on the CAP was comparable to the effect measured in scala vestibuli. Furthermore, during the presence of 4-AP, a shift of the SP in the negative direction occurred. The 4-AP-evoked changes were almost completely reversible as the recording after a subsequent ArP perfusion shows (Fig. 2; Post-drug).

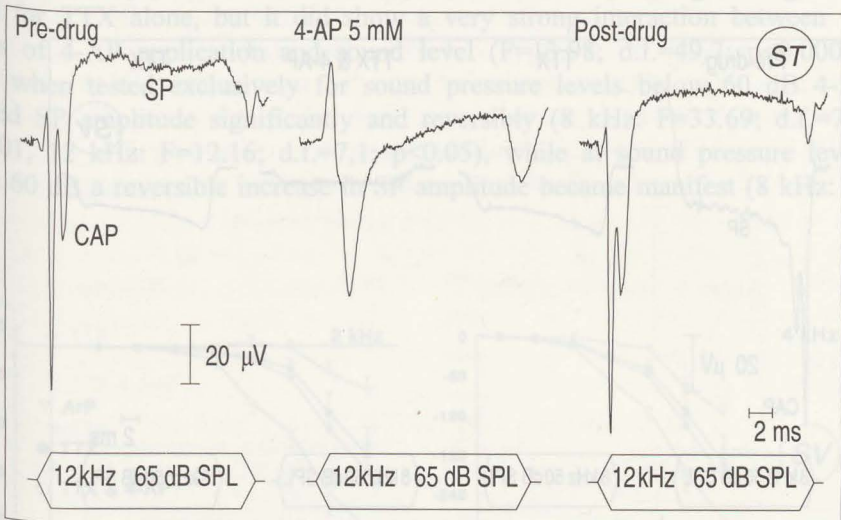


Fig. 2. Typical example of the effects of 5 mM 4-AP on the SP and the CAP measured in scala tympani (ST). The responses were recorded, after the pre-drug perfusion with ArP, after the perfusion with 5 mM 4-AP, and after the post-drug perfusion with ArP.

The results strongly suggested that the effect of 4-AP on the SP was directly related to altered nerve activity because: 1) At stimulus onset, the recording during the presence of 4-AP reaches the same level as the pre-drug SP. It is only after the onset of nerve activity that the SP shifted in the negative direction. 2) 4-AP shifted the SP in the negative direction, irrespective of the recording site (*cf.* Fig. 1 and Fig. 2). This is in contrast to the changes in the SP which are normally found as a function of stimulus frequency and level, which appear with almost opposite polarity in scala vestibuli and scala tympani (Dallos et al., 1972). 3) In our previous study with the  $K^+$  channel blocker TEA we found comparable effects on the SP which appeared to be a direct result of altered nerve activity (Van Emst et al., 1995). Therefore, we conducted experiments in which we tried to eliminate the possibility that the effects of 4-AP on the SP were related to altered nerve activity. In these experiments 10  $\mu$ M TTX, a blocker of  $Na^+$  channels, was perfused through the

cochlea preceding and during perfusion with 5 mM 4-AP. Again the sound-evoked potentials were recorded from scala vestibuli and scala tympani.

Representative 8-kHz recordings from scala vestibuli are shown in Fig. 3. The recordings at the top are typical for sound pressure levels below 60 dB, while the recordings at the bottom are typical for sound pressure levels of 60 dB and above. Comparison of the left two recordings of Fig. 3, at 50 or 60 dB SPL, shows that in this example TTX by itself almost completely removed the CAP without significantly affecting the SP. Comparison of the right three recordings in Fig. 3 shows that 4-AP, in combination with TTX, caused a re-

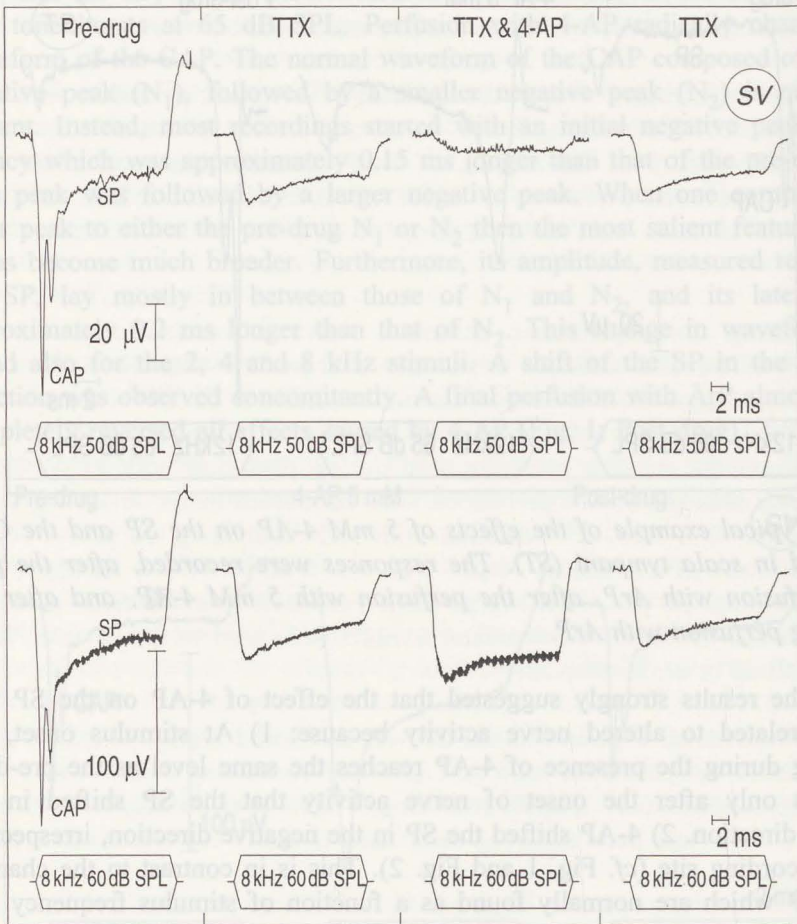


Fig. 3. Examples of the effects of 10  $\mu$ M TTX, and a combination of 10  $\mu$ M TTX and 5 mM 4-AP, on the CAP and the SP. The responses were measured in scala vestibuli (SV), after the pre-drug perfusion with ArP, after perfusion with 10  $\mu$ M TTX, after perfusion with 10  $\mu$ M TTX & 5 mM 4-AP, and after the final perfusion with 10  $\mu$ M TTX. Note that the effect of 4-AP on the SP depends critically on stimulus level.



versible decrease in the magnitude of the negative SP at 50 dB SPL, and caused a reversible increase in SP magnitude at 60 dB SPL.

The group results ( $n=8$ ) as a function of frequency and level, presented in Fig. 4, provide the average effects of TTX, TTX and 4-AP, and rinsing with TTX on the SP. TTX caused a frequency-dependent shift of the SP; at 8 and 12 kHz TTX hardly affected the SP (like in the example of Fig. 3), while at 2 and 4 kHz TTX caused a shift of the SP into the negative direction. At the higher test frequencies, 8 and 12 kHz, ANOVA showed no main effect of a subsequent 4-AP perfusion on SP amplitude, with respect to the amplitude found for TTX alone, but it did show a very strong interaction between the effects of 4-AP application and sound level ( $F=13.98$ ;  $d.f.=49,7$ ;  $p<0.0001$ ). Thus, when tested exclusively for sound pressure levels below 60 dB 4-AP reduced SP amplitude significantly and reversibly (8 kHz:  $F=33.69$ ;  $d.f.=7,1$ ;  $p<0.001$ , 12 kHz:  $F=12.16$ ;  $d.f.=7,1$ ;  $p<0.05$ ), while at sound pressure levels above 60 dB a reversible increase in SP amplitude became manifest (8 kHz: F

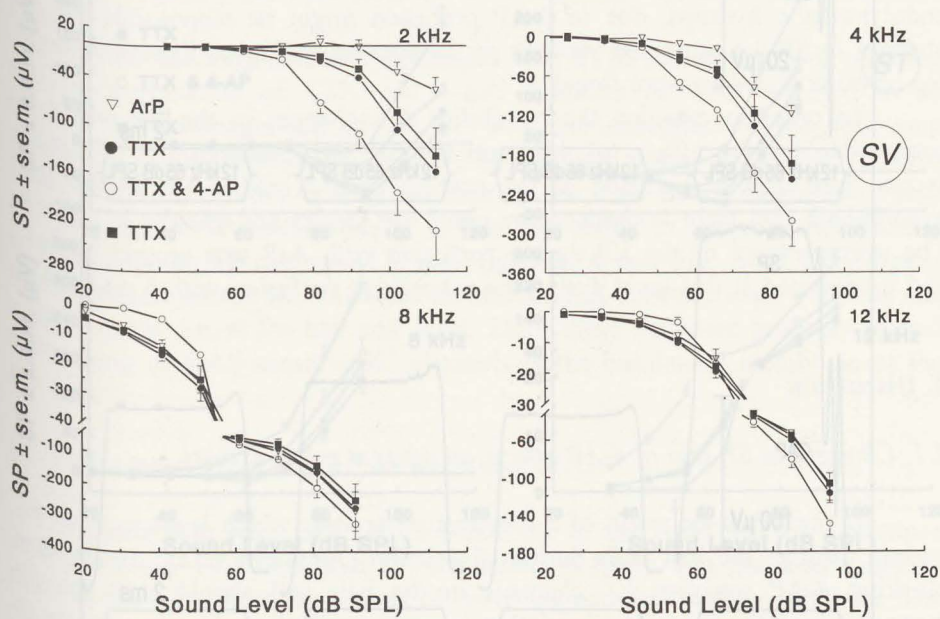


Fig. 4. Effects of 5 mM 4-AP on the SP in scala vestibuli (SV) after nerve activity had been removed via perfusion of the cochlea with TTX. SP input-output functions were recorded for 2, 4, 8 and 12 kHz stimuli. Each graph shows the input-output functions after the pre-drug perfusion with ArP ( $\nabla$ ), after perfusion with 10  $\mu$ M TTX ( $\bullet$ ), after perfusion with 10  $\mu$ M TTX & 5 mM 4-AP ( $\circ$ ), and after the final perfusion with 10  $\mu$ M TTX ( $\blacksquare$ ). Number of animals: 8.

=38.38; d.f.=7,1;  $p < 0.001$ , 12 kHz:  $F=6.83$ ; d.f.=7,1;  $p < 0.05$ ). At the lower test frequencies, 2 and 4 kHz, 4-AP, in combination with TTX, caused a significant and reversible increase in SP amplitude, with respect to the amplitude found for TTX alone ( $F=125.88$ ; d.f.=7,1;  $p < 0.001$ ).

After perfusion of the cochlea with 4-AP there was no statistically significant change in CM amplitude measured in scala vestibuli (not shown).

Representative 12-kHz recordings from scala tympani are shown in Fig. 5. The recordings at the top are typical for sound pressure levels below 70 dB, while the recordings at the bottom are typical for sound pressure levels of 70

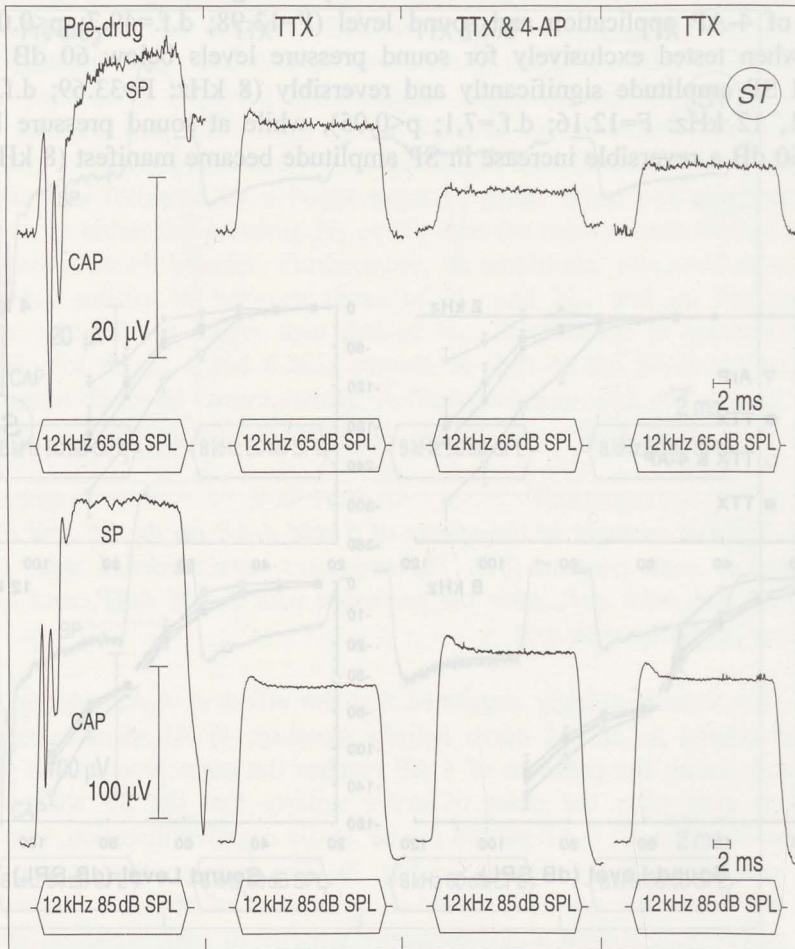


Fig. 5. Examples of the effects of  $10 \mu\text{M}$  TTX, and a combination of  $10 \mu\text{M}$  TTX and  $5 \text{ mM}$  4-AP, on the CAP and the SP. The responses were measured in scala tympani (ST), after the pre-drug perfusion with ArP, after perfusion with  $10 \mu\text{M}$  TTX, after perfusion with  $10 \mu\text{M}$  TTX &  $5 \text{ mM}$  4-AP, and after the final perfusion with  $10 \mu\text{M}$  TTX.

dB and above. Comparison of the left two recordings of Fig. 5, at 65 or 85 dB SPL, shows that TTX by itself completely removed the CAP, and caused a shift of the SP in the negative direction. Comparison of the right three recordings in Fig. 5 shows that 4-AP, in combination with TTX, caused a reversible decrease in the magnitude of the positive SP at 65 dB SPL, and a reversible increase in SP magnitude at 85 dB SPL.

The group results ( $n=8$ ) as a function of frequency and level, presented in Fig. 6, provide the average effects of TTX, TTX and 4-AP, and rinsing with TTX on the SP. In contrast to the recordings from scala vestibuli TTX caused a shift of the SP into the negative direction at all stimulus frequencies. At the highest test frequency of 12 kHz ANOVA revealed no main effect of a subsequent 4-AP perfusion on SP amplitude, with respect to the amplitude found for TTX alone, but it did show a very strong interaction between the effects of 4-AP application and sound level ( $F=5.56$ ;  $d.f.=49,7$ ;  $p<0.0001$ ). Thus, when tested exclusively for sound pressure levels below 70 dB, 4-AP re-

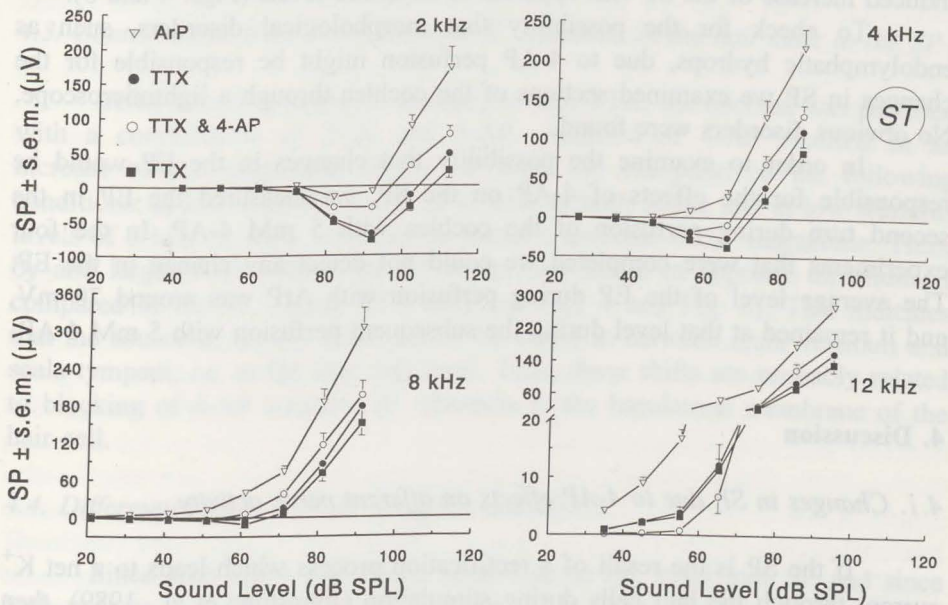


Fig. 6. Effects of 5 mM 4-AP on the SP in scala tympani (ST) after nerve activity had been removed via perfusion of the cochlea with TTX. SP input-output functions were recorded for 2, 4, 8 and 12 kHz stimuli. Each graph shows the input-output functions after the pre-drug perfusion with ArP ( $\nabla$ ), after perfusion with 10  $\mu$ M TTX ( $\bullet$ ), after perfusion with 10  $\mu$ M TTX & 5 mM 4-AP ( $\circ$ ), and after the final perfusion with 10  $\mu$ M TTX ( $\blacksquare$ ). Number of animals: 8.

duced SP amplitude significantly and reversibly ( $F=9.62$ ;  $d.f.=7,1$ ;  $p<0.05$ ), while at sound pressure levels above 70 dB there was a trend toward an increase of the SP, although not statistically significant. At the lower test frequencies, 2, 4 and 8 kHz, 4-AP, in combination with TTX, caused a significant and reversible increase in SP amplitude, with respect to the amplitude found for TTX alone ( $F=25.47$ ;  $d.f.=7,1$ ;  $p<0.01$ ).

After perfusion of the cochlea with 4-AP there was no significant change in CM amplitude measured in scala tympani.

The effects of 4-AP on the SP, once nerve activity had been removed by TTX, can be summarized as follows: at sound pressure levels below 60-70 dB the amplitude of the SP was reduced significantly and reversibly at 8 and 12 kHz in scala vestibuli and at 12 kHz in scala tympani, while at higher sound pressure levels a reversible increase in SP amplitude was found. The increase of the SP, found with 12 kHz stimuli at high levels only, became more pronounced when the stimulus frequency decreased, so that at the lower frequencies, 2 and 4 kHz in both scalae and at 8 kHz in scala tympani, a 4-AP induced increase of the SP was apparent at all sound-levels (Figs. 4 and 6).

To check for the possibility that morphological disorders, such as endolymphatic hydrops, due to 4-AP perfusion might be responsible for the changes in SP we examined sections of the cochlea through a lightmicroscope. No obvious disorders were found.

In order to examine the possibility that changes in the EP would be responsible for the effects of 4-AP on the SP, we measured the EP in the second turn during perfusion of the cochlea with 5 mM 4-AP. In the four experiments that were completed we could not detect any change in the EP. The average level of the EP during perfusion with ArP was around 70 mV, and it remained at that level during the subsequent perfusion with 5 mM 4-AP.

## 4. Discussion

### 4.1. Changes in SP due to 4-AP effects on afferent nerve activity

If the SP is the result of a rectification process which leads to a net  $K^+$  current through the hair cells during stimulation (Johnstone et al., 1989), then blocking 4-AP sensitive  $K^+$  channels in the hair cell should shift the SP measured near the place of stimulation in scala vestibuli and scala tympani in opposite directions. However, in our first series of experiments 4-AP shifted the SP in the negative direction in both scala vestibuli and scala tympani (Figs. 1 and 2). A comparable negative shift of the SP in scala tympani after 4-AP application was reported by Wang et al. (1993). 4-AP probably blocks the 4-AP sensitive  $K^+$  channel in the cochlear afferents and associated ganglion cells (Santos-Sacchi, 1993). This might result in a drastic change in the waveform of the CAP and a subsequent shift of the SP in the negative direction in both

scalae (Van Emst et al., 1995).

#### 4.2. Preventing afferent nerve related changes in SP after 4-AP application

Thus, it became clear that if we wanted to study the contribution from 4-AP sensitive  $K^+$  channels in the basolateral membrane of the hair cells to the SP we first had to block the neuronal discharges. This was done by adding the  $Na^+$  channel blocker TTX to the perfusion solutions. TTX removed the CAP, but also caused specific shifts of the SP in the negative direction in both scalae (Dolan et al., 1989; Van Emst et al., 1995). There are two reasons why this TTX effect on the SP would not originate in hair cells near the recording electrode, but most likely with nerve activity: 1) TTX effects on local hair cells should shift the SP in scala vestibuli and scala tympani in opposite directions. 2) Shifts in the same direction could originate in hair cells at a remote location with respect to the electrode position, but physiologically active  $Na^+$  channels have not been found in hair cells (Witt et al., 1994).

#### 4.3. Contributions from 4-AP sensitive $K^+$ channels in the hair cells to the SP

After blocking neuronal discharges with TTX, the cochlea was perfused with a combination of TTX and 4-AP. Addition of 4-AP resulted in an increase of the magnitude of the SP with the exception of the following conditions: at low stimulus levels of 12 kHz in both scalae and at low stimulus levels of 8 kHz in scala vestibuli we found a decrease of SP magnitude. Thus, by and large, 4-AP shifted the SP in the two scalae in opposite directions if compared to the SP during TTX only (*cf.* Fig. 4 and Fig. 6). This indicates that the source of the SP shifts has to be found in between scala vestibuli and scala tympani, i.e. at the hair cell level. Thus, these shifts are probably related to blocking of 4-AP sensitive  $K^+$  channels in the basolateral membrane of the hair cell.

#### 4.4. Differential effect of 4-AP on IHCs and OHCs

Since both IHCs and OHCs contribute to the basal turn SP and since both possess a 4-AP sensitive  $K^+$  channel it is likely that the 4-AP induced shifts in the SP reflect the effects of 4-AP on both hair cell populations. The decrease in SP magnitude was found at low and moderate stimulus levels of 8 and 12 kHz stimuli. It is generally assumed that in these conditions the SP depends mainly on contributions from the basal turn IHCs. The basal turn IHCs produce large depolarizing DC receptor potentials when stimulated with characteristic high-frequency sound, while basal turn OHCs do not produce DC responses when stimulated with these high-frequency sounds at low and moderate levels (Dallos, 1985; Russell et al., 1986; Cody and Russell, 1987). Therefore, we conclude that the decrease in SP magnitude at low and moderate

level high-frequency stimulation reflects the effects of 4-AP on the IHC.

The increase in SP with 4-AP administration was found at high levels of 8 and 12 kHz stimuli, and at all levels of 2 and 4 kHz stimuli. At high stimulus frequencies the OHCs in the basal turn start to depolarize when the stimulus reaches a high level. Therefore, we expect that with these stimulus conditions both IHCs and OHCs contribute to the SP. Furthermore, when the guinea pig cochlea is stimulated with sound frequencies below 4 kHz, the SP recorded from the basal turn can be either positive or negative, depending on frequency and level of the stimulus used (Dallos et al., 1972). When basal turn OHCs are stimulated with sound frequencies far below their characteristic frequency they produce both depolarizing and hyperpolarizing DC receptor potentials, depending on frequency and level of the stimulus in a similar manner as the extracellular SP (Dallos et al., 1982; Dallos, 1985; Russell et al., 1986; Cody and Russell, 1987). Therefore, it is generally assumed that for frequencies up to about 4 kHz the SP is dominated by contributions from OHCs (Cheatham and Dallos, 1994). At these frequencies we found an increase in SP amplitude. Thus, we conclude that the increase in SP amplitude reflects the effects of 4-AP on the OHC.

#### *4.5. Possible mechanisms behind 4-AP induced shifts in SP*

##### *4.5.1 Increase in IHC basolateral membrane resistance*

The primary effect of blocking  $K^+$  channels is an increase in the resting resistance of the basolateral membrane of the hair cell (Mammano et al., 1995). By resting resistance is meant the resistance of the basolateral membrane in the absence of stimulation. An increase in resting basolateral membrane resistance will lead to a relatively smaller contribution of the stimulus-controlled apical resistance to the total resistance. Thus, a given stimulus will evoke smaller modulations of the current flowing through the hair cell and, consequently, will lead to a smaller contribution of the hair cell to the extracellular receptor potentials. We have found a decrease in the magnitude of the extracellular DC receptor potential (SP) at low and moderate levels of 8 and 12 kHz stimuli. Above we have noted that at these conditions the SP depends mainly on contributions from basal turn IHCs. Together, these considerations suggest that the 4-AP sensitive  $K^+$  channel in the IHC as reported by Kros and Crawford (1990) is responsible for the decrease in SP after 4-AP application at low-level high-frequency stimulation. One property of the 4-AP sensitive  $K^+$  channels is that their open probability depends on the membrane potential (Kros and Crawford, 1990; Housley and Ashmore, 1992; Mammano et al., 1995), i.e. they are activated by depolarization of the membrane potential. IHCs invariably produce depolarizing DC receptor potentials (Russell et al., 1986). These potentials will increase the open probability of the 4-AP sensitive  $K^+$  channel. Because the proportion of open  $K^+$  channels is normally increased during stimulation, the effect of 4-AP on

basolateral membrane resistance is virtually enhanced. Consequently, we expect that the effect of 4-AP on the SP is larger in a situation with interaction between channel conductance and membrane potential than in a situation without. An estimate of the total effect based on the model proposed by Dallos (1983) is in agreement with the decrease in SP found in the present experiment.

#### 4.5.2. *Electro-mechanic interactions in the OHC*

Patch-clamp recordings show that the 4-AP sensitive  $K^+$  channel in the OHC is activated only at extreme depolarizations (Mammano et al., 1995). Therefore, no effect of 4-AP on OHC physiology is expected when the blocker is applied *in vivo*. However, when we perfused 4-AP through the cochlea we did find an increase in SP amplitude, especially at the lowest test frequencies where the major contribution to the SP is thought to come from OHCs. This strongly suggests that the 4-AP sensitive  $K^+$  channel in OHCs does play a role in normal physiological conditions.

Because the discussion in 4.5.1 holds also for the OHC, we should expect a decrease in SP when an operational voltage-dependent  $K^+$  channel in the OHC is blocked. Therefore, the increase in SP must be due to an additional effect occurring specifically in the OHC after the 4-AP sensitive  $K^+$  channel is blocked. It has been reported that depolarization of the OHC causes a decrease in the apical transducer conductance, equivalent to displacing the stereociliar bundle in the inhibitory direction (Russell and Kössl, 1991). This displacement may be caused by depolarization-induced contraction of the OHC body (Santos-Sacchi, 1989; Evans et al., 1991). If blocking of the 4-AP sensitive  $K^+$  channel in the OHC basolateral membrane causes a slight depolarization of the membrane potential, then this might cause a small decrease in the proportion of the transducer conductance which is open at rest. This would mean that the operating point of the apical mechano-electrical transducer function shifts to a region where stimulation of the apical transducer results in more positive intracellular DC potentials, more negative SP values in scala vestibuli and more positive SP values in scala tympani (Cheatham and Dallos, 1994). Therefore, considering the unique properties of OHCs it seems possible that blocking of the 4-AP sensitive  $K^+$  channel in the basolateral membrane could explain the increased SP magnitude at high levels of 8 and 12 kHz stimuli, and at all levels of 2 and 4 kHz stimuli. Since CM is generally assumed to be dominated by the OHC (Dallos, 1983), one might expect a concomitant change in CM. However, we observed no significant changes in CM. This reduces the set of nonlinear transfer functions that can account for the results. Yet, preliminary calculations on the basis of a Boltzmann type of transfer function, which has been shown to accurately describe transduction at the apical channel (Kros et al., 1992), demonstrated that with shifts in the operating point the SP may shift by 50 % of its maximum value while the CM amplitude varies within 5 %. In view of measurement variability such a small change in CM

may not lead to an experimentally significant change in CM amplitude.

#### 4.5.3. Other mechanisms

Other mechanisms through which increases of the SP might be explained have been considered.  $K^+$  channels are undoubtedly present in nonsensory cells lining the cochlear duct. 4-AP effects on these cells could increase the duct's resistance and consequently, increase the EP. However, a 4-AP induced increase in the EP has been ruled out as a causative factor for SP increase because we found that the EP was unaffected by 4-AP perfusion. It is not clear how blocking the  $K^+$  channels in the nonsensory cells could change the SP by other means than by changing the EP. We, therefore, assume that the changes in SP are a direct consequence of changes in the input resistance of the hair cells. In principle, a change in the hair cells' input resistance will change the EP. We calculated that this effect is too small to result in a detectable change in EP.

The SP is known to increase in situations where a displacement of the resting position of the basilar membrane is evoked (Klis and Smoorenburg, 1985), e.g. during endolymphatic hydrops (Van Deelen et al., 1987; Van Benthem et al., 1994). However, light microscopical examination of the cochlea after 4-AP perfusion revealed no sign of endolymphatic hydrops.

#### 4.6. Conclusion

In conclusion, it appears that blocking the 4-AP sensitive  $K^+$  channel in the basolateral membrane of the IHC results in a decrease of the SP magnitude, which is comparable to the effect of blocking the TEA-sensitive  $K^+$  channel in the IHC basolateral membrane (Van Emst et al., 1995). A decrease in SP magnitude can be explained in terms of known properties of the basolateral membrane. The increase in SP magnitude is probably the result of blocking the 4-AP sensitive  $K^+$  channel in the basolateral membrane of the OHC. Blocking the 4-AP sensitive  $K^+$  channel in the OHC may lead to an increase in SP because of depolarization and subsequent mechanical alterations.



## References

- Ashmore, J.F. (1991) The electrophysiology of hair cells. *Annu. Rev. Physiol.* 53, 465-476.
- Ashmore, J.F. and Meech, R.W. (1986) Ionic basis of membrane potential in outer hair cells of guinea pig cochlea. *Nature* 322, 368-371.
- Cheatham, M.A. and Dallos, P. (1994) Stimulus biasing: A comparison between cochlear hair cell and organ of corti response patterns. *Hear. Res.* 75, 103-113.
- Cody, A.R. and Russell, I.J. (1987) The responses of hair cells in the basal turn of the guinea-pig cochlea to tones. *J. Physiol.* 383, 551-569.
- Corey, D.P. and Hudspeth, A.J. (1983) Kinetics of the receptor current in bullfrog saccular hair cells. *J. Neurosci.* 3, 962-976.
- Dallos, P., Schoeny, Z.G. & Cheatham, M.A. (1972) Cochlear summing potentials. Descriptive aspects, *Acta Otolaryngol. (Stockh.) Suppl.* 302, 5-46.
- Dallos, P., Santos-Sacchi, J. and Flock, Å. (1982) Intracellular recordings from cochlear outer hair cells. *Science* 218, 582-584.
- Dallos, P. (1983) Some electrical circuit properties of the organ of Corti. I. Analysis without reactive elements. *Hear. Res.* 12, 89-119.
- Dallos, P. (1985) Response characteristics of mammalian cochlear hair cells. *J. Neurosci.* 5, 1591-1608.
- Dallos, P. and Cheatham, M.A. (1990) Effects of electrical polarization on inner hair cell receptor potentials. *J. Acoust. Soc. Am.* 87, 1636-1647.
- De Groot, J.C.M.J., Veldman, J.E. and Huizing E.H. (1987) An improved fixation method for guinea pig cochlear tissues. *Acta Otolaryngol. (Stockh.)* 104, 234-242.
- Dolan, D.F., Xi, L. and Nuttall, A.L. (1989) Characterization of an EPSP-like potential recorded remotely from the round window. *J. Acoust. Soc. Am.* 86, 2167-2171.
- Dulon, D., Sugasawa, M., Blanchet, C. and Erostequi, C. (1995) Direct measurements of  $\text{Ca}^{2+}$ -activated  $\text{K}^+$  currents in inner hair cells of the guinea-pig cochlea using photolabile  $\text{Ca}^{2+}$  chelators. *Pflügers Arch.* 430, 365-373.

Evans, B.N., Hallworth, R. and Dallos, P. (1991) Outer hair cell electromotility: The sensitivity and vulnerability of the DC component. *Hear. Res.* 52, 288-304.

Gitter, A.H., Frömter, E. and Zenner, H.P. (1992) C-type potassium channels in the lateral membrane of guinea-pig outer hair cells. *Hear. Res.* 60, 13-19.

Housley, G.D. and Ashmore, J.F. (1992) Ionic currents of outer hair cells isolated from the guinea-pig cochlea. *J. Physiol.* 448, 73-98.

Hudspeth, A.J. and Corey, D.P. (1977) Sensitivity, polarity and conductance change in the response of vertebrate hair cells to controlled mechanical stimuli. *Proc. Natl. Acad. Sci. U.S.A.* 74, 2407-2411.

Johnstone, B.M., Patuzzi, R., Syka, J. and Sykova, E. (1989) Stimulus-related potassium changes in the organ of Corti of guinea-pig. *J. Physiol.* 408, 77-92.

Klis, S.F.L. and Smoorenburg, G.F. (1985) Modulation at the guinea pig round window of summing potentials and compound action potentials by low-frequency sound. *Hear. Res.* 20, 15-23.

Klis, S.F.L. and Smoorenburg, G.F. (1994) Osmotically induced pressure difference in the cochlea and its effect on cochlear potentials. *Hear. Res.* 75, 114-120.

Kros, C.J. and Crawford, A.C. (1990) Potassium currents in inner hair cells isolated from the guinea-pig cochlea. *J. Physiol.* 421, 263-291.

Kros, C.J., Rüsç, A. and Richardson, G.P. (1992) Mechano-electrical transducer currents in hair cells of the cultured neonatal mouse cochlea. *Proc. R. Soc. Lond. B* 249, 185-193.

Lin, X., Hume, R.I. and Nuttall, A.L. (1995) Dihydropyridines and verapamil inhibit voltage-dependent  $K^+$  current in isolated outer hair cells of the guinea pig. *Hear. Res.* 88, 36-46.

Mammano, F., Kros, C.J. and Ashmore, J.F. (1995) Patch clamped responses from outer hair cells in the intact adult organ of Corti. *Pflügers arch.* 430, 745-750.

Nuttall, A.L. (1985) Influence of direct current on dc receptor potentials from cochlear inner hair cells in the guinea pig. *J. Acoust. Soc. Am.* 77, 165-175.

Russell, I.J. and Sellick, P.M. (1978) Intracellular studies of hair cells in the

mammalian cochlea. *J. Physiol.* 284, 261-290.

Russell, I.J. (1983) Origin of the receptor potential in inner hair cells of the mammalian cochlea-evidence for Davis' theory. *Nature* 301, 334-336.

Russell, I.J., Cody, A.R. and Richardson, G.P. (1986) The responses of inner and outer hair cells in the basal turn of the guinea-pig cochlea and in the mouse cochlea grown in vitro. *Hear. Res.* 22, 199-216.

Russell, I.J. and Kössl, M. (1991) The voltage responses of hair cells in the basal turn of the guinea-pig cochlea. *J. Physiol.* 435, 493-511.

Santos-Sacchi, J. (1989) Asymmetry in Voltage-Dependent Movements of Isolated Outer Hair Cells from the Organ of Corti. *J. Neurosci.* 9, 2954-2962.

Santos-Sacchi, J. (1993) Voltage-dependent ionic conductances of type I spiral ganglion cells from the guinea pig inner ear. *J. Neurosci.* 13, 3599-3611.

Van Benthem, P.P.G., Klis, S.F.L., Albers, F.W.J., de Wildt, D.J., Veldman, J.E., Huizing, E.H. and Smoorenburg, G.F. (1994) The effect of nimodipine on cochlear potentials and  $\text{Na}^+/\text{K}^+$ -ATPase activity in normal and hydropic cochleas of the albino guinea pig. *Hear. Res.* 77, 9-18.

Van Deelen G.W. and Smoorenburg, G.F. (1986) Electrocochleography for different electrode positions in guinea pig. *Acta Otolaryngol. (Stockh.)* 101, 207-216.

Van Deelen, G.W., Ruding, P.R.J.W., Veldman, J.E., Huizing, E.H. and Smoorenburg, G.F. (1987) Electrocochleographic study of experimentally induced endolymphatic hydrops. *Arch. Otorhinolaryngol.* 244, 167-173.

Van Emst, M.G., Klis, S.F.L. and Smoorenburg, G.F. (1995) Tetraethylammonium effects on cochlear potentials in the guinea pig. *Hear. Res.* 88, 27-35.

Wang, J., Li, Q., Dong, W. and Chen, J. (1993) Effects of  $\text{K}^+$ -channel blockers on cochlear potentials in the guinea pig. *Hear. Res.* 68, 152-158.

Witt, C.M., Hu, H.Y., Brownell, W.E. and Bertrand, D. (1994) Physiologically silent sodium channels in mammalian outer hair cells. *J. Neurophysiol.* 72, 1037-1040.

## Chapter 4

### Identification of the nonlinearity governing even-order distortion products in cochlear potentials

Maarten G. van Emst, Sjaak F.L. Klis and Guido F. Smoorenburg  
*submitted for publication in Hearing Research*

#### Abstract

In order to characterize the cochlear transducer nonlinearities which are involved in the generation of the summing potential (SP), we investigated the effect of a change in the electrical operating point of the cochlear transducer on the SP. The electrical operating point of the cochlear transducer was affected by suppressing reversibly the endocochlear potential (EP). In guinea pig this was realised by intravenous injection of either 30 or 80 mg/kg furosemide. A differential recording technique was used in the basal turn of the guinea pig's cochlea to measure locally generated even-order distortion products: the SP and the second harmonic component ( $2F_0$ ) of the cochlear microphonics (CM). These potentials were evoked by 2 and 8 kHz stimuli, presented at 60 dB SPL. During the reversible suppression of the EP the SP changed polarity twice. The zero crossings of the SP coincided with a minimum in the amplitude of  $2F_0$ . Concomitantly, the phase of  $2F_0$  shifted about  $120^\circ$ . The changes in the electrical even-order products were comparable to the changes that occurred in a mechanical even-order intermodulation distortion product (the difference tone oto-acoustic emission) after 80-mg/kg furosemide application (Mills et al., *J. Acoust. Soc. Am.* 94, 2108-2122 (1993)). The combined results suggest that only one sigmoidal transfer function may account for the SP,  $2F_0$  and the emission of the difference tone, and that shifts in the operating point of the transfer function would be the major cause behind the furosemide-induced changes in the even-order distortion products. The sigmoidal transfer function can possibly be associated with the mechano-electrical transducer channel at the apical pole of the OHC.

**Keywords:** Summing potential; Cochlear microphonics; Distortion products; Nonlinearities; Guinea pig

## 1. Introduction

The positive endocochlear potential (EP) and the negative membrane potential in the hair cell add to form an approximately 150 mV potential difference across the apical membrane of the hair cell. This potential difference together with the apical membrane conductance determines the current flowing through the hair cells at rest. Sound-evoked modulation of the apical membrane conductance modulates the hair cell current, which results in both an AC and a DC receptor potential (Russell, 1983). The intracellular DC potential arises due to nonlinear elements in the transduction chain, among which the apical mechano-electrical transduction process (Russell and Sellick, 1978; Corey and Hudspeth, 1983) and the basolateral voltage-dependent  $K^+$  channels (Dallos and Cheatham, 1990; Van Emst et al., 1995; 1996). Extracellularly, the AC and DC receptor potential are reflected in the cochlear microphonics (CM) and the summing potential (SP), respectively.

The voltage-dependent conductances that have been identified *in vitro* in the basolateral membrane of cochlear hair cells are primarily associated with the voltage-dependent potassium ( $K^+$ ) channels in this part of the membrane (Kros and Crawford, 1990; Housley and Ashmore, 1992). The dependence of  $K^+$  conductance on the membrane potential is nonlinear and can be described by a sigmoidal relation, the Boltzmann relation. We established that blocking the voltage-dependent  $K^+$  channels, located in either the inner hair cells (IHC) or outer hair cells (OHC), caused small changes in the SP (Van Emst et al., 1995; 1996).

The experimental results mentioned above suggest that the major contribution to the SP should come from the apical mechano-electrical transduction process. The relation between the conductance of the apical transduction channels and the position of the stereocilia is also described by a Boltzmann function (Kros et al., 1992).

We chose to examine the contribution from the apical conductance to the SP by means of manipulating electrically the operating point of the apical channel. Russell and Kössl (1991) showed that the conductance in the apical membrane of the OHC depends on the electrical operating point of the cell. One way to alter the operating point of the cochlear partition electrically is to change the EP. This can be achieved pharmacologically with loop-diuretics, such as furosemide (Kusakari et al., 1978). Furosemide causes a reversible suppression of the EP. Thus, it should cause a reversible shift in the operating point of the cochlear partition. Indeed, application of loop-diuretics resulted in reversible polarity changes of the SP (Aran and Charlet de Sauvage, 1977; Syka and Melichar, 1985).

Although the changes in SP just quoted could relate to changes in the operating point of the apical nonlinearity there might be another explanation. In both experiments a single recording electrode was used. This implies that the SP was generated by outputs from many hair cells, widely distributed over the length of the basilar membrane. One group of hair cells might have contributed a negative DC component while another group might have contributed a positive DC component (Dallos et al., 1972). Thus, the changes in polarity might just as well have reflected a change in the relative magnitude of the positive and negative contributions to the SP. This interpretation is supported by the finding that suppression of the EP by furosemide varies throughout the cochlea (Sewell, 1984).

Thus, in order to establish the role of the apical hair cell nonlinearity in SP generation we studied the effects of reversible EP suppression, evoked by furosemide, on the locally generated SP measured with a pair of differential recording electrodes (Tasaki et al., 1952). Moreover, the effects of EP suppression on the phase and amplitude of several harmonic components of the locally generated CM were studied: the fundamental or 1<sup>st</sup> harmonic ( $1F_0$ ), 2<sup>nd</sup> harmonic ( $2F_0$ ), 3<sup>rd</sup> harmonic ( $3F_0$ ) and 4<sup>th</sup> harmonic ( $4F_0$ ).

Finally, we compared the changes in the locally-generated SP and  $2F_0$  to the changes in an even-order distortion-product-otoacoustic-emission (DPOAE) that occurred after furosemide application (Mills et al., 1993). This comparison shows to what extent our products of nonlinear mechano-electrical transduction are related to mechanical distortion products.

## 2. Materials and methods

Albino female guinea pigs, Dunkin Hartley strain (Cpb/Hsd DH), were used as experimental subjects. Pre-operatively the animals were treated with Thalamonal (0.15 ml/100 g body weight, i.m.). Thalamonal is a mixture of 2.5 mg/ml droperidol and 0.05 mg/ml fentanyl. During surgery and experimental procedures the animals were anaesthetized by artificial ventilation through a cannula in the exposed trachea with a gas mixture containing 33% O<sub>2</sub>, 66% N<sub>2</sub>O and 1% halothane. Heart frequency was monitored, and body temperature was kept at about 37.7°C. The care and use of the animals were approved by the Animal Care and Use Committee of the Faculty of Medicine, Utrecht University, under number FDC-89007, GDL-20008.

The jugular vein was cannulated with polyethylene tubing to allow intravenous injection of furosemide. The cochlea was exposed using a ventrolateral approach. Two 0.2-mm holes were drilled into the wall of the cochlea for measurement of sound-evoked intracochlear potentials. One hole

opened into the scala vestibuli (SV), and the other one into the scala tympani (ST) of the basal turn. Care was taken to drill the holes in a plain perpendicular to the stria vascularis in order to situate the electrodes symmetrically on the two sides of the organ of Corti. For measuring the EP a 0.1-mm hole was drilled in the bony wall overlying the scala media (SM) of the second turn. The second turn was chosen for its easy access to SM.

Stimulus generation and data acquisition were controlled by a PC using a Cambridge Electronic Design 1401-plus laboratory interface. Tone-burst signals were calculated and stored in a revolving memory consisting of 2,500 points with 12-bit resolution. Tone bursts of 2 and 8 kHz were used to evoke responses which contain substantial SP of positive or negative polarity, respectively, and CM. The stimuli were constructed with cosine-shaped rise- and fall-times of 1 ms, to reduce spectral spread of energy, and a plateau of 14 ms. Consecutive tone bursts were presented with alternating polarity at 99-ms intervals from onset to onset. The electric stimuli were led to a Beyer DT 48 dynamic transducer, which was connected to a hollow ear bar fitted into the exposed outer ear canal. The acoustic stimuli were presented at a moderate 60 dB sound pressure level.

Sound-evoked potentials were recorded with silver-electrodes inserted into the holes in SV and ST. The electrodes had small spindle-shaped globules just behind their tip. The globules, which were formed by dipping the tip of the electrode into a flame, served to control the depth of the electrode tip and also to seal off the holes. The electrodes were insulated with enamel, except at the tip.

The potentials in SV and ST were measured in separate channels. Each intracochlear electrode was connected to the non-phase-inverting input of a differential amplifier, the phase inverting inputs were connected to a common reference electrode, a steel wire connected to the neck musculature. The signals were amplified and band-pass filtered between 1 Hz and 10 kHz. AD conversion was performed simultaneously for both channels, using sample-and-hold circuitry, at the smallest technically-possible time-interval; 40  $\mu$ s or 25 kHz. Within both channels the responses to the tone bursts of opposite polarity were averaged (max. 500 x) and stored separately. Thus, each averaging sequence yielded 4 different signals:  $SV^+$ ,  $SV^-$ ,  $ST^+$ ,  $ST^-$ . They were mathematically combined to produce:

1) Compound action potential(CAP)-and-SP responses in each of the scalae separately (by adding the recordings to the tone bursts of opposite polarity;  $SV^+ + SV^-$  &  $ST^+ + ST^-$ ).

2) CM responses in each of the scalae separately (by subtracting the recordings

to the tone bursts of opposite polarity;  $SV^+ - SV^-$  &  $ST^+ - ST^-$ ).

3) Differential SP responses (diff-SP) by subtracting the CAP-and-SP response (calculated sub-1) for scala tympani from the CAP-and-SP response (calculated sub-1) for scala vestibuli;  $(SV^+ + SV^-) - (ST^+ + ST^-)$ . This procedure reveals the locally generated SP while suppressing the CAP.

4) Differential CM responses (diff-CM) by subtracting the CM responses (calculated sub-2) for the two scalae;  $(SV^+ - SV^-) - (ST^+ - ST^-)$ . This procedure reveals the locally generated CM.

The magnitude of the diff-SP response was measured as the difference between the pre-stimulus DC level and the DC level approximately 12 ms after the start of the 16 ms tone burst. A FFT of the CM data was performed. The AD sampling frequency allowed us to study the fundamental response ( $1F_0$ ) at 2 and 8 kHz, and the 2<sup>nd</sup> ( $2F_0$ ), 3<sup>rd</sup> ( $3F_0$ ), and 4<sup>th</sup> ( $4F_0$ ) harmonic of the response to 2 kHz. Both amplitude and phase shifts were examined.

To check the symmetry of electrode placement we compared the CM responses from the two scalae to an 8 kHz tone burst (Tonndorf, 1958b). When the amplitude of the CM recorded from SV deviated less than 10 % from that of the CM from ST, and the difference in phase between the CM recorded from SV and ST was between  $170^\circ$  and  $190^\circ$ , it was decided that the electrodes had been accurately placed, and that the diff-SP and diff-CM data (sub-3 and sub-4) were acceptable.

In each experiment the cochlear responses to the stimuli at the two frequencies were recorded repeatedly before, during and after furosemide was injected, during a total period of 200 min. Furosemide (20mg/2ml) was injected until a dose of either 30 or 80 mg/kg-b.w. was reached (Furosemidum; Centrafarm, Rijswijk, the Netherlands). The compound was steadily injected over a 60 sec period.

In separate experiments the EP was recorded before, during and after injection of furosemide. The EP was measured with a glass micropipette filled with 3 M KCl (impedance 5-10 M $\Omega$ ), which was connected to a WPI 705 preamplifier through an Ag-AgCl pellet. The EP was measured relative to a chlorided silver wire in the neck musculature. AD-converted samples of the EP were taken every two seconds. Only those preparations where a stable recording of the EP of initially more than 70 mV for 10 min had been achieved were used to study the effect of furosemide on the EP.



### 3. Results

#### 3.1. Effects of 80 mg/kg furosemide

##### 3.1.1. Endocochlear Potential

Fig. 1 is a typical example of the effect of 80 mg/kg furosemide on the EP. Furosemide injection was started at time zero. The EP reached a minimum within 2 min. The average drop of the EP in 4 experiments that were fully completed was 107 mV, from about +76 mV to about -31 mV. Subsequently, the EP started to recover. The EP did not fully recover within the 200 minutes of recording.

##### 3.1.2. Odd-order responses evoked by 8 and 2 kHz stimuli at 60 dB SPL

Four experiments successfully met our criterion on accurate electrode placement (see Methods). Thus, the differential responses were obtained for these experiments. An example of the effect of furosemide on the fundamental component ( $1F_0$ ) of the 8-kHz diff-CM is shown in Fig. 2. The  $1F_0$  showed essentially the same course of events as described for the EP. The  $1F_0$  amplitude was reduced by approximately 66% within 2 min ( $n=4$ ). Subsequently, the  $1F_0$  slowly started to recover, but at the end of the experiment the amplitude of the  $1F_0$  was still below pre-injection levels. No systematic changes were observed in the phase of the  $1F_0$  component of the 8-kHz diff-CM.

Fig. 3 shows an example of the effect of furosemide on the fundamental component ( $1F_0$ ) of the 2-kHz diff-CM. At this lower stimulus frequency the amplitude of  $1F_0$  was larger than at 8 kHz, but the behaviour of the  $1F_0$  amplitude still followed that of the EP. A sharp reduction (approximately 63%) was followed by slow recovery. Again, no systematic changes were observed in the phase of  $1F_0$ . The development of the change in the  $3F_0$  component of the 2-kHz diff-CM was similar to the development of the change in the  $1F_0$  component (not shown).

##### 3.1.3. Even-order responses evoked by 8 and 2 kHz stimuli at 60 dB SPL

Fig. 4 shows an example of the 8-kHz diff-SP response. The time course of the diff-SP differs markedly from the  $1F_0$  amplitude time course. Initially, the stimulus evoked a negative diff-SP, but the sign of the diff-SP rapidly changed to positive after injection of furosemide. Subsequently, the positive diff-SP decreased in magnitude, went through zero for the second time after about 25 min, thereby regaining its original negative polarity, and started to increase in magnitude. The magnitude of the negative SP continued to increase even after it reached its original value at about 30 min. It continued to grow to extraordinarily large values. After about 93 min the diff-SP moved towards its original magnitude.

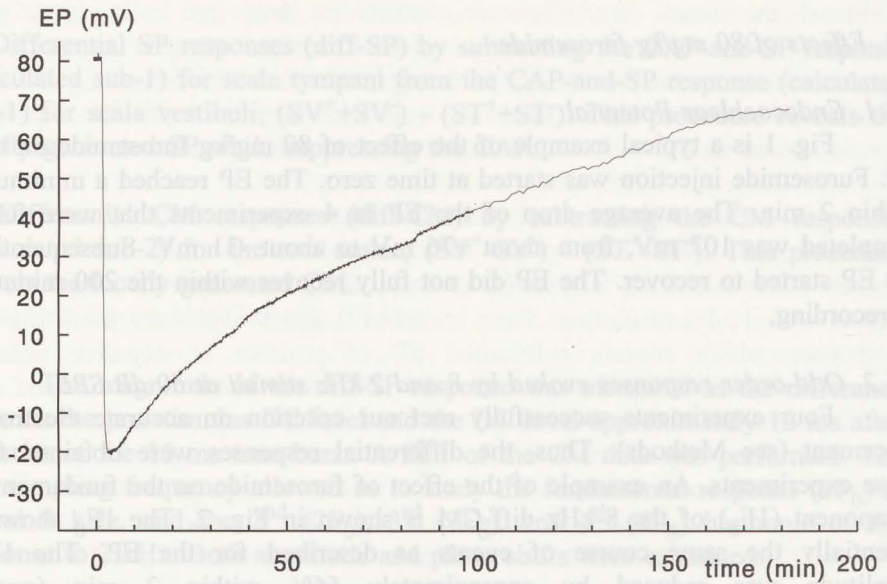


Fig. 1. Example of the effect of 80 mg/kg furosemide on the EP, which was recorded from the second-turn of scala media. The intravenous injection of furosemide took one minute, and started at time zero.

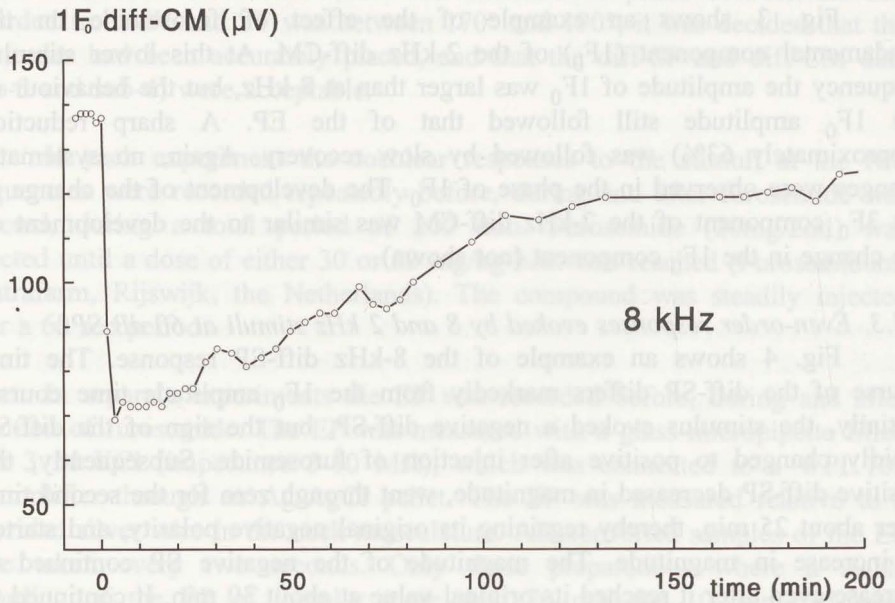


Fig. 2. Example of the effect of 80 mg/kg furosemide on the amplitude of the fundamental component of the CM evoked by an 8 kHz stimulus at 60 dB SPL. Differential recordings were made from the basal turn.

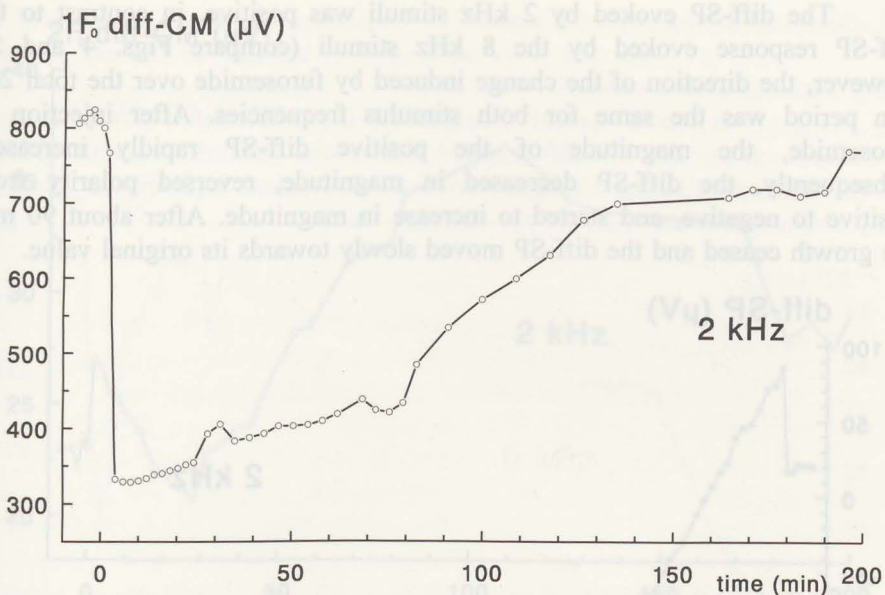


Fig. 3. Example of the effect of 80 mg/kg furosemide on the amplitude of the fundamental component of the CM evoked by a 2 kHz stimulus at 60 dB SPL. Differential recordings were made from the basal turn.

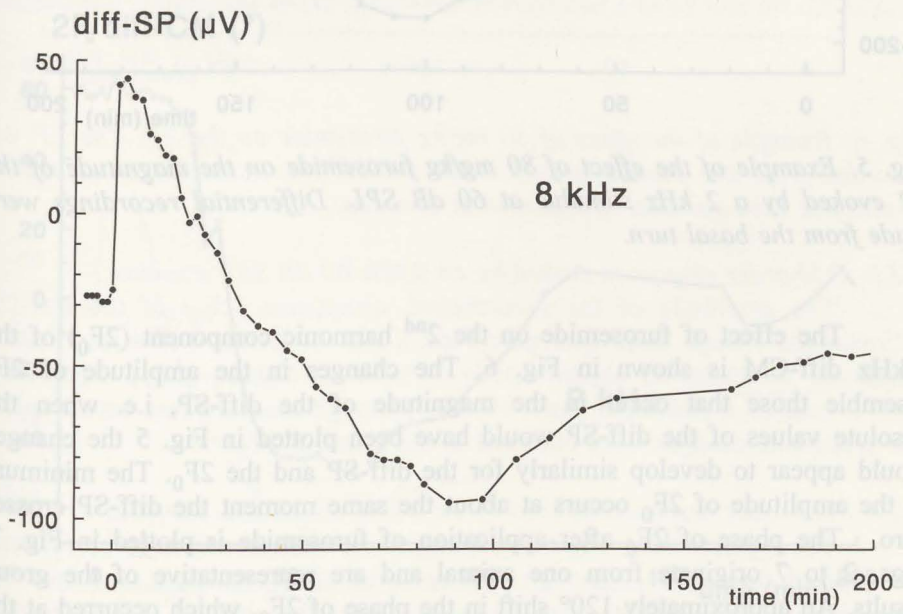


Fig. 4. Example of the effect of 80 mg/kg furosemide on the magnitude of the SP evoked by an 8 kHz stimulus at 60 dB SPL. Differential recordings were made from the basal turn.

The diff-SP evoked by 2 kHz stimuli was positive, in contrast to the diff-SP response evoked by the 8 kHz stimuli (compare Figs. 4 and 5). However, the direction of the change induced by furosemide over the total 200 min period was the same for both stimulus frequencies. After injection of furosemide, the magnitude of the positive diff-SP rapidly increased. Subsequently, the diff-SP decreased in magnitude, reversed polarity from positive to negative, and started to increase in magnitude. After about 90 min the growth ceased and the diff-SP moved slowly towards its original value.

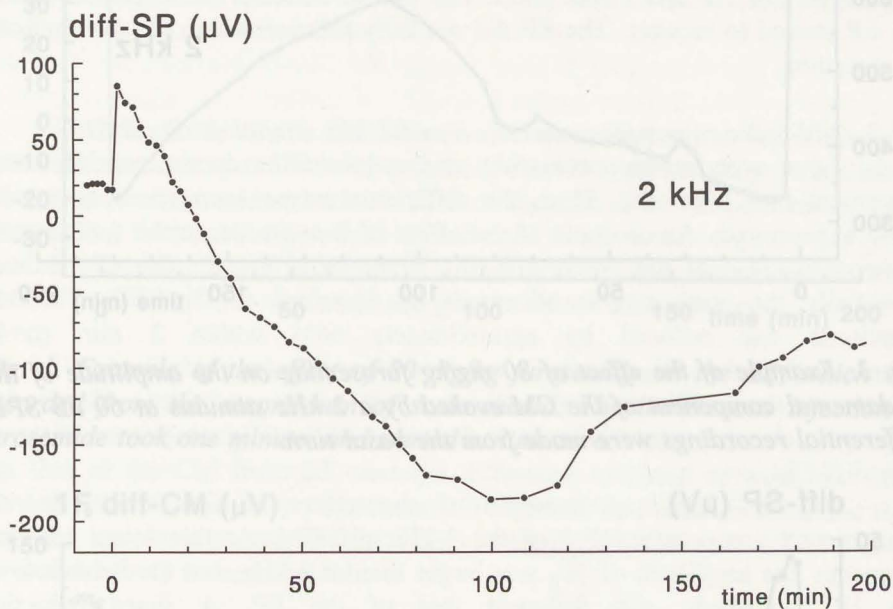


Fig. 5. Example of the effect of 80 mg/kg furosemide on the magnitude of the SP evoked by a 2 kHz stimulus at 60 dB SPL. Differential recordings were made from the basal turn.

The effect of furosemide on the 2<sup>nd</sup> harmonic component ( $2F_0$ ) of the 2-kHz diff-CM is shown in Fig. 6. The changes in the amplitude of  $2F_0$  resemble those that occur in the magnitude of the diff-SP, i.e. when the absolute values of the diff-SP would have been plotted in Fig. 5 the changes would appear to develop similarly for the diff-SP and the  $2F_0$ . The minimum in the amplitude of  $2F_0$  occurs at about the same moment the diff-SP crosses zero. The phase of  $2F_0$  after application of furosemide is plotted in Fig. 7. Figs. 2 to 7 originate from one animal and are representative of the group results. An approximately  $120^\circ$  shift in the phase of  $2F_0$ , which occurred at the moment that the amplitude went through a minimum, was the most conspicuous change. The  $4F_0$  component of the 2-kHz diff-CM showed a behaviour similar to that of  $2F_0$  (not shown).

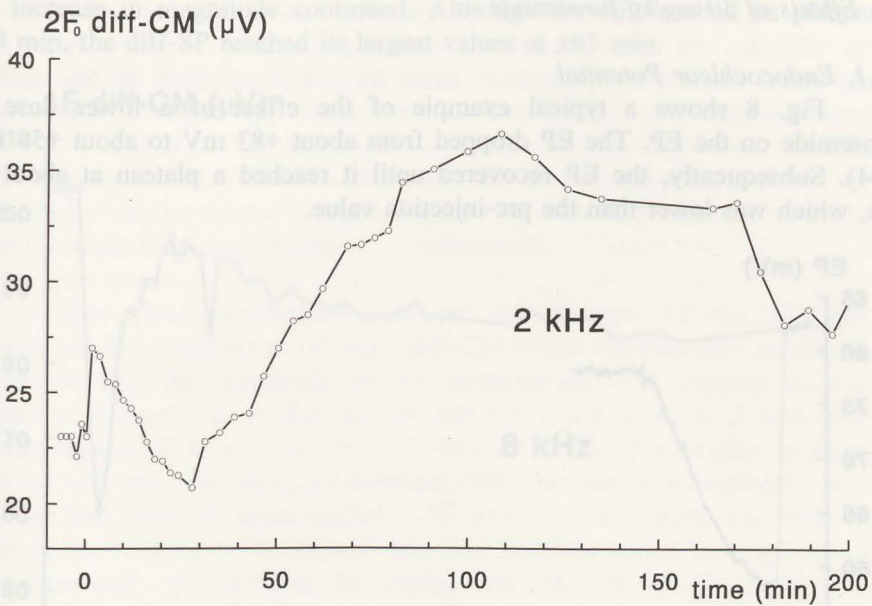


Fig. 6. Example of the effect of 80 mg/kg furosemide on the amplitude of the 2<sup>nd</sup> harmonic component (4 kHz) of the CM evoked by a 2 kHz stimulus at 60 dB SPL. Differential recordings were made from the basal turn.

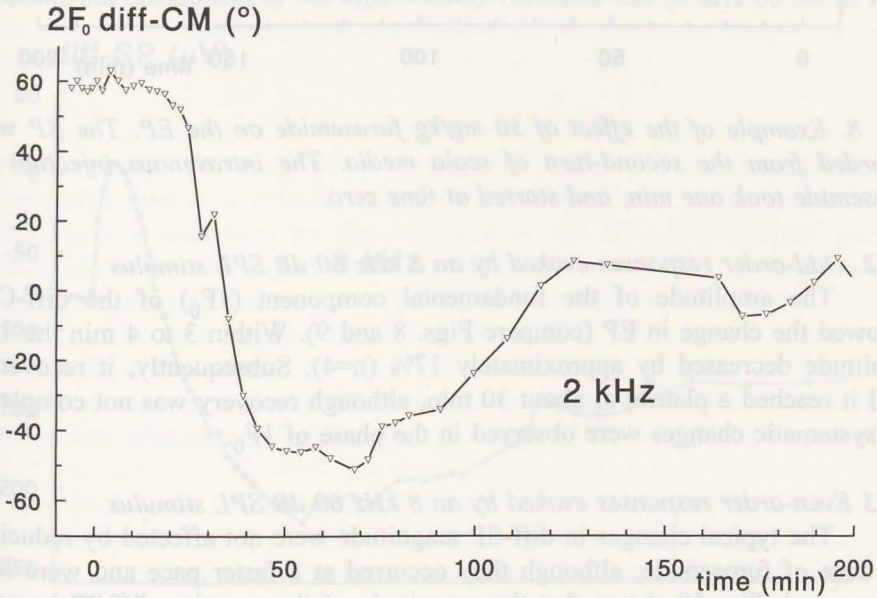


Fig. 7. Example of the effect of 80 mg/kg furosemide on the phase of the 2<sup>nd</sup> harmonic component (4 kHz) of the CM evoked by a 2 kHz stimulus at 60 dB SPL. The reference phase is arbitrary.

### 3.2. Effects of 30 mg/kg furosemide

#### 3.2.1. Endocochlear Potential

Fig. 8 shows a typical example of the effect of a lower dose of furosemide on the EP. The EP dropped from about +83 mV to about +58 mV ( $n=4$ ). Subsequently, the EP recovered until it reached a plateau at about 40 min, which was lower than the pre-injection value.

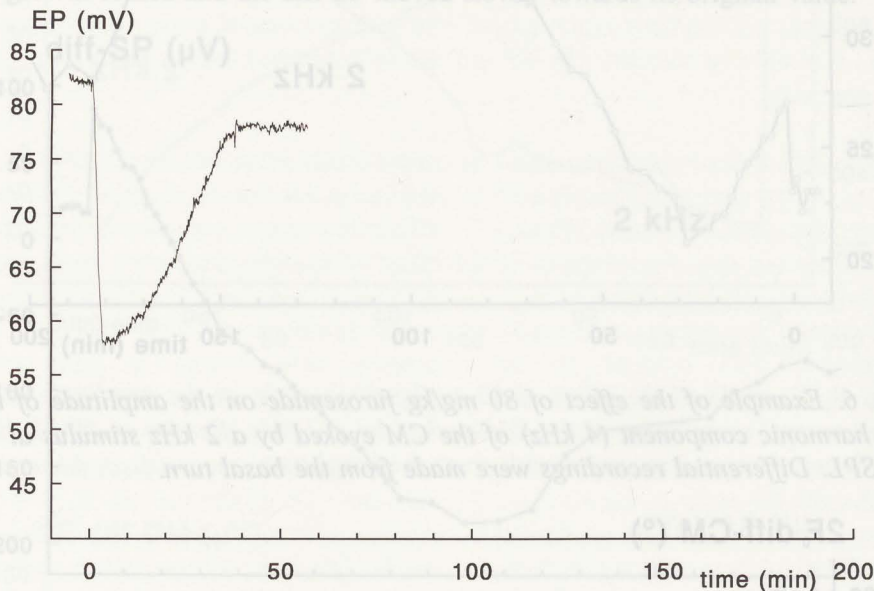


Fig. 8. Example of the effect of 30 mg/kg furosemide on the EP. The EP was recorded from the second-turn of scala media. The intravenous injection of furosemide took one min, and started at time zero.

#### 3.2.2. Odd-order responses evoked by an 8 kHz 60 dB SPL stimulus

The amplitude of the fundamental component ( $1F_0$ ) of the diff-CM followed the change in EP (compare Figs. 8 and 9). Within 3 to 4 min the  $1F_0$  amplitude decreased by approximately 17% ( $n=4$ ). Subsequently, it recovered until it reached a plateau at about 30 min, although recovery was not complete. No systematic changes were observed in the phase of  $1F_0$ .

#### 3.2.3 Even-order responses evoked by an 8 kHz 60 dB SPL stimulus

The typical changes in diff-SP magnitude were not affected by reducing the dose of furosemide, although they occurred at a faster pace and were less pronounced. Fig. 10 shows that the magnitude of the negative diff-SP became smaller, and just reached positive values. Within a few minutes the diff-SP had regained its negative polarity and started to increase in magnitude. After about 22 min the magnitude of the diff-SP had reached the pre-injection level, but

the increase in magnitude continued. Although the EP reached its plateau at  $\pm 40$  min, the diff-SP reached its largest values at  $\pm 63$  min.

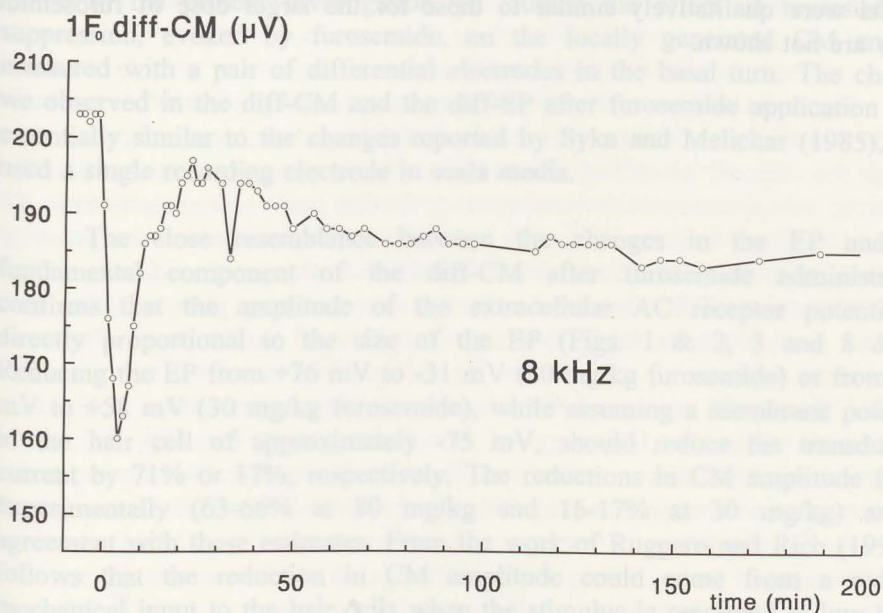


Fig. 9. Example of the effect of 30 mg/kg furosemide on the amplitude of the fundamental component of the differentially-recorded CM (8 kHz 60 dB SPL).

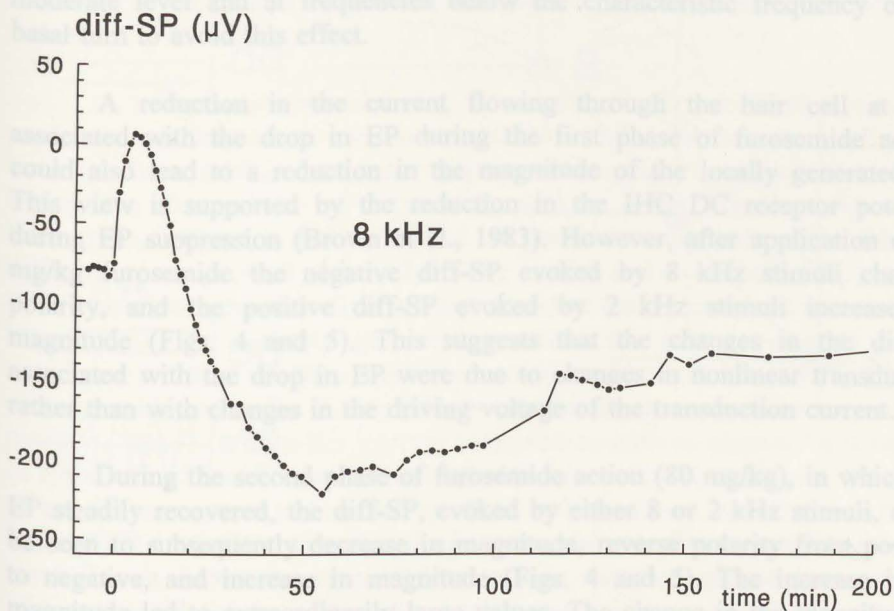


Fig. 10. Example of the effect of 30 mg/kg furosemide on the magnitude of the differentially-recorded SP evoked by an 8 kHz 60 dB SPL stimulus.

The behaviour of the odd-order and even-order responses evoked by the 2-kHz stimulus was not affected by reducing the dose of furosemide. The results were qualitatively similar to those for the larger dose of furosemide. They are not shown.

a typical example of the effect of furosemide on the EP. The EP dropped from about +83 mV to about +70 mV (n=4). Subsequently, the EP recovered until it reached a plateau at about 80 min, which was lower than the pre-injection value.



Fig. 8. Example of the effect of 30 mg/kg furosemide on the amplitude of the fundamental component of the differential-recorded CM (8 kHz 60 dB SPL).

Fig. 8. Example of the effect of 30 mg/kg furosemide on the EP. The EP was recorded from the second-turn of scala media. The intravenous injection of furosemide took one min, and started at time zero.

### 3.2.2 Odd-order responses evoked by an 8 kHz 60 dB SPL stimulus

The amplitude of the fundamental component ( $1F_0$ ) of the differential-recorded CM followed the change in EP (compare Figs. 8 and 9). Within 3 to 4 min the amplitude decreased by approximately 17% (n=4). Subsequently, it recovered until it reached a plateau at about 30 min, although recovery was not complete. No systematic changes were observed in the phase of  $1F_0$ .

### 3.2.3 Even-order responses evoked by an 8 kHz 60 dB SPL stimulus

The typical changes in diff-SP magnitude were not affected by reducing the dose of furosemide, although they occurred at a faster pace and were more pronounced. Fig. 10 shows that the magnitude of the negative diff-SP became smaller, and just reached positive values. Within a few minutes the diff-SP had returned to its pre-injection level. At 22 min the magnitude of the diff-SP was 100 uV.



#### 4. Discussion

In the present investigation we studied the effect of reversible EP suppression, evoked by furosemide, on the locally generated CM and SP measured with a pair of differential electrodes in the basal turn. The changes we observed in the diff-CM and the diff-SP after furosemide application were essentially similar to the changes reported by Syka and Melichar (1985), who used a single recording electrode in scala media.

The close resemblance between the changes in the EP and the fundamental component of the diff-CM after furosemide administration confirms that the amplitude of the extracellular AC receptor potential is directly proportional to the size of the EP (Figs. 1 & 2, 3 and 8 & 9). Reducing the EP from +76 mV to -31 mV (80 mg/kg furosemide) or from +83 mV to +58 mV (30 mg/kg furosemide), while assuming a membrane potential in the hair cell of approximately -75 mV, should reduce the transduction current by 71% or 17%, respectively. The reductions in CM amplitude found experimentally (63-66% at 80 mg/kg and 16-17% at 30 mg/kg) are in agreement with these estimates. From the work of Ruggero and Rich (1991) it follows that the reduction in CM amplitude could come from a reduced mechanical input to the hair cells when the stimulus is presented at low levels and at a frequency that is characteristic for the location of the hair cells. However, in our experiment the stimuli were deliberately presented at a moderate level and at frequencies below the characteristic frequency of the basal turn to avoid this effect.

A reduction in the current flowing through the hair cell at rest, associated with the drop in EP during the first phase of furosemide action, could also lead to a reduction in the magnitude of the locally generated SP. This view is supported by the reduction in the IHC DC receptor potential during EP suppression (Brown et al., 1983). However, after application of 80 mg/kg furosemide the negative diff-SP evoked by 8 kHz stimuli changed polarity, and the positive diff-SP evoked by 2 kHz stimuli increased in magnitude (Figs. 4 and 5). This suggests that the changes in the diff-SP associated with the drop in EP were due to changes in nonlinear transduction rather than with changes in the driving voltage of the transduction current.

During the second phase of furosemide action (80 mg/kg), in which the EP steadily recovered, the diff-SP, evoked by either 8 or 2 kHz stimuli, could be seen to subsequently decrease in magnitude, reverse polarity from positive to negative, and increase in magnitude (Figs. 4 and 5). The increase in SP magnitude led to extraordinarily large values. The change in the magnitude of the diff-SP closely resembled the change in the amplitude of the  $2F_0$  component of the diff-CM evoked by the 2-kHz stimulus (Figs. 5 and 6).

Moreover, the zero crossing of the SP coincided with an approximately 120° phase shift of  $2F_0$  (Figs. 5 and 7). These results suggest that the SP and the  $2F_0$  are generated by the same even-order components of a nonlinear transfer function.

Figure 11 illustrates how a shift in the operating point of a nonlinear transfer function can produce the observed changes in the even-order responses during the second phase of furosemide action. The transfer function is conceived as a symmetrical saturating relation. The point of symmetry is in the middle ( $f(x) = -f(-x)$ ). When the operating point lies below the point of symmetry (situation A) the stimulus is rectified in the positive direction. The Taylor expansion of the transfer function at this operating point contains both odd and even components:  $F(x) = a_0 + a_1x + a_2x^2 + \dots + a_nx^n$ . The even components, such as  $+ a_2x^2$ , account for the rectification of the stimulus. The rectified sine wave contains both a positive constant term and a component which has twice the frequency of the input ( $2F_0$ ), see Fig. 11 A. If the operating point moves to the middle then the transfer function operates symmetrically with respect to the zero point ( $f(x) = -f(-x)$ ). The even compo-

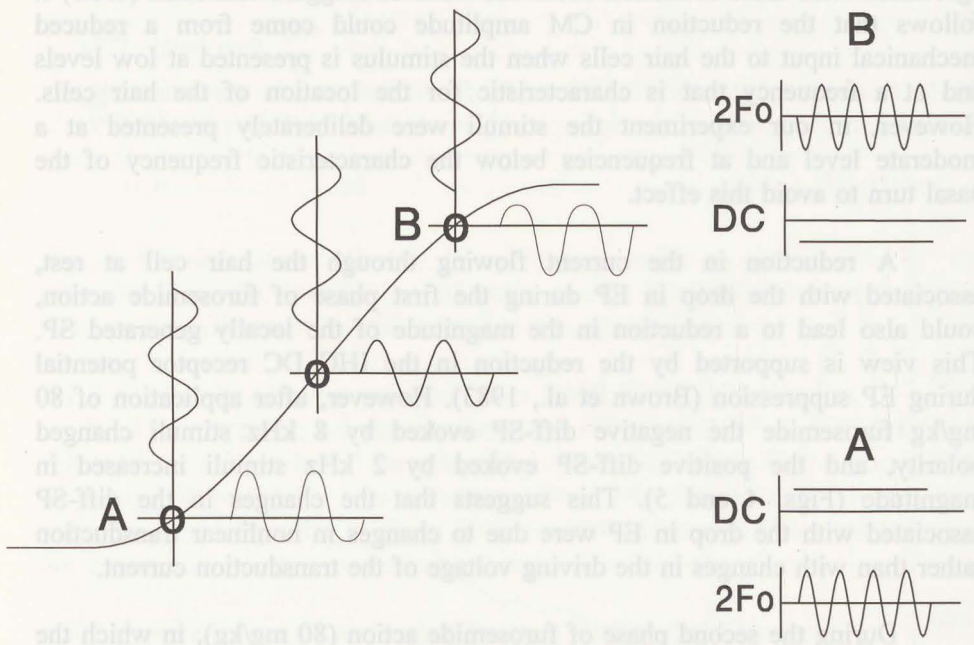


Fig. 11. A symmetrical saturating transduction function ( $f(x) = -f(-x)$ ). The resting or operating point is positioned below, at, or above the point of symmetry. For each operating point the response (horizontal) to a sinusoidal stimulus (vertical) is shown. The dominant even-order components in the responses are shown on the right hand side of the figure.

nents have disappeared from the locally expanded transfer function, and so have the even-order responses. As soon as the operating point passes the point of symmetry the sinusoidal stimulus is rectified in the negative direction (situation B). The even components in the Taylor expansion of the transfer function reappear at this operating point but with reversed polarity, e.g.  $+ a_2x^2$  (situation A) has become  $- a_2x^2$  (situation B). The rectified sine wave now contains both a negative constant term and a  $2F_0$  term whose phase has shifted  $180^\circ$  with respect to the previously generated  $2F_0$  (Fig. 11 B). Thus, a shift in the operating point of a saturating transfer function across the point of symmetry causes a change in polarity of both the constant term and the  $2F_0$  term it produces. The experimentally observed lower phase shift of  $120^\circ$  rather than  $180^\circ$  for  $2F_0$  may be expected when one takes into account that the measured  $2F_0$  represents the output of a number of generators.

The nonlinearity responsible for the change in the SP and  $2F_0$  during the second phase of furosemide action can possibly be associated with the apical mechano-electrical transduction conductance. Although asymmetrical, the sigmoidal Boltzmann function describing apical transduction possesses a point at which it could be considered to operate symmetrically (Kros et al., 1992), such that a shift in the operating point of the apical transducer across the point of local symmetry would cause a zero-crossing of the diff-SP and the  $2F_0$ . A Boltzmann function also applies to the basolateral conductances but they are too slow to be involved in the generation of the  $2F_0$  component of the response to the 2-kHz stimulus (Kros and Crawford, 1990; Housley and Ashmore, 1992).

A comparison between the behaviour of the electrical even-order products and that of an even-order DPOAE, after furosemide application, indicates that a shift in the operating point of the apical transducer also occurs during the first phase of furosemide action. After injecting 80 mg/kg furosemide, Mills et al. (1993) studied the phase and amplitude of the DPOAE difference tone ( $F_1=6.8$  and  $f_2=8.0$  kHz;  $L_1=55$  and  $L_2=45$  dB SPL), which also is an even-order distortion product. Because the difference tone and the 8-kHz diff-SP are probably generated at about the same stretch of basilar membrane we may compare these even-order responses. During the first phase of furosemide action the 8-kHz diff-SP rapidly changes sign from negative to positive (Fig. 4). Within this interval Mills and co-authors observed a sharp dip in amplitude of the difference tone. After the sharp dip in amplitude, the phase of the difference tone had shifted by about  $130^\circ$  (inferred from Fig. 3, Mills et al., 1993). As explained before, these changes in amplitude and phase could result from a shift in the operating point of the apical transducer from one side to the other side of the point of local symmetry.

Some 30 min later, during the second phase of furosemide action, we

noticed that the 8-kHz diff-SP regained its original negative polarity (Fig. 4). At about the same time, the amplitude of the difference tone reached a second minimum and the phase shifted about  $160^\circ$  (inferred from Fig. 3, Mills et al., 1993). This change could result from a shift in the operating point of the apical transducer back to the original side of the point of local symmetry.

Thus, shifts in the operating point of the apical transducer could account for the change in the diff-SP, the change in  $2F_0$ , and the change in the difference tone as measured by Mills et al. (1993) during the first and second phase of furosemide action. The nonlinearities responsible for DPOAE generation are generally assumed to reside in the OHCs (Probst et al., 1991). The similarity between DPOAE behaviour, and SP and  $2F_0$  behaviour suggests that the nonlinearity responsible for the changes in the electrical even-order responses also resides in the OHC. It seems, therefore, that the nonlinear apical conductance describing the changes in the electrical even-order responses during reversible EP suppression belongs to the OHC.

Although we might have determined the identity and location of the nonlinearity we did not yet discuss the relation between EP and the electrical even-order responses in terms of this nonlinearity. During the first phase of the response to 80-mg/kg furosemide the SP seems to be directly determined by the value of the EP (Figs. 1 & 4, 5 and 8 & 10). This can be expected from what is known about cochlear electrophysiology. The drop in EP hyperpolarizes the hair cell (Brown et al., 1983). For the OHC it has been reported that negative current injection, which also hyperpolarizes the cell, causes an increase in the apical transducer conductance (Russell and Kössl, 1991). A shift in the operating point of the apical transducer, associated with an increase in its conductance, could account for the change in polarity of the DC receptor potential. For example, if this increase in conductance shifts the operating point across the point of local symmetry of the Boltzmann function then the DC receptor potential inside the cell should change sign from positive to negative (Fig. 11). Extracellularly, the increase in apical conductance should change the polarity of the SP from negative to positive (Figs. 4 and 10).

During the second phase of the response to 80-mg/kg furosemide there is no simple unequivocal relationship between the value of the EP and the polarity and magnitude of the diff-SP. At 30 min the SP assumed its initial value while the EP value was still below normal (Figs. 1 and 4). Later, while the EP moved steadily toward its original value, the SP could reach abnormally high values. Therefore, we conclude that an additional process caused a shift in the operating point of the apical transducer. This process must cause a decrease in the apical resting conductance.

A shift in the operating point of the apical transducer induced by the

substantial increase in endolymphatic  $\text{Ca}^{++}$  concentration after injecting 80 mg/kg furosemide (Ikeda et al., 1987; Crawford, et al., 1991) can probably be dismissed as the origin of the large SP excursion. After administration of 30 mg/kg furosemide, a dosage that caused a nonsignificant increase in endolymphatic  $\text{Ca}^{++}$  concentration (Ikeda et al., 1987), the SP still showed a large excursion not unequivocally related to the EP (Figs. 8 and 10). The decrease in apical resting conductance might be due to the temporary imbalance in transport of cations in SM during EP recovery (Bosher, 1980). The imbalance in ion transport is possibly accompanied by a net flux of  $\text{H}_2\text{O}$  into the SM resulting in an increase of the pressure (a situation resembling endolymphatic hydrops (Van Benthem et al., 1994)). The increase in pressure could lead to a decrease in the OHC's apical conductance through a displacement of the basilar membrane and a subsequent deflection of the stereociliar bundle.

In conclusion, the magnitude and polarity of the diff-SP are sensitive to what appears to be the operating point of the transducer channel in the apical membrane of the OHC. This sensitivity implies that in the normal situation the SP is primarily generated by this nonlinear apical conductance. However, this conclusion is limited to certain frequency-place combinations. When the basal turn is stimulated with sound at its high, characteristic frequency then the OHCs do not produce DC potentials, while IHCs produce large positive DC potentials (Russell et al., 1986). In that case we may assume that elements in the basal turn IHCs, among which the apical nonlinear conductance, are responsible for high-frequency SP generation.

## References

- Aran, J.-M. and Charlet de Sauvage, R. (1977) Evolution of CM, SP and AP during etacrynic acid intoxication in the guinea pig. *Acta Otolaryngol.* (Stockh.) 83, 153-159.
- Bosher, S.K. (1980) The nature of the ototoxic actions of ethacrynic acid upon the mammalian endolymph system. *Acta Otolaryngol.* 89, 407-418.
- Brown, M.C., Nuttall, A.L., Masta, R.I. and Lawrence, M. (1983) Cochlear inner hair cells: Effects of transient asphyxia on intracellular potentials. *Hear. Res.* 9, 131-144.
- Corey, D.P. and Hudspeth, A.J. (1983) Kinetics of the receptor current in bullfrog saccular hair cells. *J. Neurosci.* 3, 962-976.
- Crawford, A.C., Evans, M.G. and Fettiplace, R. (1991) The actions of calcium on the mechano-electrical transducer current of turtle hair cells. *J. Physiol.* 434, 369-398.
- Dallos, P., Schoeny, Z.G. and Cheatham, M.A. (1972) Cochlear summing potentials. Descriptive aspects. *Acta Otolaryngologica Suppl.* 302, 5-46.
- Dallos, P. and Cheatham M.A. (1990) Effects of electrical polarization on inner hair cell receptor potentials. *J. Acoust. Soc. Am.* 87, 1636-1647.
- Housley, G.D. and Ashmore, J.F. (1992) Ionic currents of outer hair cells isolated from the guinea-pig cochlea. *J. Physiol.* 448, 73-98.
- Ikeda, K., Kusakari, J., Takasaka, T. and Saito, Y. (1987) The  $Ca^{2+}$  activity of cochlear endolymph of the guinea pig and the effect of inhibitors. *Hear. Res.* 26, 117-125.
- Kros, C.J. and Crawford, A.C. (1990) Potassium currents in inner hair cells isolated from the guinea-pig cochlea. *J. Physiol.* 421, 263-291.
- Kros, C.J., Rüsçh, A. and Richardson, G.P. (1992) Mechano-electrical transducer currents in hair cells of the cultured neonatal mouse cochlea. *Proc. R. Soc. Lond. B* 249, 185-193.
- Kusakari, J., Ise, I., Comegys, T.H., Thalmann, I. and Thalmann, R. (1978) Effect of ethacrynic acid, furosemide, and ouabain upon the endolymphatic potential and upon high energy phosphates of the stria vascularis. *Laryngoscope* 88, 12-37.
- Mills, D.M., Norton, S.J. and Rubel, E.W. (1993) Vulnerability and adaptation of distortion product otoacoustic emissions to endocochlear potential variation.

- J. Acoust. Soc. Am. 94, 2108-2122.
- Probst, R., Lonsbury-Martin, B.L. and Martin, G.K. (1991) A review of otoacoustic emissions. *J. Acoust. Soc. Am.* 89, 2027-2067.
- Ruggero, M.A. and Rich, N.C. (1991) Furosemide alters organ of Corti mechanics: evidence for feedback of outer hair cells upon the basilar membrane. *J. Neurosci.* 11, 1057-1067.
- Russell, I.J. and Sellick, P.M. (1978) Intracellular studies of hair cells in the mammalian cochlea. *J. Physiol.* 284, 261-290.
- Russell, I.J. (1983) Origin of the receptor potential in inner hair cells of the mammalian cochlea-evidence for Davis' theory. *Nature* 301, 334-336.
- Russell, I.J., Cody, A.R. and Richardson, G.P. (1986) The responses of inner and outer hair cells in the basal turn of the guinea-pig cochlea and in the mouse cochlea grown in vitro. *Hear. Res.* 22, 199-216.
- Russell, I.J. and Kössl, M. (1991) The voltage responses of hair cells in the basal turn of the guinea pig cochlea. *J. Physiol.* 435, 493-511.
- Sewell, W.F. (1984) The effects of furosemide on the endocochlear potential and auditory-nerve fiber tuning curves in cats. *Hear. Res.* 14, 305-314.
- Syka, J. and Melichar, I. (1985) The effect of loop diuretics upon summing potentials in the guinea pig. *Hear. Res.* 20, 267-273.
- Tasaki, I., Davis, H. and Legoux, J.P. (1952) The space-time pattern of the cochlear microphonics (guinea pig), as recorded by differential electrodes. *J. Acoust. Soc. Am.* 24, 502-518.
- Tonndorf, J. (1958b) Localization of aural harmonics along the basilar membrane of guinea pigs. *J. Acoust. Soc. Am.* 30, 938-943.
- Van Emst, M.G., Klis, S.F.L. and Smoorenburg, G. F. (1995) Tetraethylammonium effects on cochlear potentials in the guinea pig. *Hear. Res.* 88, 27-35.
- Van Emst, M.G., Klis, S.F.L. and Smoorenburg, G. F. (1996) 4-Aminopyridine effects on summing potentials in the guinea pig. *Hear. Res.*, In Print.
- Van Benthem, P.P.G., Klis, S.F.L., Albers, F.W.J., de Wildt, D.J., Veldman, J.E., Huizing, E.H. and Smoorenburg, G.F. (1994) The effect of nimodipine on cochlear potentials and  $\text{Na}^+/\text{K}^+$ -ATPase activity in normal and hydropic cochleas of the albino guinea pig. *Hear. Res.* 77, 9-18.

## Chapter 5

### Generation of DC receptor potentials in a computational model of the organ of Corti with voltage-dependent $K^+$ channels in the basolateral membrane of inner hair cells

Maarten G. van Emst, Christian Giguère and Guido F. Smoorenburg

#### Abstract

A computational model of the organ of Corti is described to assist in the interpretation of electrophysiological data concerning the role of the  $K^+$  channels in the basolateral membrane of cochlear hair cells. Recent *in vivo* data from van Emst et al. (Hear. Res. 88, 27-35 (1995); Hear. Res. in print (1996)) obtained through selective blocking of  $K^+$  channels indicate that they affect the magnitude of the summing potential (SP). In order to understand the nature of this effect, the model of Dallos (Hear. Res. 14, 281-291 (1984)) was extended to account for the voltage and time-dependent properties of the  $K^+$  channels in the basolateral membrane of the inner hair cell (IHC) (Kros and Crawford, J. Physiol. 421, 262-291 (1990)). The model simulations show that the  $K^+$  channels produce a shift of the mean IHC basolateral conductance in the presence of high-frequency stimuli. As a result, cochlear transduction moves to a different electrical operating state and this is the source of a marked adaptation in the stimulus-evoked DC response of the IHC. Extracellularly, in contrast, the shift to a different electrical operating state increases the magnitude of the DC response. Thus,  $K^+$  channels modify the high-frequency DC response. At low frequencies, the  $K^+$  channels also respond to the stimulus waveform on a cycle-by-cycle basis. The waveform distortion associated with this dynamic impedance produces a further decrease in the intracellular stimulus-evoked DC response of the IHC. Thus,  $K^+$  channels appear directly involved in the generation of the low-frequency DC receptor potential.

**Keywords:** DC receptor potential; Summing potential; Nonlinear conductance; Hair cell model



## 1. Introduction

The DC receptor potentials in the cochlea are related to nonlinear elements in the mechano-electrical transduction chain. In particular, the nonlinear conductance associated with the stimulus-controlled transducer channel at the apical pole of cochlear hair cells is considered to play an important part in the generation of the DC receptor potentials (Kros et al., 1992). *In vitro*, nonlinear conductances have also been identified at the basolateral pole of hair cells. These conductances are primarily associated with the voltage-dependent potassium ( $K^+$ ) channels across this part of the cell membrane (Kros and Crawford, 1990). However, it is not clear whether and/or how these nonlinear conductances are involved in the generation of DC potentials. The present paper focuses on this aspect.

In the inner hair cell (IHC), two types of  $K^+$  channels have been characterized *in vitro*; one that can be blocked by tetraethylammonium (TEA) and one that can be blocked by 4-aminopyridine (4-AP) (Kros and Crawford, 1990). The conductance associated with single channels is inherently nonlinear in that a channel is either open or closed. The open probability of channels increases with electrical depolarization of the membrane, i.e. they activate with depolarization. This voltage dependence is nonlinear and is active over a limited range of membrane potentials. The activation process seen when recording from the whole-cell shows a smooth time course because it is based on a number of channels with slightly different open probabilities. The time constant related to the activation of the TEA-sensitive  $K^+$  channels (0.15-0.35 ms) is much smaller than that related to the activation of the 4-AP sensitive  $K^+$  channels (2-10 ms).

In the outer hair cell (OHC), several calcium ( $Ca^{++}$ ) and voltage-dependent  $K^+$  channels (K(Ca)-channels) have been found *in vitro* (Housley and Ashmore, 1992; Mammano et al., 1995). With a fixed concentration of intracellular  $Ca^{++}$  the open probability of K(Ca) channels increases with depolarization of the membrane (Barret et al., 1982). One type can also be blocked by 4-AP. The time constant related to the activation of this channel is 10-20 ms. Another  $Ca^{++}$  and voltage-dependent  $K^+$  channel can be blocked by  $Cs^+$ . This channel reacts even slower to transmembrane voltage changes.

The *in vitro* experiments referred to above provide valuable information about the nonlinear properties of  $K^+$  channels, but do not specifically address their role *in vivo*. A type of *in vivo* experiment that has been carried out to shed some light on this problem uses electrical biasing (Nuttall, 1985; Russell et al., 1986; Dallos and Cheatham, 1990). Dallos and Cheatham injected constant current into the IHC which, through changes in the transmembrane potential, was assumed to affect the state of the voltage-dependent  $K^+$

channels. Hyperpolarizing current enlarged the AC receptor potential, and conversely, depolarizing current reduced it. This could be explained by changes in the driving force for  $K^+$  ions in combination with the effect of changes in transmembrane potential on the number of  $K^+$  channels conducting current, i.e. on the gross resistance and filtering properties of the basolateral membrane. In other words, the  $K^+$  channels appeared to modify the size of the AC receptor potentials, but without being necessarily involved in their generation. However, in these experiments current injection affected the DC component of the IHC receptor potential to a larger extent than the AC component, especially for stimuli below 600 Hz. This suggested direct involvement of the dynamics of a voltage or current-sensitive basolateral nonlinearity in shaping the receptor potential waveform.

In our own *in vivo* experiments we tried to find out whether basolateral voltage-dependent  $K^+$  channels rectify the sound induced AC signal (Van Emst et al., 1995, 1996). We perfused the perilymphatic spaces of the guinea pig's cochlea with the  $K^+$  channel blocker TEA and with 4-AP. Subsequently, we measured the extracellular DC receptor potential, which is called the summing potential (SP), in the basal turn of the cochlea. Since the basal turn SP consists of contributions from both the IHCs and the OHCs, and since each type of hair cell dominates the extracellular response at certain frequencies, we were able to relate the changes in SP to the effects of the blockers specifically on the IHC or OHC. We concluded that blocking the TEA and the 4-AP sensitive  $K^+$  channel in the IHC reduced the SP magnitude at high frequencies (8-12 kHz sound). Since OHCs probably dominate SP generation at low stimulus frequencies (< 4kHz) (Cheatham and Dallos, 1994), we assumed that a possible effect of these channels on low-frequency receptor potentials in the IHC would not be visible in the extracellular SP. Blocking the 4-AP sensitive  $K^+$  channel in the OHC seemed to be responsible for the increase in SP magnitude, found predominantly at the lowest stimulus frequency used (2 kHz).

The experiments described above all indicate that  $K^+$  channels may be involved in modifying and/or generating DC receptor potentials. However, the interpretation of the data from our *in vivo* experiments is complicated because comparisons are made between situations in which  $K^+$  channels are normally operating and situations in which  $K^+$  channels are affected. Affecting the  $K^+$  channels could also affect other aspects of hair cell physiology. For example, the use of either current injection or chemical blockers will affect the resistance of the basolateral membrane at rest. Thus, the hair cell will start already from a different electrical operating point when the stimulus is presented.

An alternative approach to studying the role of  $K^+$  channels in generating DC receptor potentials is via mathematical modelling of the organ of Corti. A first attempt was made by McMullen and Mountain (1985) who studied the responses of a hair cell circuit model which included voltage-dependent basolateral membrane conductances. These conductances generated a DC component in both the intracellular and extracellular voltage response. However, their use of a 880 mV battery in the hair cell was unrealistic. Zeddies and Siegel (1995) developed a physiologically-based model of a single IHC. They incorporated the characteristics of the fast TEA-sensitive  $K^+$  channel and the slow 4-AP sensitive  $K^+$  channel characterised by Kros and Crawford (1990). Delivering sinusoidal stimuli through the nonlinear apical transducer channel produced depolarizing intracellular DC receptor potentials. Direct injection of sinusoidal current into the cell, bypassing the apical stimulus-controlled conductance, produced hyperpolarizing intracellular DC voltage responses. The latter finding suggests that the basolateral  $K^+$  channels, with their nonlinear properties, generate DC receptor potentials.

In this paper, we explore the role of hair cell basolateral conductance nonlinearities in determining the size of the intracellular and extracellular cochlear potentials, especially the DC potential, via a computational model of a segment of the organ of Corti. For this purpose, the circuit model of Dallos (1983, 1984) was extended to incorporate the voltage and time-dependent characteristics of  $K^+$  channels in the basolateral membrane of the IHC (Kros and Crawford, 1990), and the model was adapted to the situation in the basal turn of the cochlea. Specifically, we are seeking to study (1) the influence of the basolateral conductance on the distribution of the potentials in the organ of Corti when there is no acoustic stimulation, (2) the effects of blocking the fast TEA-sensitive and slow 4-AP sensitive  $K^+$  channels in the IHC on the extracellular stimulus-evoked potentials, and (3) whether these basolateral channels could be a source of DC receptor potentials.

## 2. The Model

### 2.1. Electrical circuit representation

A model for the generation of potentials by the organ of Corti is developed in this section. The starting point for this model is the equivalent circuit of Dallos (1983, 1984) given for a radial cross-section of the cochlea. The main advantage of this type of model is that the identity of the circuit elements and sources is firmly based on the electroanatomy of the cochlea. The IHCs, the OHCs, and the stria vascularis complex are represented as separate entities, thus allowing to simulate the main intracellular and extracellular potentials of interest in the organ of Corti.

In the original formulation of the model (Dallos, 1983, 1984), the apical membrane resistance of the hair cells changed in direct proportion to the mechanical stimulation. The basolateral membrane resistance of the hair cells was held constant. The main modifications in this study are to account for the saturation of the transducer channels with increasing level at the apical pole of the hair cells, and to replace the constant resistance at the basolateral pole of the IHCs by a voltage and time-dependent conductance.

The resulting circuit is shown in Fig. 1. Each hair cell is represented by apical and basolateral membrane impedances, and by an electrochemical battery  $E_1$  associated with the Nernst potential across the basolateral membrane arising from the different ionic compositions of the cytoplasm and perilymph. In this study it is assumed that hair cell currents are mainly carried by  $K^+$  ions, so  $E_1$  corresponds to the reversal potential for  $K^+$  ions. Moreover, battery  $E_1$  is taken to be identical for IHCs and OHCs. The apical hair cell membrane impedance is represented by the parallel combination of variable resistance  $R_a(t)$  and constant capacitance  $C_a$ . Likewise, the basolateral hair cell membrane impedance is represented by the parallel combination of variable resistance  $R_b(t)$  and constant capacitance  $C_b$ .

The model of Fig.1 is completed by an equivalent circuit for the effects of the extracellular components on a radial cross-section of the cochlea (Dallos, 1983). Element  $R_3$  is the Thevenin resistance between the organ of Corti (OC) and the body ground. Elements  $E_T$  and  $R_T$  are the Thevenin equivalent circuit for the stria vascularis source and the various resistive pathways between the scala media (SM) and the body ground. A shunt capacitive element  $C_T$  was added in this study to account for the ionic barriers associated with the SM-ground pathway, and the lowpass filtering of the AC component observed in the experimental data for SM recordings. According to Dallos (1984), ionic barriers are unlikely for the OC-ground pathway, and thus no capacitance is used in conjunction with  $R_3$ .

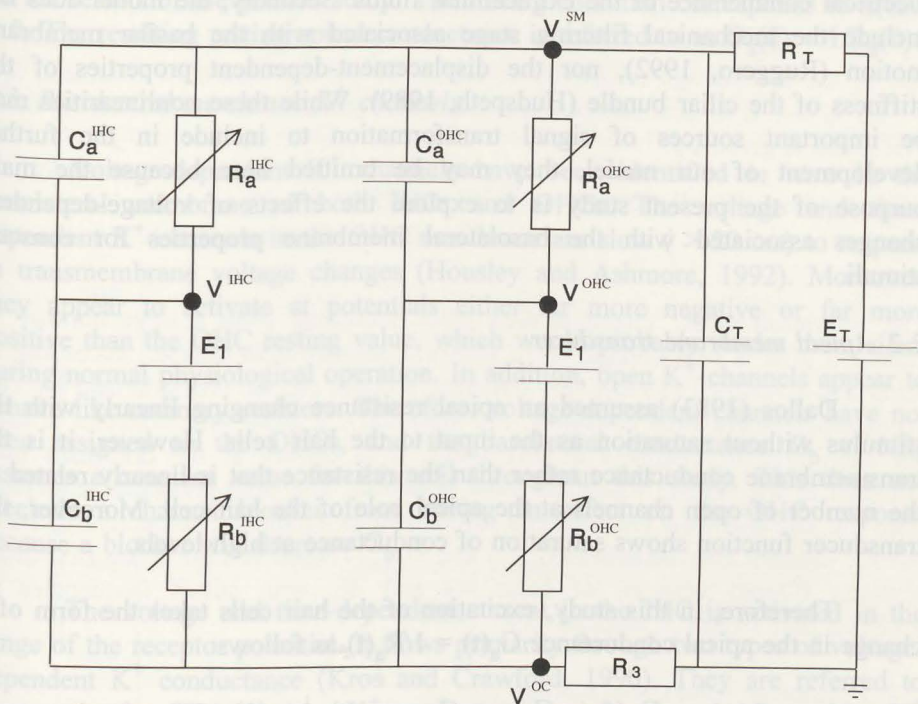


Figure 1. Electrical circuit representation of the organ of Corti model (adapted from Dallos (1984)). Arrows indicate variable elements.

The electrical circuit allows to access several intracellular and extracellular potentials of interest. These are represented by  $V^{IHC}(t)$  and  $V^{OHC}(t)$  for the IHC and OHC receptor potentials, respectively, and by  $V^{SM}(t)$  and  $V^{OC}(t)$  for the scala media and organ of Corti potentials, respectively. The scala vestibuli and scala tympani potentials are not explicitly represented in the circuit. To a first approximation, they are linearly related to  $V^{SM}(t)$  and  $V^{OC}(t)$ , respectively.

The model contains a number of simplifying assumptions. Firstly, it is a model of a single cross-section through the organ of Corti, i.e. it does not formally simulate the electrical coupling across adjacent sections of the cochlea. Fortunately, this does not seem to be a very serious constraint for the simulation of the intracellular potentials, owing to the much larger hair cell impedances compared to the extracellular components, which effectively decouples neighbouring hair cells (Dallos, 1983). However, the validity of the model for the simulation of extracellular potentials is limited to stimulus frequencies around the characteristic frequency at the cochlear place corresponding to the cross-section being simulated, owing to the relatively high

electrical conductance of the extracellular fluids. Secondly, the model does not include the mechanical filtering stage associated with the basilar membrane motion (Ruggero, 1992), nor the displacement-dependent properties of the stiffness of the ciliar bundle (Hudspeth, 1989). While these nonlinearities may be important sources of signal transformation to include in the further development of our model, they may be omitted here because the main purpose of the present study is to explore the effects of voltage-dependent changes associated with the basolateral membrane properties for constant stimuli.

## 2.2. Apical membrane transducer

Dallos (1983) assumed an apical resistance changing linearly with the stimulus without saturation as the input to the hair cells. However, it is the transmembrane conductance rather than the resistance that is linearly related to the number of open channels at the apical pole of the hair cell. Moreover, the transducer function shows saturation of conductance at high levels.

Therefore, in this study, excitation of the hair cells takes the form of a change in the apical conductance  $G_a(t) = 1/R_a(t)$  as follows:

$$G_a(t) = G_{leak} + G_{max} p_o(t) \quad (1)$$

where  $G_{leak}$  is the constant leakage conductance through the cell membrane (Kros and Crawford, 1990),  $G_{max}$  is the maximum conductance of the transducer channels, and  $p_o(t)$  is the probability of transducer channels of being open as a function of time. We had to assign a leakage conductance to the apical membrane in order to limit the maximum modulation of the apical conductance  $G_a(t)$ , or equivalently the maximum AC receptor potential, within the physiological range. From the work of Crawford et al. (1991) and Kros et al. (1992), the open channel probability  $p_o(t)$  is chosen as a second-order Boltzmann relation:

$$p_o(t) = \frac{1}{1 + e^{(x_2 - x(t))} (1 + e^{(x_1 - ax(t))})} \quad (2)$$

where  $x_1$ ,  $x_2$  and  $a$  are scalar constants<sup>1</sup>, and  $x(t)$  is the instantaneous ciliar bundle disturbance in response to external acoustic stimulation. In this study,  $x(t)$  acts directly as the input to the model, and is assumed identical for IHC and OHCs. We did not include a differentiation in the input to IHCs to account for their velocity dependence at low-frequency stimulation (Dallos et al., 1982). The phase difference between the IHC low-frequency response and the OHC low-frequency response may be neglected here because it does not bear

on the results of the present study. The resting condition corresponds to  $x(t \leq 0) = 0$ . The resulting resting apical conductance is referred to as  $G_a(0) = 1/R_a(0)$ .

### 2.3. Basolateral membrane $K^+$ channels

Voltage-dependent  $K^+$  channels have been identified *in vitro* in the basolateral membrane of both IHCs and OHCs. The voltage and time-dependent  $K^+$  channels in the OHC membrane are slow ( $> 20$  ms) to respond to transmembrane voltage changes (Housley and Ashmore, 1992). Moreover, they appear to activate at potentials either far more negative or far more positive than the OHC resting value, which would probably render them silent during normal physiological operation. In addition, open  $K^+$  channels appear to behave like ordinary resistors. Therefore, voltage-dependent channels have not been assigned to the OHCs, and the basolateral conductance  $G_b = 1/R_b$  assumes a constant value for this cell throughout this study. This does not preclude a channel blocker from having an effect on the OHC response because a blocker will decrease  $G_b$ .

The voltage and time-dependent current in the IHC is activated in the range of the receptor potential. It flows primarily through two types of voltage-dependent  $K^+$  conductance (Kros and Crawford, 1990). They are referred to here as the fast TEA-sensitive  $K^+$  conductance and the slow 4-AP-sensitive  $K^+$  conductance. The fast channels have an activation time course typically about 5-20 times shorter than the slow channels, and a maximum conductance approximately 2-3 times larger than the slow channels. In this study, we assumed that the total IHC basolateral conductance  $G_b(t) = 1/R_b(t)$  is made up of contributions from these two types of channels, i.e.:

$$G_b(t) = G_{fast}(t) + G_{slow}(t) \quad (3)$$

where  $G_{fast}(t)$  and  $G_{slow}(t)$  are the conductances associated with the fast and slow channels, respectively. From the work of Kros and Crawford (1990), a first-order Boltzmann function is used to characterize the voltage-dependence of the fast and slow channel conductances as follows:

$$G_{fast}(t) = \frac{G_f}{1 + e^{(V_f - V^{tm}(t)) / S_f}} \quad (4a)$$

$$G_{slow}(t) = \frac{G_s}{1 + e^{(V_s - V^{tm}(t)) / S_s}} \quad (4b)$$

where  $G_f$  and  $G_s$  are the maximum conductances of the fast and slow channels,  $V_f$  and  $V_s$  are the half-activation setpoints of the fast and slow channels,  $S_f$  and  $S_s$  are the voltage sensitivity constants of the fast and slow channels, and  $V^{tm}(t)$  is the IHC basolateral transmembrane potential as a function of time. The latter is given by:

$$V^{tm}(t) = V^{IHC}(t) - V^{OC}(t) \quad (5)$$

The activation of  $K^+$  channels seen when recording from a large number of channels after a step voltage drive shows a smooth time course. According to Kros and Crawford (1990), this dynamic process can be characterized by two voltage-dependent time constants. For simplicity, a fixed time constant is used for each type of channels in this study. It is chosen as the dominant time constant at the resting transmembrane potential. The time constants associated with the fast and slow channels are referred to as  $T_f$  and  $T_s$ , respectively. Thus, the  $K^+$  channel conductances  $G_{fast}(t)$  and  $G_{slow}(t)$  used in Eqn. 3 are first-order lowpass filtered versions of Eqns. 4a and 4b, with cutoff frequencies of  $1/(2\pi T_f)$  and  $1/(2\pi T_s)$ , respectively.

#### 2.4. Parameter values and scaling

The model parameter values are listed in Table I. They were selected to model a radial cross-section of the organ of Corti in the basal turn of the guinea pig's cochlea. The parameter values ( $x_1$ ,  $x_2$ ,  $a$ )<sup>1</sup> describing the shape of the apical transducer function, Eqn. 2, of the IHC and OHCs, and those for the shape and time constant of the voltage-dependent IHC basolateral conductances ( $V_f$ ,  $S_f$ ,  $T_f$ ,  $V_s$ ,  $S_s$ ,  $T_s$ ) are based on Kros et al. (1992) and Kros and Crawford (1990), respectively. The values for the extracellular elements, the resting element values at the apical and basolateral poles of the hair cells, and the overall scaling of the model are from Dallos (1983, 1984).

In the isolated IHC and OHC preparations the apical transducer channel operated at a point at which the rate of change in sensitivity was near its maximum, i.e. the point at which the second derivative of the Boltzmann relation (Eqn. 2) reaches its maximum (Kros et al., 1992). At this point the Boltzmann relation would produce a large DC potential which agrees with the presence of a large positive DC potential in basal turn IHCs during high-frequency stimulation (Cody and Russell, 1987). Therefore, in our model the IHC's apical transducer is chosen to operate at this point. This point corresponds to a channel's probability of being open of 9.2% (Fig. 2). Noticeably, basal turn OHCs do not generate DC potentials during high-frequency stimulation (Cody and Russell, 1987). This implies that the apical transducer channel of the *in-vivo* OHC does not operate at the point at which



the rate of change of sensitivity is at its maximum, but closer to the point of maximum sensitivity. Therefore, the OHC's apical transducer is chosen to operate at the point at which the slope of the Boltzmann relation is steepest. This corresponds to a channel's probability of being open of 27.3% (Fig. 2), and is expected to generate essentially symmetrical receptor potentials upon stimulation. As a consequence of this choice of parameters, the IHCs are expected to dominate the extracellular DC potential, i.e. the SP, and the OHCs the extracellular AC potential, i.e. the CM.

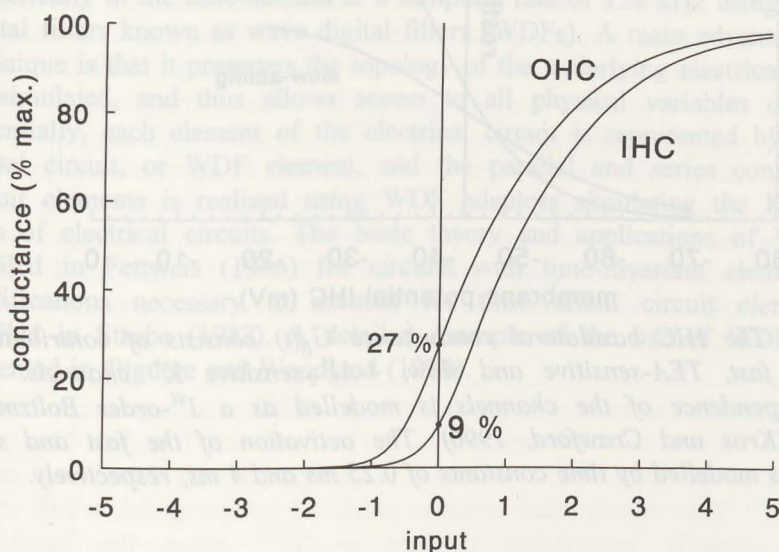


Figure 2. The apical stimulus-controlled transducer conductance is modelled as a 2<sup>nd</sup>-order Boltzmann function (Kros et al., 1992). The operating points of the hair cell transducer functions are set such that the IHC and OHCs dominate the extracellular DC and AC responses, respectively. Input in arbitrary units.

The setpoints of voltage-dependent IHC basolateral channels were selected as follows. From the data in Kros and Crawford (1990), the half-activation voltage of the slow channels found *in vitro* is very close to that of the resting potential of the IHCs in the basal turn of the cochlea found *in vivo*, so  $V_s$  is taken as the resting transmembrane potential  $V^{tm}(0)$  in this study. In other words, the slow channel's probability of being open is taken as 50% at rest. The half-activation voltage of the fast channels is typically a few millivolts above the resting potential of the IHCs, so  $V_f$  is set at 5 mV above the transmembrane potential in this study. This corresponds to a fast channel's probability of being open of about 30% at rest (Fig. 3).

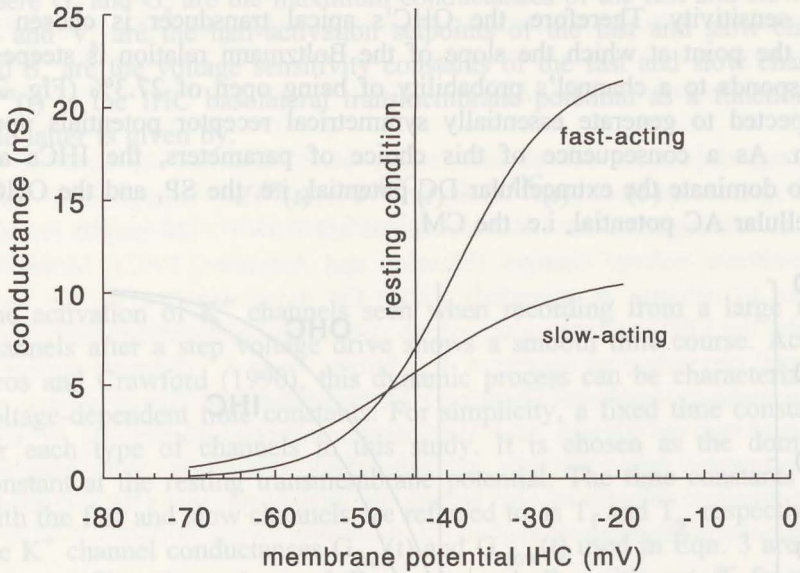


Figure 3. The IHC basolateral conductance  $G_b(t)$  consists of contributions from the fast, TEA-sensitive and slow, 4-AP sensitive  $K^+$  channels. The voltage-dependence of the channels is modelled as a 1<sup>st</sup>-order Boltzmann function (Kros and Crawford, 1990). The activation of the fast and slow channels is modelled by time constants of 0.25 ms and 4 ms, respectively.

The apical  $C_a$  and basolateral  $C_b$  capacitances of the IHC and OHC circuits are held constant in this study. The time constants associated with each of these capacitances and the corresponding membrane resistances at rest are made identical at the apical and basolateral poles of hair cells ( $R_a(0)C_a = R_b(0)C_b = 0.25$  ms), and for both types of cells.

Finally, the values for the IHC and OHC circuit elements in Fig. 1 must be properly scaled to account for the different number of IHCs and OHCs in the cochlea, and for the effective length of electrical interaction between intracellular and extracellular components (Dallos, 1983). Firstly, the OHC apical  $R_a$  and basolateral  $R_b$  resistance values are divided by a factor of 3.8, the ratio  $R$  of OHCs to IHCs in the entire guinea pig's cochlea. Likewise, the OHC apical  $C_a$  and basolateral  $C_b$  capacitance values are multiplied by the same factor. This brings the total impedance of the OHC circuit in proper balance with that of the IHC in one cross-section of the cochlea. Secondly, the extracellular potential arises from the summated response of multiple cross-sections of the cochlea. This is achieved by dividing the apical  $R_a$  and basolateral  $R_b$  resistances of the IHC and OHC circuit by a factor of 100, the estimated number  $N$  of summing cross-sections necessary to reproduce the

correct ratio between the extracellular and intracellular response (Dallos, 1983). The apical  $C_a$  and basolateral  $C_b$  capacitances of both cells are also multiplied by the same factor. This brings the parallel impedance of the IHC and OHC circuits in proper balance with that of the extracellular components.

### 2.5. Numerical implementation

The electrical circuit model of the organ of Corti was simulated numerically in the time-domain at a sampling rate of 128 kHz using a class of digital filters known as wave digital filters (WDFs). A main advantage of this technique is that it preserves the topology of the underlying electrical circuit to be simulated, and thus allows access to all physical variables of interest. Essentially, each element of the electrical circuit is represented by a simple digital circuit, or WDF element, and the parallel and series connection of circuit elements is realized using WDF adaptors simulating the Kirchhoff's laws of electrical circuits. The basic theory and applications of WDFs are detailed in Fettweis (1986) for circuits with time-invariant elements. The modifications necessary to account for time-variant circuit elements are detailed in Strube (1982). A detailed example of the use of WDFs is also presented in Giguère and Woodland (1994).

#### Footnote:

- 1 Constants  $x_1$  and  $x_2$  are numerically equal to  $a_1DV_1$  and  $a_2DV_2$  in Kros et al. (1992), respectively, and input  $x(t)$  is equivalent to  $a_2DV(t)$ . Constant  $a$  is equal to the ratio  $a_1/a_2$ .

### 3. Results and Discussion

#### 3.1. Resting values

The resting potentials predicted by the model in the IHC, OHC, SM and OC for the default parameter values from Table I are:  $V^{\text{IHC}} = -43.6$  mV,  $V^{\text{OHC}} = -59.5$  mV,  $V^{\text{SM}} = +68.6$  mV, and  $V^{\text{OC}} = +0.5$  mV, respectively. These values are consistent with the resting state of the guinea pig's cochlea (Dallos, 1985). Figure 4 shows how these resting potentials are affected by changes in the resting basolateral conductance  $G_b(0)$  of the hair cells from the default model parameters. Increasing basolateral conductance of the IHC (Fig. 4a) or OHC (Fig. 4b) causes the resting potential of the corresponding hair cell to approach the  $K^+$  equilibrium potential  $E_1$  of -80 mV, while decreasing this conductance causes the resting value of the hair cell to approach the potential in SM, i.e. the endocochlear potential (EP). The latter is very close to the potential of the stria vascularis source  $E_T$ , which is 70 mV. Changes in the basolateral conductance of either type of hair cell have a much smaller effect on the potentials outside that cell and virtually do not affect the potential in the other type of hair cell.

In our previous *in vivo* experiments we blocked voltage-dependent  $K^+$  channels in the basolateral membrane of the hair cell and found no changes in the resting potential of SM, i.e. the EP remained constant (Van Emst et al., 1995, 1996). This experimental result is predicted by the model, which shows no experimentally measurable changes in  $V^{\text{SM}}$  when the basolateral conductance is varied over a 3 decade range. Thus, intracellular potentials are much more sensitive to changes in the basolateral conductance of hair cells than extracellular potentials.

Figure 5 shows how the resting potentials are affected by changing the resting conductance  $G_a(0)$  at the apical pole of the hair cells. Increasing apical membrane conductance of the IHC (Fig. 5a) or OHC (Fig. 5b) causes the resting potential of the corresponding hair cell to approach the EP, while decreasing apical membrane conductance causes the resting potential of the hair cell to approach the  $K^+$  equilibrium potential  $E_1$ . The only sizable effect on extracellular potentials is seen in SM when the apical conductance of the OHC is changed; the EP is reduced by a few mV when apical conductance is increased by 1 decade, and enlarged by a few mV when the apical conductance is decreased by the same extent.

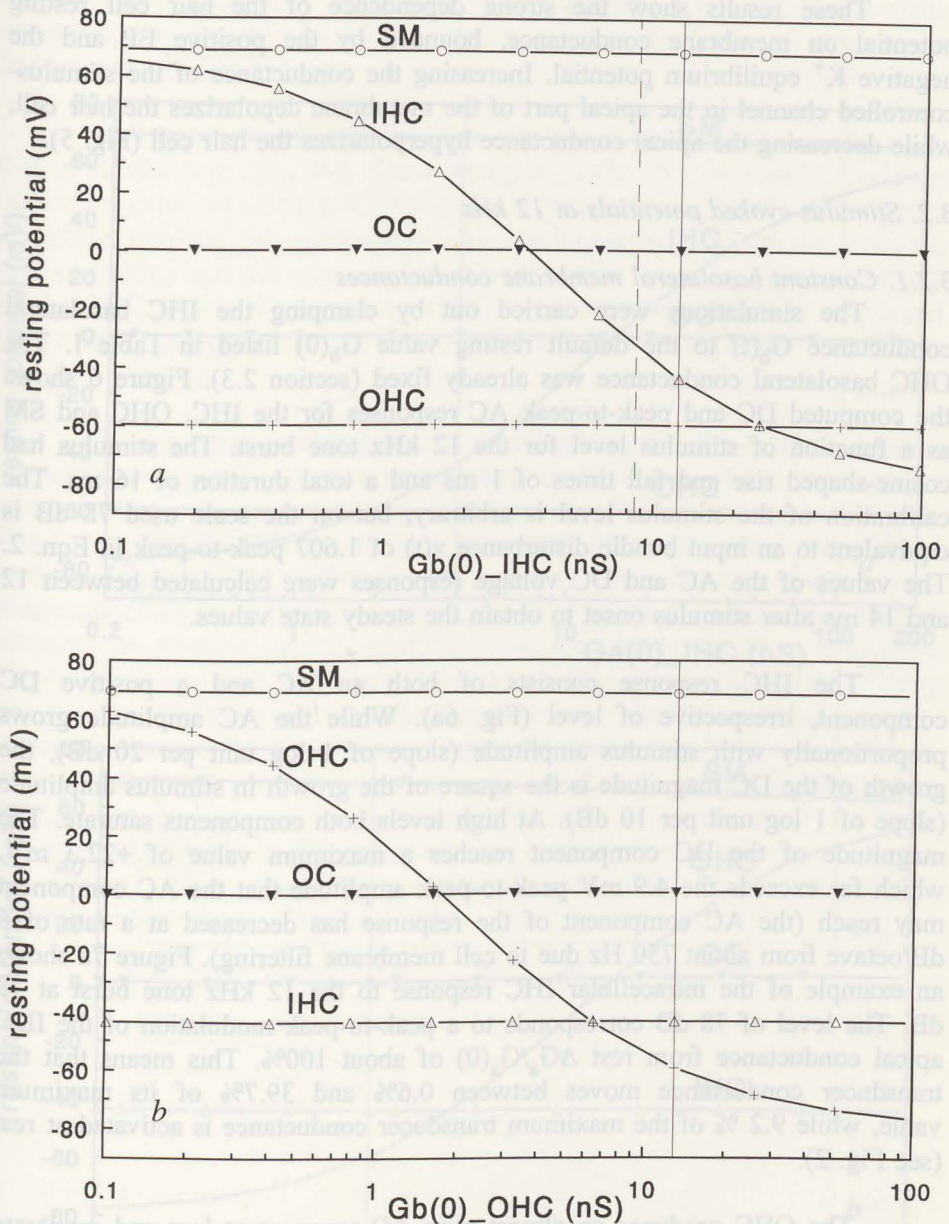


Figure 4. Evolution of the resting potentials in the model for changes in the resting basolateral conductance  $G_b(0)$  of (a) the IHC or (b) the OHC. All other model parameters are from Table I. The resting potentials corresponding to the default model parameters are shown by a thin vertical line. The resting potentials corresponding to the situation in which the fast-acting conductance in the IHC basolateral membrane is blocked are shown by the dashed vertical line.

These results show the strong dependence of the hair cell resting potential on membrane conductance, bounded by the positive EP and the negative  $K^+$  equilibrium potential. Increasing the conductance of the stimulus-controlled channel in the apical part of the membrane depolarizes the hair cell, while decreasing the apical conductance hyperpolarizes the hair cell (Fig. 5).

### 3.2. Stimulus-evoked potentials at 12 kHz

#### 3.2.1. Constant basolateral membrane conductances

The simulations were carried out by clamping the IHC basolateral conductance  $G_b(t)$  to the default resting value  $G_b(0)$  listed in Table I. The OHC basolateral conductance was already fixed (section 2.3). Figure 6 shows the computed DC and peak-to-peak AC responses for the IHC, OHC and SM as a function of stimulus level for the 12 kHz tone burst. The stimulus had cosine-shaped rise and fall times of 1 ms and a total duration of 16 ms. The calibration of the stimulus level is arbitrary, but on the scale used 78 dB is equivalent to an input bundle disturbance  $x(t)$  of 1.607 peak-to-peak in Eqn. 2. The values of the AC and DC voltage responses were calculated between 12 and 14 ms after stimulus onset to obtain the steady state values.

The IHC response consists of both an AC and a positive DC component, irrespective of level (Fig. 6a). While the AC amplitude grows proportionally with stimulus amplitude (slope of 1 log unit per 20 dB), the growth of the DC magnitude is the square of the growth in stimulus amplitude (slope of 1 log unit per 10 dB). At high levels both components saturate. The magnitude of the DC component reaches a maximum value of +22.3 mV, which far exceeds the 4.9 mV peak-to-peak amplitude that the AC component may reach (the AC component of the response has decreased at a rate of 6 dB/octave from about 750 Hz due to cell membrane filtering). Figure 7a shows an example of the intracellular IHC response to the 12 kHz tone burst at 78 dB. The level of 78 dB corresponds to a peak-to-peak modulation of the IHC apical conductance from rest  $\Delta G_a/G_a(0)$  of about 100%. This means that the transducer conductance moves between 0.6% and 39.7% of its maximum value, while 9.2 % of the maximum transducer conductance is activated at rest (see Fig. 2).

The OHC produces an almost pure AC response at low and moderate stimulus levels (Fig. 6b). It is only at high stimulus levels that the OHC starts to produce a substantial positive DC potential. The stimulus-evoked DC potential rises rapidly (slope of 1 log unit per 5 dB) and then saturates. The AC component reaches a maximum peak-to-peak value of 2.7 mV, the DC component a value of +6.5 mV. An example of the intracellular OHC response at 78 dB is shown in Fig. 7b. This response corresponds to a peak-to-peak modulation of the apical conductance from rest  $\Delta G_a/G_a(0)$  of about 200%. This

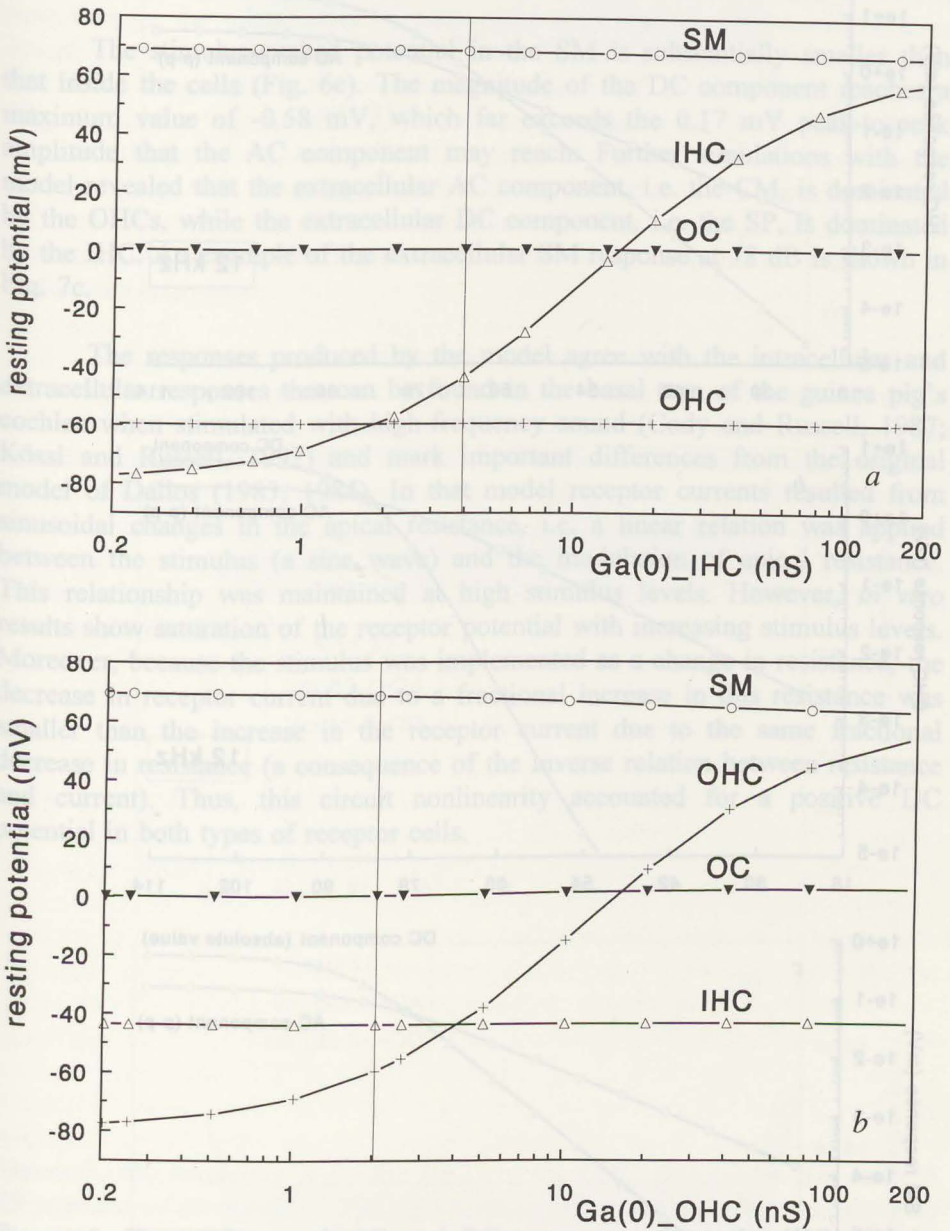
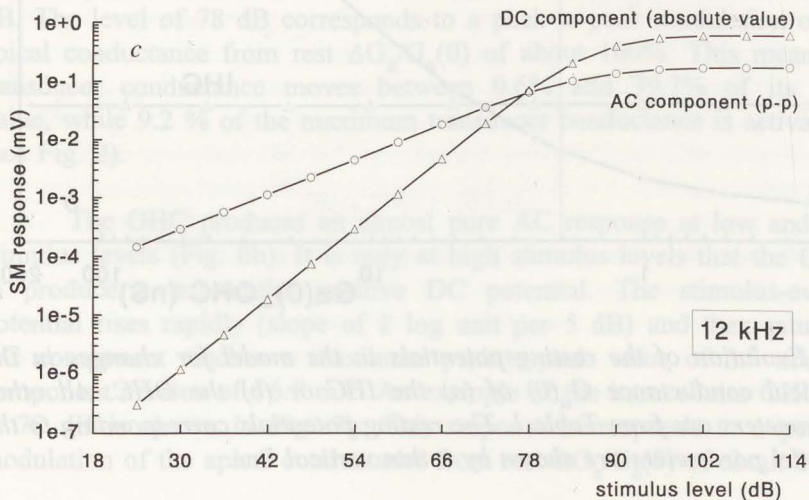
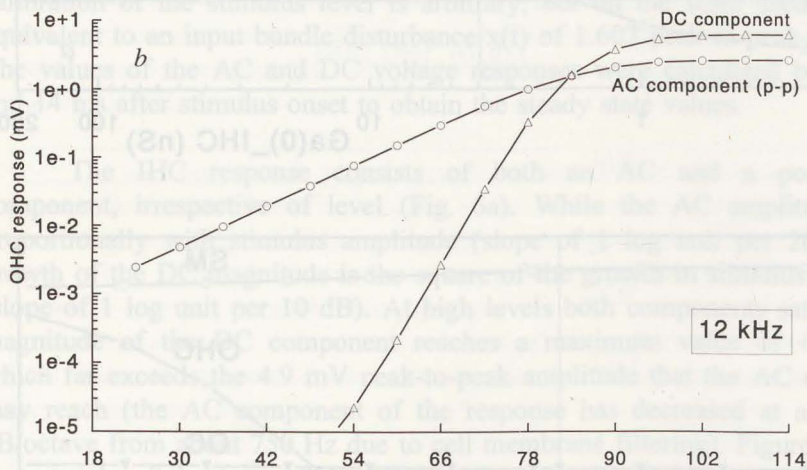
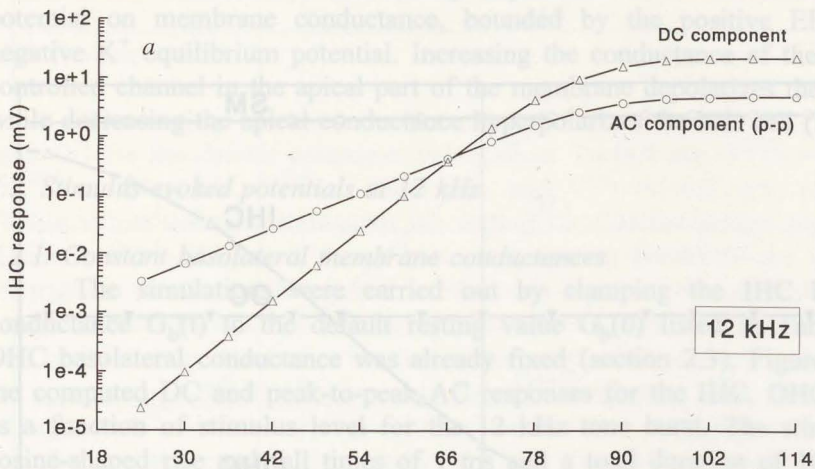


Figure 5. Evolution of the resting potentials in the model for changes in the resting apical conductance  $G_a(0)$  of (a) the IHC or (b) the OHC. All other model parameters are from Table I. The resting potentials corresponding to the default model parameters are shown by a thin vertical line.





means that the transducer conductance moves between 3.5% and 55.9% of its maximum value, while 27.3 % of the maximum transducer conductance is activated at rest (see Fig. 2).

The stimulus-evoked potential in the SM is substantially smaller than that inside the cells (Fig. 6c). The magnitude of the DC component reaches a maximum value of -0.58 mV, which far exceeds the 0.17 mV peak-to-peak amplitude that the AC component may reach. Further simulations with the model revealed that the extracellular AC component, i.e. the CM, is dominated by the OHCs, while the extracellular DC component, i.e. the SP, is dominated by the IHC. An example of the extracellular SM response at 78 dB is shown in Fig. 7c.

The responses produced by the model agree with the intracellular and extracellular responses that can be found in the basal turn of the guinea pig's cochlea when stimulated with high-frequency sound (Cody and Russell, 1987; Kössl and Russell, 1992) and mark important differences from the original model of Dallos (1983, 1984). In that model receptor currents resulted from sinusoidal changes in the apical resistance, i.e. a linear relation was applied between the stimulus (a sine wave) and the modulation of apical resistance. This relationship was maintained at high stimulus levels. However, *in vivo* results show saturation of the receptor potential with increasing stimulus levels. Moreover, because the stimulus was implemented as a change in resistance, the decrease in receptor current due to a fractional increase in this resistance was smaller than the increase in the receptor current due to the same fractional decrease in resistance (a consequence of the inverse relation between resistance and current). Thus, this circuit nonlinearity accounted for a positive DC potential in both types of receptor cells.

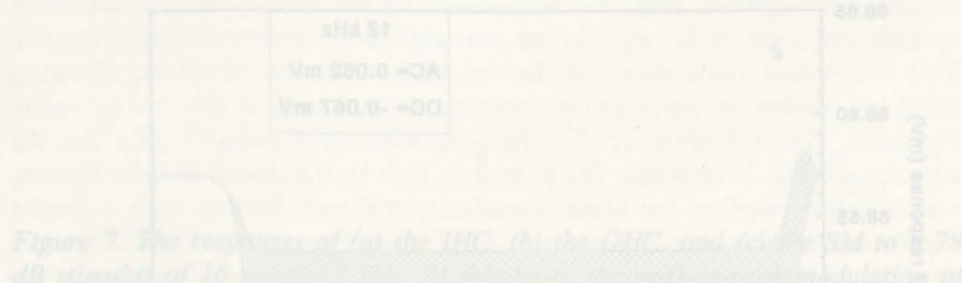
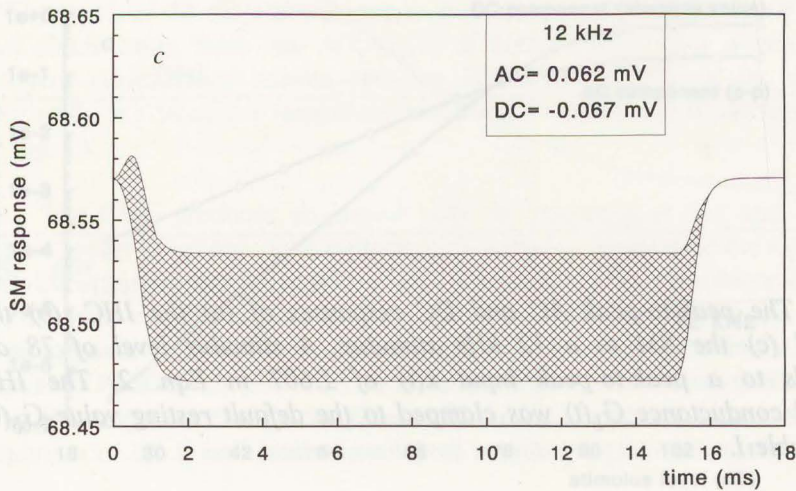
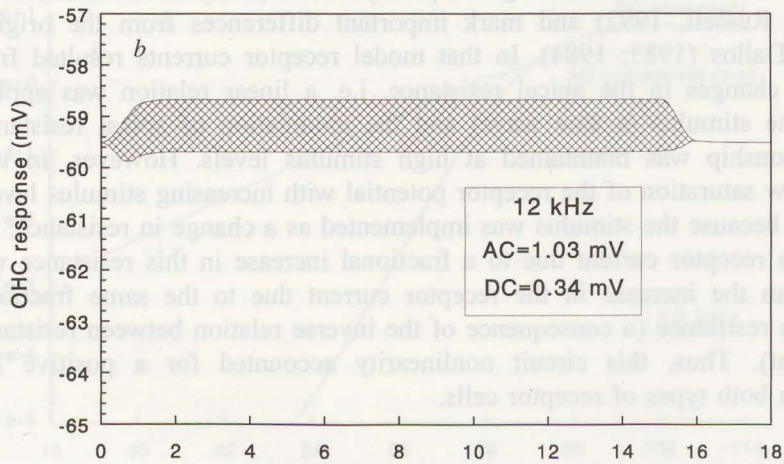
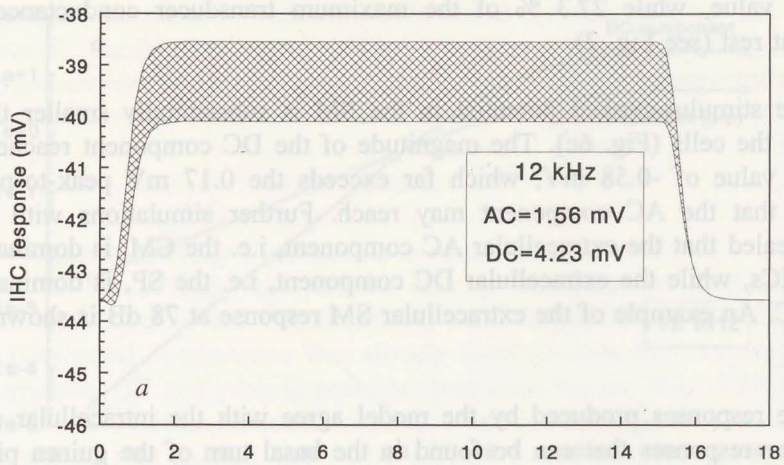


Figure 6. The peak-to-peak AC and DC responses of (a) the IHC, (b) the OHC, and (c) the SM to a 12 kHz stimulus. A stimulus level of 78 dB corresponds to a peak-to-peak input  $x(t)$  of 1.607 in Eqn. 2. The IHC basolateral conductance  $G_b(t)$  was clamped to the default resting value  $G_b(0)$  listed in Table I.



We used the second-order Boltzmann function to relate the stimulus (a sine wave) to the stimulus-induced change in conductance, as described by Kros et al. (1992). The IHC's apical transducer was set to operate in such a way that, in the presence of symmetric input (a sine wave), the increase in apical conductance exceeded the decrease. Consequently, a stimulus-evoked DC flows into the IHC. This results in a negative DC receptor potential in SM (Fig. 7c) and a large positive DC receptor potential in the IHC (Fig. 7a). The rates at which the DC and AC components of the IHC intracellular receptor potential grow with stimulus level are a direct reflection of the stimulus-evoked AC and DC changes in the apical conductance. The saturation of the receptor potential, which occurs at high levels, is due to the "sigmoidal" shape of the Boltzmann transducer.

The OHC's apical transducer was chosen to operate in such a way that, in the presence of symmetric input (a sine wave), the increase in apical conductance equalled the decrease. This results in an almost symmetrical receptor potential at low and moderate levels. However, because this operating point corresponds to a 27.3% probability of being open, i.e. 27.3% of the total conductance is activated at rest, the hyperpolarizing phase of the receptor potential eventually saturates more quickly than the depolarizing phase and, consequently, a positive DC receptor potential arises at moderate to high stimulus levels (Fig. 6b).

Figure 7. The responses of (a) the IHC, (b) the OHC, and (c) the SM to a 78 dB stimulus of 16 ms at 12 kHz. At this level, the peak-to-peak modulation of the IHC and OHC apical conductance from rest is about 100% and 200%, respectively. Only the envelope of the responses is shown for clarity. The inserted boxes give the values of the stimulus-evoked DC and peak-to-peak AC voltages calculated between 12 and 14 ms. The IHC basolateral conductance  $G_b(t)$  was clamped to the default resting value  $G_b(0)$  listed in Table I.

### 3.2.2. Voltage and time-dependent IHC basolateral membrane conductances

The upper curve of Fig. 8a shows the response of the total IHC basolateral conductance  $G_b(t)$  to the 12 kHz stimulus at 78 dB, once the voltage and time-dependent properties of the fast and slow channel are assigned. During the presence of the stimulus there is a general increase of +1.36 nS in the basolateral conductance, with only a very small alternating response. In other words, the operating point of the basolateral conductance moves from the resting position  $G_b(0)=12.32$  nS to a higher value of 13.68 nS, but is unable to respond to the stimulus waveform on a cycle-by-cycle basis. This positive DC shift in basolateral conductance is due to the combined activation of both the fast and slow acting conductances (bottom curves Fig. 8a). With stimulation at 78 dB the former moves from  $G_{fast}(0)=6.75$  nS to  $G_{fast}(12ms)=7.75$  nS and the latter from  $G_{slow}(0)=5.57$  nS to  $G_{slow}(12ms)=5.93$  nS. Fig. 8b shows the corresponding intracellular voltage response of the IHC to the 12 kHz stimulus. Due to the active conductances in the basolateral membrane the DC response of the IHC shows pronounced adaptation and offset hyperpolarization (compare Fig. 7a with Fig. 8b). In contrast, the AC amplitude is hardly affected by the voltage and time-dependence of the basolateral conductance (compare Fig. 7a with Fig. 8b). Fig. 9 shows the stimulus-evoked response in the SM. The magnitude of the negative DC response in SM is larger with active conductances in the IHC basolateral membrane than without (compare Fig. 7c with Fig. 9), in contrast to the changes in the intracellular IHC DC component. The AC component in SM has remained essentially constant.

Figure 8 reveals that at high stimulus frequencies the interaction between the receptor potential and the basolateral conductance occurs in the domain of the DC responses. As described in section 3.2.1., the apical transducer in the IHC causes a large positive DC potential to arise at the moment the stimulus starts (Fig. 7a). Consequently, both fast and slow conductances activate (Fig. 8a) and a shift of the membrane potential back towards the negative  $K^+$  equilibrium potential occurs concomitantly (Fig. 8b). This is revealed more clearly at the end of the stimulus where the operating point has shifted in the negative direction as compared to the resting value. Moreover, the activation of  $K^+$  channels leads to a reduced gain for the stimulus-evoked intracellular DC potential. That is, the direct receptor current, which is generated by the apical transducer, will now flow through a greater basolateral conductance, thereby producing a smaller voltage drop. Together, the shift of the membrane operating potential in the negative direction and the reduced gain for the DC receptor potential accounted for the adaptation seen in the positive DC receptor potential of the IHC with active, fast and slow basolateral conductances (compare Fig. 7a with Fig. 8b). The quantitative details are presented in Table II.

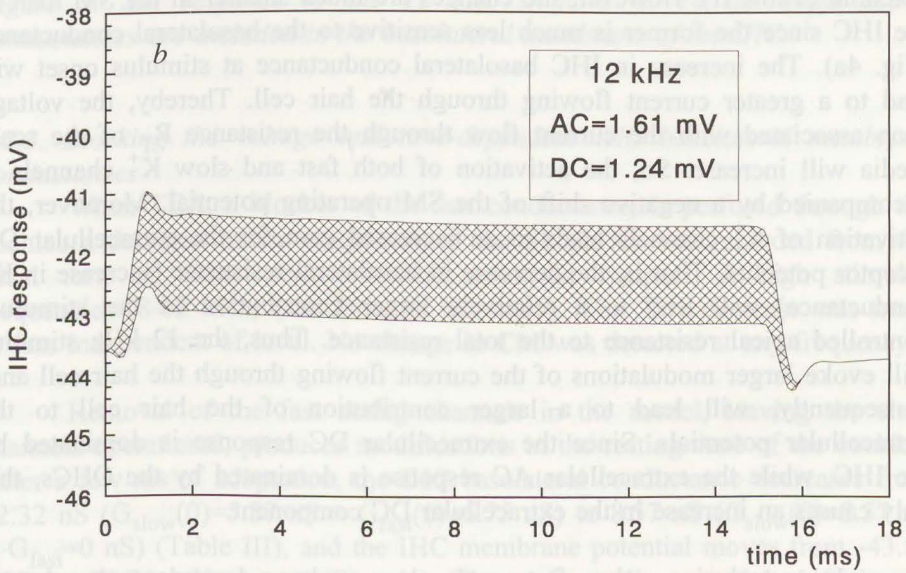
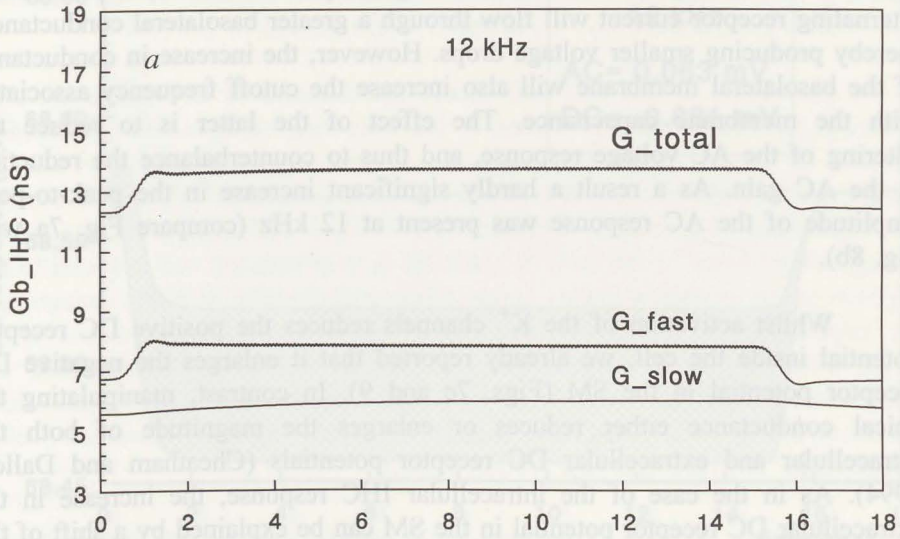


Figure 8a-b. The upper curve of Fig. 8a shows the combined response of the active conductances  $G_b(t)$  in the basolateral membrane of the IHC to a 78 dB stimulus of 16 ms at 12 kHz. The stimulus evoked shift in the basolateral conductance is +1.36 nS. The resting conductance  $G_b(0)$  is 12.32 nS. The bottom two curves of Fig. 8a show the individual responses of the fast and slow-acting conductances. Fig. 8b shows the corresponding response of the IHC to the same stimulus.

The increase in IHC basolateral conductance at stimulus onset will also lead to a reduced gain for the AC voltage response. That is, a part of the alternating receptor current will flow through a greater basolateral conductance, thereby producing smaller voltage drops. However, the increase in conductance of the basolateral membrane will also increase the cutoff frequency associated with the membrane capacitance. The effect of the latter is to reduce the filtering of the AC voltage response, and thus to counterbalance the reduction in the AC gain. As a result a hardly significant increase in the peak-to-peak amplitude of the AC response was present at 12 kHz (compare Fig. 7a with Fig. 8b).

Whilst activation of the  $K^+$  channels reduces the positive DC receptor potential inside the cell, we already reported that it enlarges the negative DC receptor potential in the SM (Figs. 7c and 9). In contrast, manipulating the apical conductance either reduces or enlarges the magnitude of both the intracellular and extracellular DC receptor potentials (Cheatham and Dallos, 1994). As in the case of the intracellular IHC response, the increase in the extracellular DC receptor potential in the SM can be explained by a shift of the operating potential and a change in the gain for the extracellular DC receptor potential (Table II). However, the changes are much smaller in the SM than in the IHC since the former is much less sensitive to the basolateral conductance (Fig. 4a). The increase in IHC basolateral conductance at stimulus onset will lead to a greater current flowing through the hair cell. Thereby, the voltage drop associated with the current flow through the resistance  $R_T$  of the scala media will increase. So, the activation of both fast and slow  $K^+$  channels is accompanied by a negative shift of the SM operating potential. Moreover, the activation of  $K^+$  channels leads to an increased gain for the extracellular DC receptor potential. That is, the decrease in basolateral resistance (increase in  $K^+$  conductance) will lead to a relatively larger contribution of the stimulus-controlled apical resistance to the total resistance. Thus, the 12 kHz stimulus will evoke larger modulations of the current flowing through the hair cell and, consequently, will lead to a larger contribution of the hair cell to the extracellular potentials. Since the extracellular DC response is dominated by the IHC, while the extracellular AC response is dominated by the OHCs, this only causes an increase in the extracellular DC component.

In conclusion, the fast and slow voltage-dependent basolateral conductances are probably not directly involved in the generation of the high-frequency DC receptor potentials, but they can nonetheless have a relatively large effect on the size of the measured DC potential, especially intracellularly.

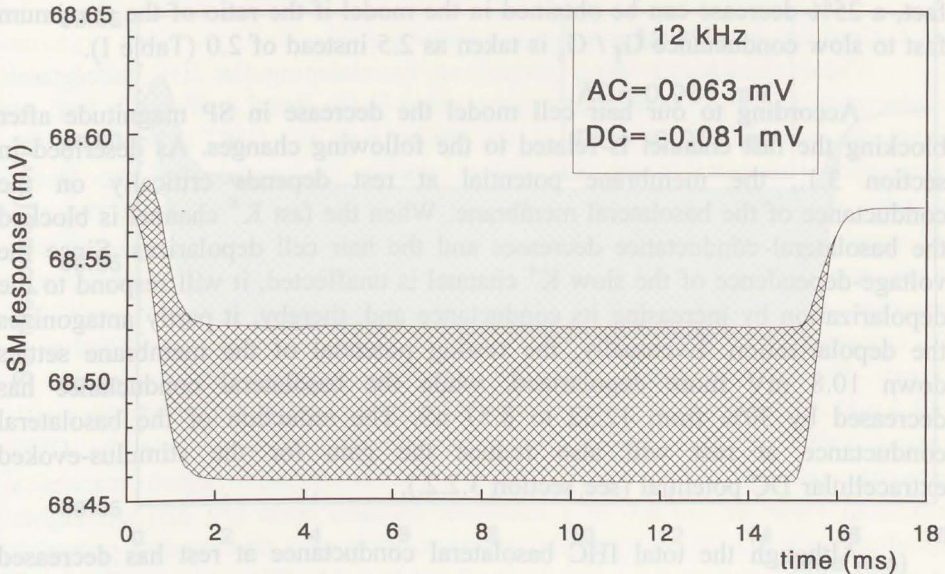


Figure 9. SM response to the 12 kHz stimulus at 78 dB when active conductances are included in the basolateral membrane of the IHC.

### 3.2.3. Blocking the voltage and time-dependent IHC basolateral membrane conductances

When TEA, a blocker of the fast conductance, is perfused through the cochlea a decrease in the magnitude of the SP (25%) was recorded from the basal turn of either scala vestibuli or scala tympani at high stimulus frequencies (8-12 kHz) (van Emst et al., 1995). The 25% decrease was more or less independent of level. No change in CM was detected at any frequency.

Removal of the fast acting channels in the model, leaving the slow channels operational, produces modifications in the resting state of the cochlea. After a few ms of adaptation, the IHC basolateral conductance decreases from 12.32 nS ( $G_{\text{slow}}(0)=5.57$  nS +  $G_{\text{fast}}(0)=6.75$  nS) to 8.57 nS ( $G_{\text{slow}}(0)=8.57$  nS +  $G_{\text{fast}}=0$  nS) (Table III), and the IHC membrane potential moves from -43.59 mV to -32.74 mV at rest (Fig. 4a). The scala media potential shifted only slightly from +68.57 mV to +68.61 mV.

Figure 10 shows the stimulus-evoked voltage response in SM which arises after such a removal of the fast acting conductance. The magnitude of the extracellular negative DC component has been reduced by 17.3%, compared to the situation in which both basolateral channels were active (Fig. 9). The CM is essentially unchanged. This effect was virtually independent of

level. The value of 17.3% compares well to the 25% found experimentally. In fact, a 25% decrease can be obtained in the model if the ratio of the maximum fast to slow conductance  $G_f / G_s$  is taken as 2.5 instead of 2.0 (Table I).

According to our hair cell model the decrease in SP magnitude after blocking the fast channel is related to the following changes. As described in section 3.1., the membrane potential at rest depends critically on the conductance of the basolateral membrane. When the fast  $K^+$  channel is blocked the basolateral conductance decreases and the hair cell depolarizes. Since the voltage-dependence of the slow  $K^+$  channel is unaffected, it will respond to the depolarization by increasing its conductance and, thereby, it partly antagonizes the depolarization. Eventually, the resting potential of the membrane settles down 10.8 mV more depolarized, while the basolateral conductance has decreased by 30% from 12.32 to 8.57 nS. The reduction of the basolateral conductance at rest will also reduce the gain for the stimulus-evoked extracellular DC potential (see section 3.2.2.).

Although the total IHC basolateral conductance at rest has decreased from  $G_b(0)=12.32$  nS to 8.57 nS after removal of the fast conductance, the resting conductance  $G_{slow}(0)$  associated with the slow  $K^+$  channel has increased from 50% to 77% of its maximum value  $G_s=11.14$  nS (Table III). Because the fast channel is blocked and the slow channel is now almost fully open the voltage sensitivity of the basolateral conductance has decreased (Fig. 3). Consequently, less additional basolateral conductance is activated at stimulus onset. Specifically, the IHC basolateral conductance increases from  $G_b(0)=8.57$  nS to  $G_b(12ms)=9.13$  nS during stimulation at 78 dB, which is less than the increase in basolateral conductance that occurs when both channels are operative (12.32 nS to 13.68 nS) (Table III). By now, the total reduction in  $G_b(t)$  from 13.68 nS to 9.13 nS during stimulation is responsible for a 15.4% decrease in gain for the extracellular DC receptor potential. Moreover, because the positive DC response of the basolateral conductance at stimulus onset shifts the SM operating potential in the negative direction this shift is reduced after removal of the fast conductance. Altogether, these two effects account for the 17.3% reduction in the magnitude of the negative extracellular DC receptor potential after blocking the fast-acting conductance.

In conclusion, the decrease in the magnitude of the high-frequency SP after TEA perfusion probably arises from a decrease in IHC basolateral conductance at rest, and a change in the modification of the extracellular DC potential by active basolateral conductances during stimulation.



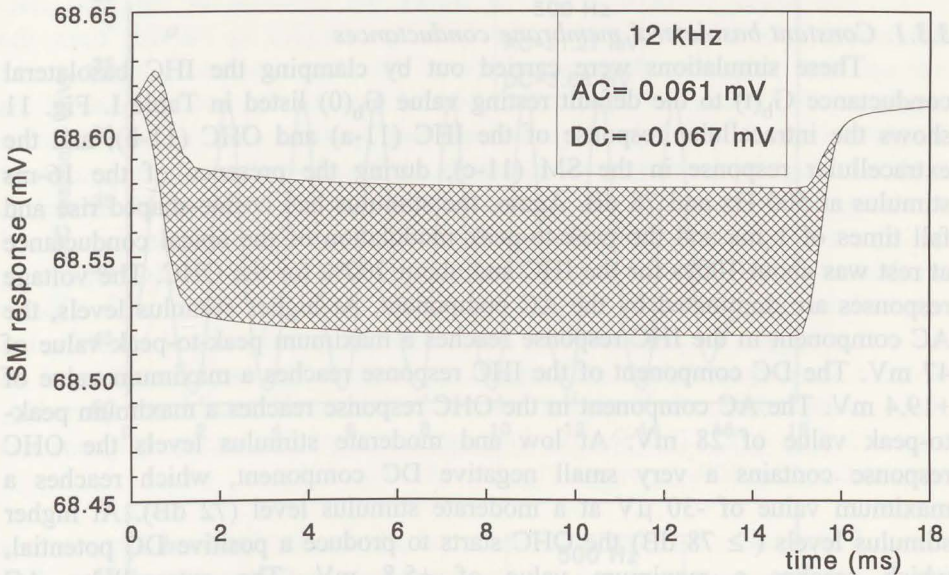


Figure 10. SM response to the 12 kHz stimulus at 78 dB when the fast-acting conductance in the basolateral membrane of the IHC is blocked.

When 4-AP, a blocker of the slow conductance, is perfused through the cochlea a substantial decrease in the magnitude of the SP was recorded from the basal turn of either scala vestibuli and scala tympani at high-frequency (12 kHz) low-level stimulation (Van Emst et al., 1996). Initially, we attributed this effect to the blocking of the slow  $K^+$  channel in the basolateral membrane of the IHC. However, this interpretation is not supported by the present model. After removal of the slow-acting conductance the changes in the resting condition of the IHC are minimal:  $G_b(0)$  moves from 12.32 nS to 10.55 nS and  $V^{IHC}(0)$  from -43.59 mV to -39.22 mV. This means that  $G_{fast}(0)$  has increased from 30% (6.75 nS) to 47% (10.55 nS) of its maximum value  $G_f$  (22.28 nS) and, thereby, has become more sensitive to voltage changes (Fig. 3). As a result, the positive DC response of the basolateral conductance at stimulus onset is hardly affected (Table III). Consequently, the extracellular DC receptor potential produced by the model shows no substantial changes after removal of the slow-acting conductance. Further simulations are needed to reveal how critical the TEA and 4-AP predictions depend on the choice of channel parameters.

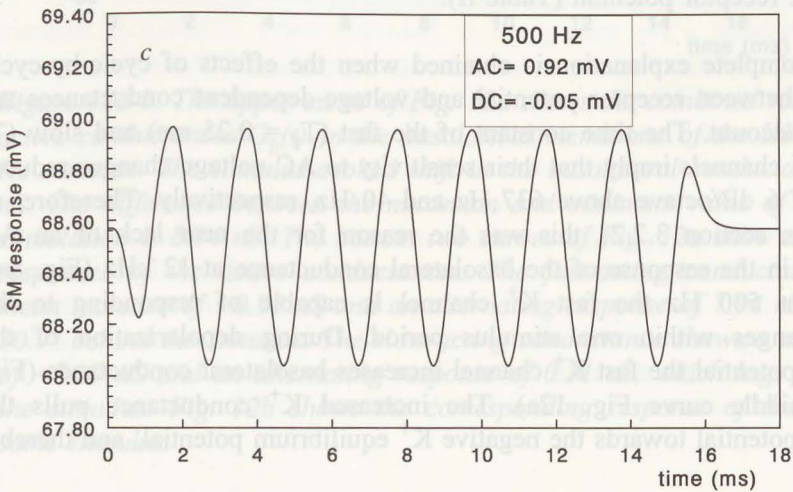
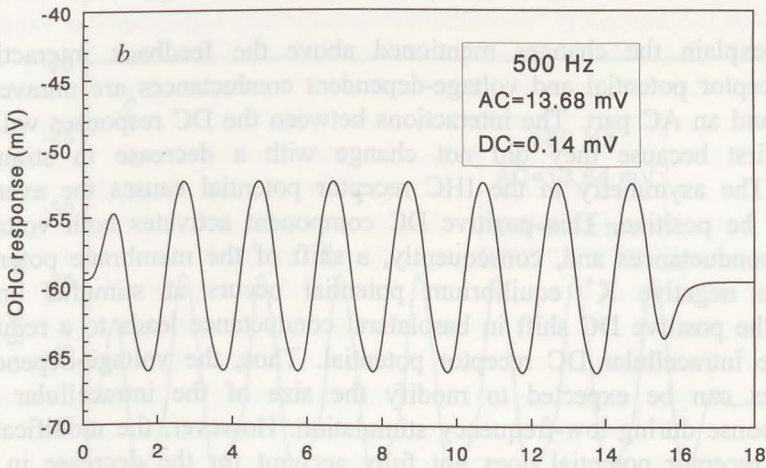
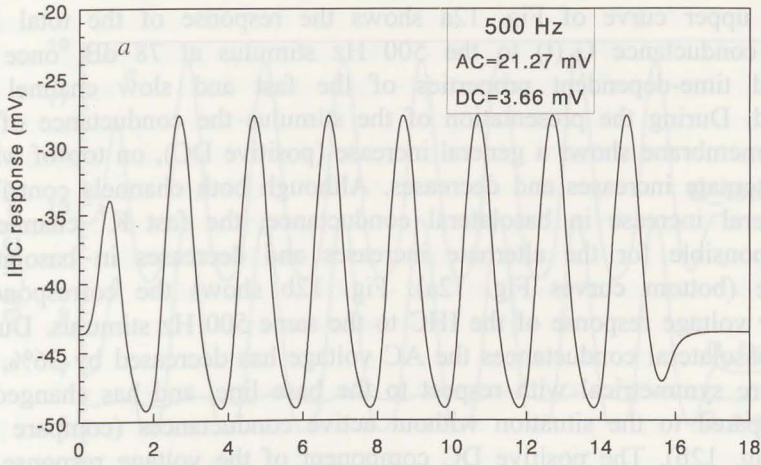
### 3.3. Stimulus-evoked potentials at 500 Hz

#### 3.3.1. Constant basolateral membrane conductances

These simulations were carried out by clamping the IHC basolateral conductance  $G_b(t)$  to the default resting value  $G_b(0)$  listed in Table I. Fig. 11 shows the intracellular response of the IHC (11-a) and OHC (11-b), and the extracellular response in the SM (11-c), during the presence of the 16-ms stimulus at 500 Hz and 78 dB. Again, the stimulus had cosine-shaped rise and fall times of 1 ms and the peak-to-peak modulation of the apical conductance at rest was about 100% for the IHC and about 200% for the OHC. The voltage responses are dominated by the AC component. At higher stimulus levels, the AC component in the IHC response reaches a maximum peak-to-peak value of 47 mV. The DC component of the IHC response reaches a maximum value of +19.4 mV. The AC component in the OHC response reaches a maximum peak-to-peak value of 28 mV. At low and moderate stimulus levels the OHC response contains a very small negative DC component, which reaches a maximum value of -30  $\mu$ V at a moderate stimulus level (72 dB). At higher stimulus levels ( $\geq 78$  dB) the OHC starts to produce a positive DC potential, which reaches a maximum value of +5.8 mV. The extracellular AC component, i.e. the CM, is dominated by the OHCs, while the extracellular DC component, i.e. the SP, is dominated by the IHC. The stimulus-evoked DC potential in the SM has a negative polarity, irrespective of stimulus level.

The IHC results conform to the responses of an IHC in the basal turn of the guinea pig's cochlea when stimulated with 600 Hz sound (Cody and Russell, 1987). However, the presence of a substantial negative DC receptor potential in basal turn OHCs at moderate sound pressure levels of the above stimulus is not reproduced by our model. This is a consequence of the apical transducer's setpoint. Accordingly, the model also does not account for the positive SP which is recorded in the basal turn of the SM of the guinea pig's cochlea when stimulated with low-level low-frequency sound. Thus, the following discussion concerning the consequences of active conductances in the IHC basolateral membrane will be limited to the intracellular response.

*Figure 11. The responses of (a) the IHC, (b) the OHC, and (c) the SM to a 78 dB stimulus of 16 ms at 500 Hz. At 78 dB the peak-to-peak modulation of the IHC and OHC apical conductance is about 100% and 200% of their respective resting value. The values of the stimulus-evoked peak-to-peak AC and DC voltages were calculated between 12 and 14 ms. The IHC basolateral conductance  $G_b(t)$  was clamped to the default resting value  $G_b(0)$  listed in Table I.*



### 3.3.2. Voltage and time-dependent IHC basolateral membrane conductances

The upper curve of Fig. 12a shows the response of the total IHC basolateral conductance  $G_b(t)$  to the 500 Hz stimulus at 78 dB, once the voltage and time-dependent properties of the fast and slow channel are incorporated. During the presentation of the stimulus the conductance of the basolateral membrane shows a general increase (positive DC), on top of which it shows alternate increases and decreases. Although both channels contribute to the general increase in basolateral conductance, the fast  $K^+$  channel is mainly responsible for the alternate increases and decreases in basolateral conductance (bottom curves Fig. 12a). Fig. 12b shows the corresponding intracellular voltage response of the IHC to the same 500 Hz stimulus. Due to the active basolateral conductances the AC voltage has decreased by 36%, has become more symmetrical with respect to the base line, and has changed its shape, compared to the situation without active conductances (compare Fig. 11a with Fig. 12b). The positive DC component of the voltage response has been reduced by 80% (compare Fig. 11a with Fig. 12b).

To explain the changes mentioned above the feedback interactions between receptor potential and voltage-dependent conductances are unravelled into a DC and an AC part. The interactions between the DC responses will be discussed first because they did not change with a decrease in stimulus frequency. The asymmetry in the IHC receptor potential causes the average response to be positive. This positive DC component activates both voltage-dependent conductances and, consequently, a shift of the membrane potential towards the negative  $K^+$  equilibrium potential occurs at stimulus onset. Moreover, the positive DC shift in basolateral conductance leads to a reduced gain for the intracellular DC receptor potential. Thus, the voltage-dependent conductances can be expected to modify the size of the intracellular DC voltage response during low-frequency stimulation. However, the modification of the DC receptor potential does not fully account for the decrease in the positive DC receptor potential (Table II).

A complete explanation is obtained when the effects of cycle-by-cycle interaction between receptor potential and voltage-dependent conductances are taken into account. The time constant of the fast ( $T_f = 0.25$  ms) and slow ( $T_s = 4$  ms)  $K^+$  channels imply that their sensitivity to AC voltage changes reduces at a rate of 6 dB/octave above 637 Hz and 40 Hz, respectively. Therefore, as explained in section 3.2.2., this was the reason for the near lack of an AC component in the response of the basolateral conductance at 12 kHz (Fig. 8a). However, at 500 Hz the fast  $K^+$  channel is capable of responding to the voltage changes within one stimulus period. During depolarization of the membrane potential the fast  $K^+$  channel increases basolateral conductance (Fig. 11a and middle curve Fig. 12a). The increased  $K^+$  conductance pulls the membrane potential towards the negative  $K^+$  equilibrium potential, and thereby

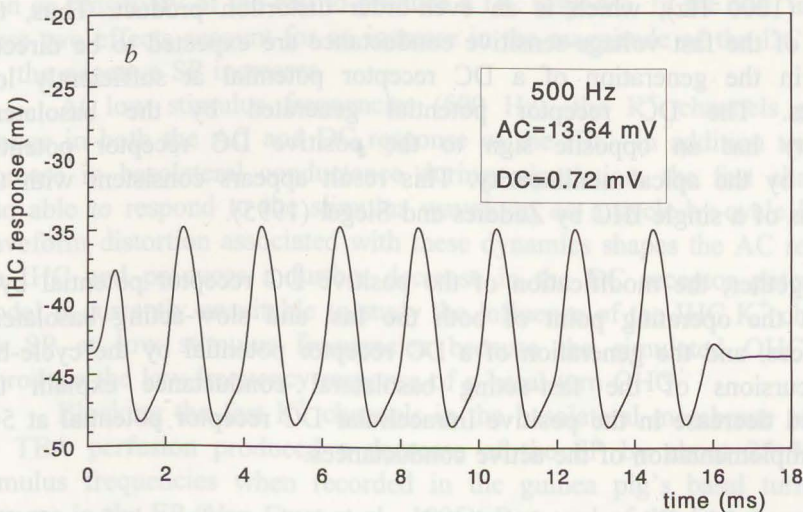
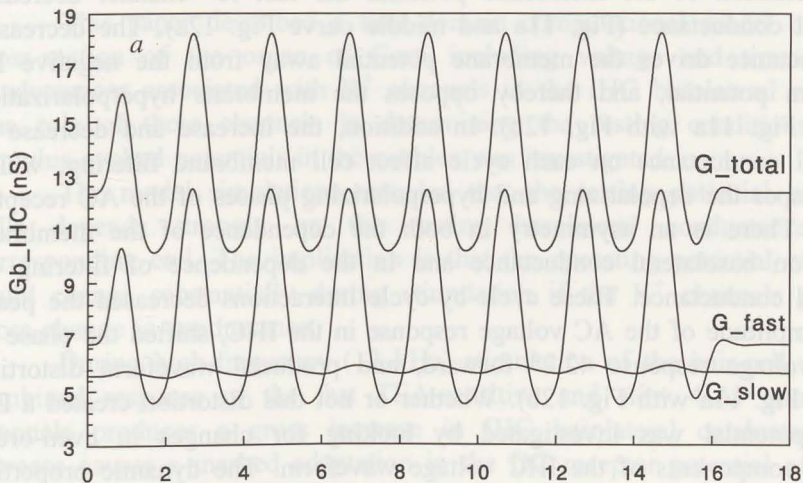


Figure 12a-b. The upper curve of Fig. 12a shows the combined response of the active conductances  $G_b(t)$  in the basolateral membrane of the IHC to the 500 Hz stimulus. The stimulus-evoked shift in the basolateral conductance is +1.14 nS. The difference between the maximum and minimum value of  $G_b(t)$  during stimulation is 8.14 nS. The bottom two curves of Fig. 12a show the individual responses of the active conductances. The fast-acting conductance shows a mean increase of +0.95 nS and an alternating response of 7.94 nS, which lags  $30.9^\circ$  behind the stimulus. The slow-acting conductance shows a mean increase of +0.19 nS and an alternating response of 0.31 nS, which lags  $75.9^\circ$  behind the stimulus. Fig. 12b shows the corresponding response of the IHC to the same stimulus.

opposes the membrane depolarization (compare Fig. 11a and Fig. 12b). During hyperpolarization of the membrane potential the fast  $K^+$  channel decreases basolateral conductance (Fig. 11a and middle curve Fig. 12a). The decreased  $K^+$  conductance drives the membrane potential away from the negative  $K^+$  equilibrium potential, and thereby opposes the membrane hyperpolarization (compare Fig. 11a with Fig. 12b). In addition, the increase and decrease in basolateral conductance on each cycle affect cell membrane filtering, which further shapes the depolarizing and hyperpolarizing phases of the AC receptor potential. There is an asymmetry in both the dependence of the membrane potential on basolateral conductance and in the dependence of filtering on basolateral conductance. These cycle-by-cycle interactions decreased the peak-to-peak amplitude of the AC voltage response in the IHC, shifted the phase of the AC voltage response  $42.2^\circ$  forward, and produced waveform distortion (compare Fig. 11a with Fig. 12b). Whether or not this distortion created a DC receptor potential was investigated by looking for changes in even-order distortion components of the IHC voltage waveform. The dynamic properties of the fast voltage-dependent conductance substantially affected the second harmonic (1000 Hz), which is an even-order distortion product. Thus, the dynamics of the fast voltage-sensitive conductance are expected to be directly involved in the generation of a DC receptor potential at sufficiently low frequencies. The DC receptor potential generated by the basolateral nonlinearity has an opposite sign to the positive DC receptor potential generated by the apical nonlinearity. This result appears consistent with the simulations of a single IHC by Zeddes and Siegel (1995).

Together, the modification of the positive DC receptor potential by a change in the operating point of both the fast and slow-acting basolateral conductances, and the generation of a DC receptor potential by the cycle-by-cycle excursions of the fast-acting basolateral conductance explain the pronounced decrease in the positive intracellular DC receptor potential at 500 Hz after implementation of the active conductances.

The model offers an explanation for an experimental result from Dallos and Cheatham (1990). They injected negative current into an IHC, and observed that the increase in the DC voltage response to tones above 600 Hz was twice as large (in decibels) as in the AC response. Below 600 Hz the increase in the DC component was more than twice the increase in the AC component. It was argued that waveform distortion due to voltage-dependent conductances residing in the basolateral membrane produced the excess vulnerability of the DC response at low frequency stimulation. Their argument is supported by our model work, which shows that active basolateral conductances distort the waveform of the low-frequency receptor potential.

#### 4. Conclusions

This paper described a time-domain computational model of a radial cross-section of the organ of Corti including voltage and time-dependent conductances associated with  $K^+$  channels in the IHC basolateral membrane. The role of these channels in determining the resting conditions and the stimulus-evoked potentials in the cochlea was investigated.

The model simulations revealed that the resting potential of the hair cells depends strongly on the resting basolateral conductance of the corresponding cell. The implication is that the operating potential of the IHC could change substantially during stimulation if the  $K^+$  channels produce a gross change in conductance.

During high-frequency (12 kHz) stimulation of the hair-cell model the combined response of the fast TEA-sensitive and slow 4-AP sensitive  $K^+$  channels produces a gross increase in IHC basolateral conductance. This increase causes a marked adaptation in the DC receptor potential of the IHC via (1) a shift in the operating potential of the IHC, and (2) a change in the gain or sensitivity of the cell to produce a DC response. In the SM, in contrast, these two effects account for an increase in the magnitude of the DC response, i.e. the negative SP increases.

At low stimulus frequencies (500 Hz), the  $K^+$  channels produce a change in both the AC and DC response of the IHC. In addition to the gross increase in basolateral conductance during stimulation, the fast channels are also able to respond to the stimulus waveform on a cycle-by-cycle basis. The waveform distortion associated with these dynamics shapes the AC response of the IHC and produces a further decrease in the DC receptor potential. The model is currently unsuitable to study the influence of the IHC  $K^+$  channels on the SP at low stimulus frequencies because the simulated OHCs do not reproduce the low-frequency response of a basal turn OHC.

Blocking the fast  $K^+$  channels in the basolateral membrane of the IHC by TEA perfusion produced a decrease of the SP by about 25 % at high stimulus frequencies when recorded in the guinea pig's basal turn, and no changes in the EP (Van Emst et al., 1995). Removal of the fast channels in the model produces a change of less than 0.05 mV in the EP and a 17% decrease in SP. The decrease in SP after removal of the fast channels in the model arises from a gross decrease in basolateral conductance at rest, and a reduced responsiveness of the basolateral conductance during stimulation. The CM is essentially unaffected in both the *in vivo* experiment and in the model. Removal of the slow 4-AP sensitive channel from the IHC's basolateral membrane produced only a very small effect on the SP in the model in contrast to experimental data (Van Emst et al., 1996). This may indicate that the effects of 4-AP on the SP are due to blocking of the 4-AP sensitive  $K^+$  channels in the basolateral membrane of the OHC (Mammano et al., 1995).

Finally, the model offers an explanation for the large vulnerability of the DC response over the AC response that has been repeatedly found experimentally (Durrant and Dallos, 1972; Nuttall, 1985; Dallos and Cheatham, 1990). Manipulation of the basolateral conductance in the model has much larger effects on the intracellular DC response than on the AC response. Extracellularly, the SP can change by about 17% without a substantial change in the CM. The main source of variability of the DC voltage response appears to be the gross shift of the basolateral conductance during stimulation and the associated changes in the operating potentials of the cochlea, particularly intracellularly. This effect seems to have been disregarded previously.



Table I: Model parameter values (column 1) and resting conditions (column 2).

Extracellular components:

$$E_T = 70 \text{ mV}$$

$$R_T = 10.0 \text{ k}\Omega$$

$$R_3 = 3.6 \text{ k}\Omega$$

$$R_T C_T = 0.25 \text{ ms}$$

$$V^{SM}(0) = 68.572 \text{ mV}$$

$$V^{OC}(0) = 0.514 \text{ mv}$$

IHC:

$$E_1 = -80 \text{ mV}$$

$$C_a = 0.985 \text{ pF}$$

$$C_b = 3.080 \text{ pF}$$

$$V^{IHC}(0) = -43.593 \text{ mV}$$

$$V^{tm}(0) = -44.107 \text{ mV}$$

$$G_{leak} = 2.96 \text{ nS}$$

$$G_{max} = 10.65 \text{ nS}$$

$$x_1 = 0.9541$$

$$x_2 = 1.0032$$

$$a = 2.9375$$

$$p_o(0) = 9.2\%$$

$$G_a(0) = 3.94 \text{ nS}$$

$$G_f = 22.28 \text{ nS}$$

$$V_f = V^{tm}(0) + 5 \text{ mV}$$

$$S_f = 6.0 \text{ mV}$$

$$T_f = 0.25 \text{ ms}$$

$$G_{fast}(0) = 6.75 \text{ nS}$$

$$G_s = 11.14 \text{ nS}$$

$$V_s = V^{tm}(0)$$

$$S_s = 9.0 \text{ mV}$$

$$T_s = 4.0 \text{ ms}$$

$$G_{slow}(0) = 5.57 \text{ nS}$$

$$G_b(0) = 12.32 \text{ nS}$$

OHC:

$$E_1 = -80 \text{ mV}$$

$$C_a = 0.506 \text{ pF}$$

$$C_b = 3.247 \text{ pF}$$

$$V^{OHC}(0) = -59.506 \text{ mV}$$

$$G_b = 12.99 \text{ nS};$$

$$G_{leak} = 1.013 \text{ nS}$$

$$G_{max} = 3.72 \text{ nS}$$

$$x_1 = -0.4982$$

$$x_2 = 0.5088$$

$$a = 2.9375$$

$$p_o(0) = 27.3\%$$

$$G_a(0) = 2.03 \text{ nS};$$

Scaling:

$$R = 3.8$$

$$N = 100$$

Note: The parameter values for IHC and OHC refer to single cells. For the calculation of extracellular potentials these values are scaled by the ratio R of OHCs to IHC in the cochlea, and by the number N of summing cross-sections (see text).

Table II: Adaptation of the stimulus-evoked DC response in the model at 78 dB due to active IHC basolateral conductances. Measured adaptation is the difference in DC response between simulations with a constant conductance  $G_b = G_b(0)$  (Figs. 7a, 7c, 11a) and with active, fast and slow IHC basolateral conductances (Figs. 8b, 9, 12b). Predicted adaptation is based on model simulations using two constant values of the IHC basolateral conductance  $G_b$ . The first value is the resting basolateral conductance  $G_b(0) = 12.32$  nS and the second value is the operating point of  $G_b$  during stimulation with active conductances. The latter is defined as the resting conductance  $G_b(0)$  plus the steady-state DC increase in basolateral conductance during stimulation (Figs. 8a, 12a). At 12 kHz, the measured adaptation is equal to the sum of the adaptation in resting potential and DC response predicted from constant conductances. The former effect is dominant. At 500 Hz, the prediction from constant IHC basolateral conductances is smaller than the measured adaptation.

$G_b$ (nS)	12 kHz			12 kHz		500 Hz	
	$V^{IHC}(0)$ (mV)	DC $V^{IHC}(t)$ (mV)	$V^{SM}(0)$ (mV)	DC $V^{SM}(t)$ (mV)	$V^{IHC}(0)$ (mV)	DC $V^{IHC}(t)$ (mV)	
12.32	-43.593	4.232	68.572	-0.067	-43.593	3.662	
13.46	-	-	-	-	-45.940	3.513	
13.68	-46.363	4.015	68.561	-0.070	-	-	
	-----	-----	-----	-----	-----	-----	
	$\Delta = -2.770$	$\Delta = -0.217$	$\Delta = -0.011$	$\Delta = -0.003$	$\Delta = -2.347$	$\Delta = -0.149$	
predicted adaptation:	-2.987			-0.014		-2.520	
measured adaptation:	-2.987			-0.014		-2.944	
	(Fig. 7a vs. Fig. 8b)			(Fig. 7c vs. Fig. 9)		(Fig. 11a vs. Fig. 12b)	

Table III: The conductances associated with the fast ( $G_{fast}(t)$ ) and slow ( $G_{slow}(t)$ )  $K^+$  channels at rest and during the presence of the 78 dB stimulus of 16 ms at 12 kHz when both channels are operative, the slow channel is operative, and the fast channel is operative. The bottom row gives the total conductance of the basolateral membrane ( $G_b(t)$ ) at rest and during the presence of the stimulus. The right column gives the maximum conductances ( $G_f$  and  $G_s$ ) associated with the individual channels. All conductances are given in nS.

	normal rest	normal stimulation	fast off rest	fast off stimulation	slow off rest	slow off stimulation	maximum
$G_{fast}(t)$	6.75	7.75	$\phi$	$\phi$	10.55	11.74	$G_f = 22.28$
$G_{slow}(t)$	5.57	5.93	8.57	9.13	$\phi$	$\phi$	$G_s = 11.14$
-----	-----	-----	-----	-----	-----	-----	
$G_b(t)$	12.32	13.68	8.57	9.13	10.55	11.74	

## References

- Ashmore, J.F. (1991) The electrophysiology of hair cells. *Annu. Rev. Physiol.* 53, 465-476.
- Barrett, J.N., Magleby, K.L. and Pallotta, B.S. (1982) Properties of single calcium-activated potassium channels in cultured rat muscle. *J. Physiol.* 331, 211-230.
- Cheatham, M.A. and Dallos, P. (1994) Stimulus biasing: a comparison between cochlear hair cell and organ of Corti response patterns. *Hear. Res.* 75, 103-113.
- Cody, A.R. and Russell, I.J. (1987) The responses of hair cells in the basal turn of the guinea-pig cochlea to tones. *J. Physiol.* 383, 551-569.
- Crawford, A.C., Evans, M.G. and Fettiplace, R. (1991) The actions of calcium on the mechano-electrical transducer current of turtle hair cells. *J. Physiol.* 434, 369-398.
- Dallos, P., Santos-Sacchi, J. and Flöck, Å. (1982) Intracellular recordings from cochlear outer hair cells. *Science* 218, 582-584.
- Dallos, P. (1983) Some electrical circuit properties of the organ of Corti. I. Analysis without reactive elements. *Hear. Res.* 12, 89-119.
- Dallos, P. (1984) Some electrical circuit properties of the organ of Corti. II. Analysis including reactive elements. *Hear. Res.* 14, 281-291.
- Dallos, P. (1985) Response characteristics of mammalian cochlear hair cells. *J. Neurosci.* 5, 1591-1608.
- Dallos, P. and Cheatham, M.A. (1990) Effects of electrical polarization on inner hair cell receptor potentials. *J. Acoust. Soc. Am.* 87, 1636-1647.
- Durrant, J.D. and Dallos, P. (1972) Influence of direct-current polarization of the cochlear partition on the summing potentials. *J. Acoust. Soc. Am.* 52, 542-552.
- Fettweis, A. (1986) Wave digital filters: theory and practice. *Proc. IEEE* 74, 270-327.
- Giguère C. and Woodland, P.C. (1994) A computational model of the auditory periphery for speech and hearing research. I. Ascending path. *J. Acoust. Soc. Am.* 95, 331-342.

- Housley, G.D and Ashmore, J.F. (1992) Ionic currents of outer hair cells isolated from the guinea-pig cochlea. *J. Physiol.* 448, 73-98.
- Hudspeth, A.J. (1989) How the ear's works work. *Nature* 341, 397-341.
- Kössl, M. and Russell, I.J. (1992) The phase and magnitude of hair cell receptor potentials and frequency tuning in the guinea pig cochlea. *J. Neurosci.* 12, 1575-1586.
- Kros, C.J. and Crawford, A.C. (1990) Potassium currents in inner hair cells isolated from the guinea-pig cochlea. *J. Physiol.* 421, 262-291.
- Kros, C.J., Rüsçh, A. and Richardson, G.P. (1992) Mechano-electrical transducer currents in hair cells of the cultured neonatal mouse cochlea. *Proc. R. Soc. Lond. B* 249, 185-193.
- Mammano, F., Kros, C.J. and Ashmore, J.F. (1995) Patch clamped responses from outer hair cells in the intact adult organ of Corti. *Pflügers arch.* 430, 745-750.
- McMullen, T.A. and Mountain, D.C. (1985) Model of d.c. potentials in the cochlea: Effects of voltage-dependent cilia stiffness. *Hear. Res.* 17, 127-141.
- Nuttall, A.L. (1985) Influence of direct current on dc receptor potentials from cochlear inner hair cells in the guinea pig. *J. Acoust. Soc. Am.* 77, 165-175.
- Ruggero, M.A. (1992) Responses to sound of the basilar membrane of the mammalian cochlea. *Current Opinion in Neurobiology* 2, 449-456.
- Russell, I.J., Cody, A.R. and Richardson, G.P. (1986) The responses of inner and outer hair cells in the basal turn of the guinea-pig cochlea grown in vitro. *Hear. Res.* 22, 199-216.
- Strube, H.W. (1982) Time-varying wave digital filters for modelling analog systems. *IEEE Trans. Acoust. Speech Signal Process.* 30, 864-868.
- Van Emst, M.G., Klis, S.F.L. and Smoorenburg, G.F. (1995) Tetraethylammonium effects on cochlear potentials in the guinea pig. *Hear. Res.* 88, 27-35.
- Van Emst, M.G., Klis, S.F.L. and Smoorenburg, G.F. (1996) 4-aminopyridine effects on summing potentials in the guinea pig. *Hear. Res.*, in print.
- Zeddies, D.G. and Siegel, J.H. (1995) Physiologically-based model of the inner hair cell. *ARO Abstracts*, 18: 153.

# Chapter 6

## Summary

The summing potential (SP) is probably the least understood component of the gross cochlear potentials. Knowledge about this potential will improve our understanding of cochlear transduction and will increase our understanding about the pathophysiology of diseases in which the SP is affected, e.g., Ménière's disease.

The SP is a nonlinear response, because it is a DC potential evoked by pure sinusoidal (sound) stimulation. The objective of this thesis is to investigate which nonlinear elements in the cochlear transduction chain contribute to the generation of the SP. We focused our investigations on nonlinear conductances in cochlear hair cells, which have been investigated *in vitro* by others.

In the first experiments we concentrated on the basolateral  $K^+$  channels. Isolated hair cells express several types of  $K^+$  channels in their basolateral membrane (Kros and Crawford, 1990; Housley and Ashmore, 1992). Each type of  $K^+$  channel can be selectively blocked by applying drugs to the fluid surrounding the isolated hair cell. Therefore, we studied the contribution from these channels to the SP by blocking them pharmacologically. The perilymphatic perfusion technique was used to introduce the  $K^+$ -channel blockers into the cochlea of the guinea pig. The results are presented in chapters 2 and 3.

### **Chapter 2: Tetraethylammonium effects on cochlear potentials in the guinea pig,**

reports on the effects of the  $K^+$  channel blocker tetraethylammonium (TEA) on the SP. TEA caused a small (25 %) decrease in the magnitude of the negative SP recorded from SV and the positive SP recorded from ST (both basal turn), for the highest stimulus-frequencies only (8-12 kHz). Because basal turn OHCs do not produce DC potentials when excited with low and moderate level stimuli at high frequencies the TEA-sensitive  $K^+$  channel in the IHC is held responsible for the effect of TEA on the SP.

This result suggests that only a minor contribution to the SP comes from the TEA-sensitive  $K^+$  channel in the basolateral membrane of the IHC. Non-linearities situated at different locations in the transduction chain, e.g. the apical mechano-electrical transduction process, are probably mainly responsible for the generation of the stimulus-evoked DC potentials.

### Chapter 3: 4-Aminopyridine effects on summing potentials in the guinea pig,

describes the effects of the  $K^+$  channel blocker 4-aminopyridine (4-AP) on the SP. 4-AP produced frequency- and level-dependent changes in the magnitude of the SP. At low and moderate levels of 8 and 12 kHz stimuli 4-AP caused a substantial decrease in SP magnitude (up to 50%), while at higher sound pressure levels an increase in SP magnitude was found. The increase of the SP, found with 8 and 12 kHz stimuli at high levels only, became more pronounced when the stimulus frequency decreased, so that at the lower frequencies, 2 and 4 kHz, a 4-AP induced increase of the SP was apparent at all sound levels. These effects occurred in both SV and ST of the basal turn.

In chapter 3 we concluded that the substantial reduction of the SP magnitude at low-level high-frequency stimulation resulted from blocking the 4-AP sensitive  $K^+$  channel in the basolateral membrane of the IHC. This indicates that this channel imparts a strong asymmetry on stimulus transduction, i.e. makes a considerable contribution to the SP.

The stimuli at which we found an increased SP roughly correspond to stimuli at which the OHCs produce a DC receptor potential. We concluded that the increased SP resulted from blocking the 4-AP sensitive  $K^+$  channel in the basolateral membrane of the OHC. However, blocking a conductance in the basolateral membrane of a hair cell is unlikely to increase the DC receptor current through the hair cell. The explanation for the increased SP probably involves additional changes in OHC physiology. Mammano et al. (1995) showed that blocking the 4-AP sensitive  $K^+$  channel depolarizes the OHC. Injecting positive current into the OHC, which should also depolarize the cell, is known to reduce the conductance associated with the apical transducer, equivalent to displacing the stereociliar bundle in the inhibitory direction (Russell and Kössl, 1991). This displacement may be caused by depolarization-induced contraction of the OHC body (Santos-Sacchi 1991). Thus, blocking the 4-AP sensitive  $K^+$  channel probably causes a reduction of the OHC's apical conductance at rest. This would increase the asymmetry in mechano-electrical transduction and, consequently, result in an increase of the stimulus-evoked DC potential.

The results from chapters 2 and 3 have shown that the main nonlinearity responsible for SP generation is not connected to the basolateral  $K^+$  channels. The major contribution probably originates with the apical mechano-electrical transduction process. Because blocking the apical transduction channel abolishes stimulus transduction we studied the effect of a

gradual change in apical conductance on the SP. Russell and Kössl (1991) have shown that the apical conductance of the OHC depends on the membrane potential. Therefore, we chose to examine the contribution from the apical conductance to the SP by means of manipulating electrically the operating point of the apical channels. For this purpose, furosemide was administered intravenously to guinea pigs to affect the endocochlear potential (EP).

#### **Chapter 4: Identification of the nonlinearity governing even-order distortion products in cochlear potentials,**

reports on the effects of a furosemide-induced shift in the EP on the SP and the 2<sup>nd</sup> harmonic ( $2F_0$ ) of the cochlear microphonics (CM). Shifting the operating point of the cochlear transducer electrically by changing the EP produced drastic changes in the SP. The most conspicuous change was a reversal in the polarity of the SP. At about the same moment the SP crossed zero, the amplitude of the  $2F_0$  showed a dip and the phase of the  $2F_0$  shifted over about 120°. These changes can be explained by a shift in the operating point of a sigmoidal Boltzmann-like transfer function. The sigmoidal transfer function can be attributed to the mechano-electrical transduction channel in the apical membrane of the OHC.

The sensitivity of the SP to the operating point of the apical transducer channel implies that in the normal situation the SP is primarily generated by this nonlinear conductance.

An alternative approach to studying the role of the various hair cell conductances in generating DC receptor potentials is via mathematical modelling of the organ of Corti and subsequent computation of the receptor potentials. For this purpose we modified the circuit model of Dallos (1983, 1984). The first modification involved the incorporation of the characteristics of the apical mechano-electrical transducer channel, as determined *in vitro* by Kros et al. (1992). Secondly, the model was extended to account for the voltage and time-dependent properties of basolateral  $K^+$  channels found in *in vitro* experiments (Kros and Crawford, 1990; Housley and Ashmore, 1992).

#### **Chapter 5: Generation of DC receptor potentials in a computational model of the organ of Corti with voltage-dependent $K^+$ channels in the basolateral membrane of inner hair cells,**

shows how DC receptor potentials are generated by the apical transducer conductance and modulated by the basolateral voltage and time-dependent  $K^+$  conductances.



Incorporating a transduction channel in the apical membrane of the hair cells that followed a Boltzmann function was sufficient to reproduce the intra and extracellular DC receptor potentials found *in vivo*. The magnitude and polarity of the DC receptor potential showed a strong dependence on the operating point of the Boltzmann function, i.e. on the percentage of the maximum apical conductance activated at rest. When the apical transducer is 9% activated at rest, a value reported for isolated hair cells, sinusoidal stimulation evokes a large positive DC receptor potential in the hair cell and a negative SP in the SM (the DC receptor potential in SV is directly related to the DC receptor potential in SM).

With a delay of a few ms, the basolateral voltage and time-dependent conductances in our model respond to the depolarization of the hair cell with an increase in conductance. The increase in basolateral conductance shifts the potential in the hair cell towards the negative  $K^+$  equilibrium potential. Because the potential in SM is connected with the intracellular potentials through the apical conductance, the potential in SM shifts in the negative direction as well. The shift of the potentials in the negative direction during stimulation decreases the magnitude of the positive intracellular DC response and increases the magnitude of the SP. Thus, the magnitude of the DC receptor potentials is modulated by the nonlinear basolateral conductances. However, the predicted increase in SP due to the activity of the basolateral conductances is small.

Removing a basolateral  $K^+$  channel from the model produced small decreases in the magnitude of the SP, comparable to the effect of blocking the TEA sensitive  $K^+$  channels in the basolateral membrane of the IHC (chapter 2). In chapter 3 we concluded that blocking the 4-AP sensitive  $K^+$  in the basolateral membrane of the IHC caused the substantial reduction in SP magnitude at low-level, high-frequency stimulation. This large effect of 4-AP on the SP is not predicted by the model. Because the 4-AP induced decrease in SP was found for stimuli at which the IHCs are assumed to dominate the SP we still consider the decreased SP to reflect a reduced contribution from the IHC to the SP. But, based upon the results from the model, we do no longer think that the reduced contribution from the IHC to the SP is purely the result of blocking the 4-AP sensitive  $K^+$  channel in the basolateral membrane of the IHC.

Russell, J.J. and Katsuki, M. (1981) The voltage responses of hair cells in the basal turn of the guinea-pig cochlea. *J. Physiol.* 425, 493-511.

Santos-Sacchi, J. (1991) Reversible inhibition of voltage-dependent outer hair cell motility and capacitance. *J. of Neurosci.* 11, 3096-3110.

## Future research

In chapter 3 we reported on the frequency and level-dependent effects of 4-AP on the SP. The decreased SP at low-level high-frequency stimulation was attributed to a reduced contribution from the IHC to the SP. The increased SP at high-level high-frequency stimulation, and at all levels of low-frequency stimulation, was attributed to an increased contribution from the OHC to the SP. The increased OHC contribution was explained by membrane depolarization, due to blocking the 4-AP sensitive  $K^+$  channel in the OHC, and subsequent mechanical alterations. The latter process of reverse transduction (see Introduction) has not yet been included into our model. It would be interesting to study whether we could, by implementing reverse transduction, explain the increased contribution from the OHC to the SP after blocking a basolateral  $K^+$  channel. Whether or not 4-AP affects the operating point of the OHC could be tested *in vivo* by looking for changes in distortion-product-otoacoustic-emissions (DPOAEs) after 4-AP perfusion (Probst et al., 1991). DPOAEs are generally assumed to reflect the process of reverse transduction in the OHCs (Hubbard and Mountain, 1990).

It has been shown that affecting the operating point of basal turn OHCs causes pronounced reductions in the DC receptor potential of the neighbouring IHC for low-level characteristic-frequency stimulation (Brown and Nuttall, 1984; Nuttall, 1985). This is taken as evidence that the OHCs feed energy back into the motion of the basilar membrane, via reverse transduction, and thereby enhance the voltage response of the neighbouring IHC. Therefore, we would like to explore the possibility that the reduced contribution from the IHC to the SP at low-level high-frequency stimulation is related to a change in the operating point of the OHC.

## References

- Brown, M.C. and Nuttall, A.L. (1984) Efferent control of cochlear inner hair cell responses in the guinea-pig. *J. Physiol.* 354, 625-646.
- Dallos, P. (1983) Some electrical circuit properties of the organ of Corti. I. Analysis without reactive elements. *Hear. Res.* 12, 89-119.
- Dallos, P. (1984) Some electrical circuit properties of the organ of Corti. II. Analysis including reactive elements. *Hear. Res.* 14, 281-291.
- Housley, G.D. and Ashmore, J.F. (1992) Ionic currents of outer hair cells isolated from the guinea-pig cochlea. *J. Physiol.* 448, 73-98.
- Hubbard, A.E. and Mountain, D.C. (1990) Haircell forward and reverse transduction: Differential suppression and enhancement. *Hear. Res.*, 43, 269-272.
- Kros, C.J. and Crawford, A.C. (1990) Potassium currents in inner hair cells isolated from the guinea-pig cochlea. *J. Physiol.* 421, 263-291.
- Kros, C.J., Rüsçh, A. and Richardson, G.P. (1992) Mechano-electrical transducer currents in hair cells of the cultured neonatal mouse cochlea. *Proc. R. Soc. Lond. B* 249, 185-193.
- Mammano, F., Kros, C.J. and Ashmore, J.F. (1995) Patch clamped responses from outer hair cells in the intact adult organ of Corti. *Pflügers arch.* 430, 745-750.
- Nuttall, A.L. (1985) Influence of direct current on DC receptor potentials from cochlear inner hair cells in the guinea pig. *J. Acoust. Soc. Am.* 77, 165-177.
- Probst, R., Lonsbury-Martin, B.L. and Martin, G.K. (1991) A review of otoacoustic emissions. *J. Acoust. Soc. Am.* 89, 2027-2067.
- Russell, I.J. and Kössel, M. (1991) The voltage responses of hair cells in the basal turn of the guinea-pig cochlea. *J. Physiol.* 435, 493-511.
- Santos-Sacchi, J. (1991) Reversible inhibition of voltage-dependent outer hair cell motility and capacitance. *J. of Neurosci.* 11, 3096-3110.

## Samenvatting

### Het doel van dit proefschrift

In deze dissertatie wordt een speurtocht beschreven naar de oorsprong van de cochleaire SommatiePotentiaal (SP). Tijdens stimulatie met een zuivere toon (een sinus) kan deze gelijkspanning in de extracellulaire vloeistoffen van de cochlea gemeten worden. Dit maakt de SP per definitie een niet-lineaire receptorpotentiaal. De relatie tussen stimulus en SP is complex: de polariteit van de SP hangt af van zowel de frequentie als de intensiteit van de stimulus. Dit heeft er voor gezorgd dat de SP tot nu toe de minst begrepen cochleaire respons is. Waar komt de SP vandaan, en wat vertelt zij ons over het signaal-transductie proces in de cochlea? Meer kennis omtrent de oorsprong van de SP zou kunnen leiden tot een beter inzicht in cochleaire aandoeningen waarbij een afwijkende SP gemeten wordt, zoals de ziekte van Ménière.

*In vivo* metingen hebben een paar belangrijke aanwijzingen omtrent de oorsprong van de SP opgeleverd. Ten eerste, de SP is gerelateerd aan de DC receptorpotentialen die in de binnenste en buitenste haarcellen gemeten kunnen worden. Ten tweede, de DC receptorpotentiaal in de haarcel is op zijn beurt weer gerelateerd aan een globale verandering in de weerstand van de haarcelmembraan tijdens stimulatie. *In vitro* metingen aan geïsoleerde haarcellen van de cavia hebben aangetoond dat de membraan verschillende variabele conductanties bevat. De basolaterale membraan van de haarcellen bevat voornamelijk kanalen die specifiek permeabel zijn voor  $K^+$  ionen, de zogenoemde spanningsafhankelijke  $K^+$  kanalen. De conductantie van deze kanalen voor  $K^+$  is niet constant maar hangt af van de spanning over de membraan waarin deze kanalen zich bevinden. De relatie tussen membraan spanning en conductantie is niet lineair, maar kan beschreven worden door een sigmoïdale curve, de Boltzmann curve. De apicale membraan van de haarcel bevat een aspecifiek ionkanaal waarvan de conductantie varieert met de door de stimulus opgewekte afbuiging van de haarbundel. De relatie tussen apicale conductantie en afbuiging van de haarbundel kan ook beschreven worden met een Boltzmann curve. Het apicale kanaal wordt het mechano-elektrische transductie kanaal genoemd.

Zowel de kanalen in de apicale als basolaterale membraan van de haarcel zouden verantwoordelijk kunnen zijn voor de op niet-lineaire wijze aan de stimulus gerelateerde verandering in membraanconductantie, en dus voor het opwekken van de SP. Het doel van deze dissertatie is dan ook het bepalen van de bijdragen van deze niet-lineaire conductanties aan de SP *in vivo*.

## Samenvatting van de experimentele resultaten

In de eerste experimenten hebben we ons geconcentreerd op de basolaterale  $K^+$  kanalen. *In vitro* is aangetoond dat elk type  $K^+$  kanaal selectief geblokkeerd kan worden door het toedienen van een blokkeerder aan de vloeistof waarin de geïsoleerde haarcel zich bevindt. Op basis hiervan hebben wij getracht de bijdragen van de verschillende typen  $K^+$  kanalen aan de SP te bepalen door ze selectief uit te schakelen met blokkeerders. De blokkeerders werden m.b.v. de perilymfatische perfusietechniek in de cochlea van de cavia gebracht.

**Hoofdstuk 2** beschrijft wat er met de SP gebeurt na het toedienen van de  $K^+$  kanaal blokker tetraethylammonium (TEA). TEA veroorzaakte een geringe afname, zo'n 25%, in de grootte van de SP. Deze afname werd alleen bij de hoogste test-frequenties (8-12 kHz) waargenomen, zowel bij de afleidingen in scala vestibuli als scala tympani. Bij deze stimuluscondities domineren de binnenste haarcellen de SP. Daarom nemen wij aan dat het TEA-gevoelige  $K^+$  kanaal in de binnenste haarcel verantwoordelijk is voor het effect van TEA op de SP. De geringe afname in SP duidt er op dat de bijdrage van het TEA-gevoelige  $K^+$  kanaal aan de SP gering is. Niet-lineaire processen op een andere locatie in de transductie keten, zoals het apicale mechano-elektrische transductie proces, zijn waarschijnlijk van groter belang voor het ontstaan van de SP.

**Hoofdstuk 3** rapporteert over de effecten van de  $K^+$ -kanaal blokker 4-aminopyridine (4-AP) op de SP. De effecten van 4-AP op de SP waren tweeledig. 4-AP veroorzaakte een substantiële afname (50%) van de SP wanneer hoog-frequente (8-12 kHz) tonen op een laag tot middelmatig geluidsdrukniveau (70 dB SPL) werden aangeboden. Bij hogere niveaus (> 70 dB SPL) sloeg de afname om in een toename. De toename in SP werd duidelijker bij het verlagen van de stimulusfrequentie, zodat bij de laagste frequenties (2-4 kHz) de toename van de SP bij alle geluidsdruk niveaus voorkwam.

We concludeerden, conform de TEA-resultaten, dat de substantiële afname van de SP het gevolg was van het blokkeren van het 4-AP gevoelige  $K^+$  kanaal in de basolaterale membraan van de binnenste haarcel. Dit wijst erop dat dit 4-AP gevoelige  $K^+$  kanaal een grotere bijdrage levert aan de SP dan het TEA gevoelige  $K^+$  kanaal. Op grond van de eigenschappen van het 4-AP gevoelige kanaal werd echter een geringere bijdrage van dit kanaal verwacht.

De stimuluscondities waarbij de SP toenam zijn ruwweg gelijk aan de condities waarbij de buitenste haarcellen de SP domineren. Hieruit maakten wij

op dat de toename van de SP het gevolg was van het blokkeren van het 4-AP gevoelige  $K^+$  kanaal in de buitenste haarcel. Een toegenomen DC receptorstroom valt echter niet te rijmen met een verminderde basolaterale conductantie. Waarschijnlijk treden er additionele veranderingen op in de fysiologie van de buitenste haarcel die zorgen voor een verhoogde bijdrage van deze cel aan de SP. Blokkeren van het 4-AP kanaal zal ongetwijfeld leiden tot een depolarisatie van de buitenste haarcel. Het is bekend dat depolarisatie van de buitenste haarcel leidt tot een verminderde apicale conductantie. Dus, een geblokkeerd 4-AP kanaal kan zorgen voor een verminderde apicale conductantie. Dit zou de asymmetrie in het apicale mechano-elektrische transductie proces verhogen, en dus ook de SP.

De resultaten van hoofdstuk 2 en 3 laten zien dat de basolaterale  $K^+$  kanalen niet de belangrijkste bron van de SP zijn. Een grotere bijdrage aan de SP kan komen van het apicale transductiekanaal. Omdat blokkeren van dit kanaal het transductie proces stopzet hebben we de conductantie van het apicale transductiekanaal geleidelijk veranderd tijdens het meten van de SP. Wij hebben geprobeerd de conductantie ofwel het werkpunt van de apicale transducer via een tijdelijke verlaging van de endocochleaire potentiaal (EP) te veranderen. Wij kwamen op dit idee omdat bekend was dat de apicale conductantie van de buitenste haarcel in rust afhankelijk is van de membraanpotentiaal, en de membraanpotentiaal afhangt van de EP. De EP werd tijdelijk onderdrukt door cavia's een intraveneuse injectie met furosemide te geven.

**Hoofdstuk 4** beschrijft de effecten van de EP onderdrukking op de SP en de aan de SP verwante tweede harmonische component van de cochleaire microfonie ( $2F_0$ ). Het verschuiven van het werkpunt van de cochleaire transducer middels een reversibele EP onderdrukking veroorzaakte drastische veranderingen in de SP. De meest opvallende verandering was een ommekeer in de polariteit van de SP. Op hetzelfde moment dat de SP van teken veranderde, bereikte de amplitude van  $2F_0$  een absoluut minimum en de fase van  $2F_0$  verschoof  $120^\circ$ . De veranderingen in SP en  $2F_0$  kunnen verklaard worden door een verschuiving in het werkpunt van een sigmoïdale Boltzmann-achtige overdrachtsfunctie. Wij schrijven de sigmoïdale overdrachtsfunctie toe aan het apicale mechano-elektrische transductiekanaal.

De gevoeligheid van de SP voor een verandering in het werkpunt van de apicale transducer impliceert dat de oorsprong van de SP ligt bij deze apicale niet-lineariteit.

Een andere manier om de bijdrage van de conductanties in de membraan aan de SP te schatten is via de ontwikkeling van een cochleair

model. Wij zijn uitgegaan van het wiskundige model dat Peter Dallos ontwikkelde om de elektrische activiteit in een sectie van het orgaan van Corti te kunnen simuleren. Met dit model is het mogelijk om zowel de intra- als de extracellulaire receptorpotentialen te berekenen. De eerste wijziging die we aanbrachten in het model was het incorporeren van de eigenschappen van het apicale transductiekanaal. Daarna hebben we de spannings- en tijdsafhankelijke eigenschappen van de basolaterale  $K^+$  kanalen ingebouwd.

**Hoofdstuk 5** laat zien dat de apicale niet-lineariteit de DC receptorpotentiaal genereert en de basolaterale niet-lineariteiten de DC receptorpotentiaal modificeren. Na het implementeren van een Boltzmann-functie, om de overdrachtsfunctie van het apicale transductiekanaal te simuleren, waren we in staat om realistische intra- en extracellulaire DC receptorpotentialen op te wekken. De grootte en polariteit van de SP hingen sterk af van het werkpunt van de Boltzmann-functie, ofwel van het percentage apicale kanalen dat open is tijdens rust. Kozen we voor 9% activatie, een waarde die *in vitro* is gevonden, dan zorgde sinusoidale stimulatie voor een grote positieve DC potentiaal in de haarcel en een negatieve DC potentiaal in de scala media (de respons in scala vestibuli is rechtstreeks gekoppeld aan die in scala media).

Na een paar milliseconden nam de conductantie van de basolaterale  $K^+$  kanalen in ons model toe. De toename in basolaterale conductantie zorgde ervoor dat de potentiaal in de cel verschoof in de richting van de negatieve  $K^+$  evenwichtspotentiaal. Omdat de potentiaal in de haarcel via het apicale transductiekanaal gekoppeld is aan de potentiaal in scala media verschoof ook deze potentiaal in negatieve richting. De verschuiving van de potentialen in de negatieve richting tijdens stimulatie zorgde voor een afname van de positieve DC respons in de cel en een geringe toename in de grootte van de SP. Kortom, de  $K^+$  kanalen modificeerden de DC receptorpotentiaal die opgewekt werd door het apicale transducer kanaal.

Wanneer wij één van de basolaterale  $K^+$  kanalen in ons model uitschakelden dan veroorzaakte dat een geringe afname van de SP, vergelijkbaar met het effect van TEA op de SP. In hoofdstuk 3 vermeldden wij dat het blokkeren van het 4-AP gevoelige  $K^+$  kanaal in de binnenste haarcel verantwoordelijk was voor de forse afname van de SP bij stimulatie met hoogfrequente tonen van laag niveau. Het model voorspelt echter een veel geringere afname van de SP na blokkeren van het 4-AP kanaal. Wij zijn er nog steeds van overtuigd dat de forse afname van de SP na het toedienen van 4-AP te maken heeft met een verminderde bijdrage van de binnenste haarcel aan de SP. Maar, gebaseerd op de voorspelling van het model, denken we nu dat nog andere factoren een rol spelen bij deze verminderde bijdrage.

## Toekomstig onderzoek

In hoofdstuk 3 rapporteerden wij dat de effecten van 4-AP op de SP frequentie- en niveau afhankelijk waren. Bij het aanbieden van hoog-frequente tonen op een laag niveau zorgde 4-AP voor een forse afname van de SP. Bij het aanbieden van laag-frequente tonen en hoog-frequente tonen op een hoog niveau zorgde 4-AP voor een toename van de SP. De afname in SP schreven wij toe aan een verminderde bijdrage van de binnenste haarcel, en de toename aan een verhoogde bijdrage van de buitenste haarcel. Volgens ons kon de verhoogde bijdrage van de buitenste haarcel na perfusie met 4-AP verklaard worden door depolarisatie van de membraanpotential en de daarop volgende mechanische veranderingen. De terugkoppeling van elektrisch naar mechanisch wordt omgekeerde transductie genoemd en is uniek voor de buitenste haarcel. Dit proces van omgekeerde transductie zit nog niet in ons model. Het zou interessant zijn om na te gaan of we met het inbouwen van omgekeerde transductie in staat zijn de vergrote SP, na het toedienen van 4-AP, te verklaren. Of 4-AP het werkpunt van de buitenste haarcel verandert kan experimenteel onderzocht worden door het karakteriseren van veranderingen in distorsie-produkt-otoakoestische-emissies na toediening van 4-AP. Distorsie-produkt-otoakoestische-emissies zijn namelijk een uiting van het omgekeerde transductieproces in de buitenste haarcel.

Het is bekend dat een verandering in het werkpunt van de buitenste haarcel resulteert in een forse afname van de DC receptorpotential in de nabijgelegen binnenste haarcellen. Dit soort resultaten onderbouwt het concept dat de buitenste haarcellen energie terugvoeren naar de beweging van het basilair membraan, via omgekeerde transductie, en zo de respons van de nabijgelegen binnenste haarcellen versterken. Daarom willen we nog modelmatig onderzoeken of de verminderde bijdrage van de binnenste haarcellen aan de SP, bij stimulatie met hoog-frequente tonen op een laag niveau, een gevolg is van een verandering in het werkpunt van de buitenste haarcel.



## Een woord van dank

In de eerste plaats wil ik mijn waardering uitspreken voor mijn ouders. Ongevraagd stonden ze dag en nacht voor mij klaar zodat ik meer tijd had om aan mijn onderzoek te besteden.

Helma, twee jaar geleden kwam jij in mijn leven en gelukkig ben je gebleven. Eindelijk iemand om op te bouwen en mijn problemen aan toe te vertrouwen.

Beste collega's, toen ik vier jaar geleden onder de koffie binnenkwam waren jullie slechts vreemde gezichten. Gelukkig veranderde dat snel en hebben jullie mij altijd het gevoel gegeven dat ik thuis was. Jullie hebben ervoor gezorgd dat ik nog nooit een dag met tegenzin naar mijn werk ben gegaan. Bedankt hiervoor. Tot een aantal collega's wil ik in het bijzonder een woord richten.

Sjaak, altijd had je wel wat aan te merken op mijn werk, maar daarmee heb je er wel voor gezorgd dat ik mijn werk tot een goed einde heb gebracht. Van mij mag je dat co- wel weg laten.

Prof. Smoorenburg, bedankt voor de vrijheid die u mij gegeven heeft bij het uitvoeren van het onderzoek. De uitgebreide en zorgvuldige besprekingen van mijn teksten met u hebben er hopelijk voor gezorgd dat dit proefschrift een prettig leesbaar geheel is geworden.

John, Frits en Ferry wil ik bedanken voor de ondersteuning op alle mogelijke fronten. John, geen vraag zo raar of er stond wel een artikel of boek in je kast met het antwoord. Ook wil ik je bedanken voor het nakijken van mijn eerste manuscripten. Frits, bedankt voor de vrolijke noot in ons team. Ferry, jouw praktisch inzicht heeft ervoor gezorgd dat mijn buffers bufferden en mijn oplossingen helder waren.

Finally, I would like to thank Chris. Chris, I admire the speed with which you were able to translate my biological ideas or questions into mathematical formulas. Working with you has been a pleasant experience and I hope that we can keep combining biology and physics.

## Curriculum Vitae

The author of this thesis was born on September 12<sup>th</sup> 1967 in Utrecht, The Netherlands. He obtained his Athenaeum certificate in 1986 after passing exams for Dutch, English, Mathematics, Physics, Biology, Geography, and Chemistry at the "College Blaucapel" in Utrecht. Hereafter, he started to study Biology at the Rijksuniversiteit Utrecht. The three research projects he performed to obtain his Drs. title ( $\approx$  M.Sc. degree) were:

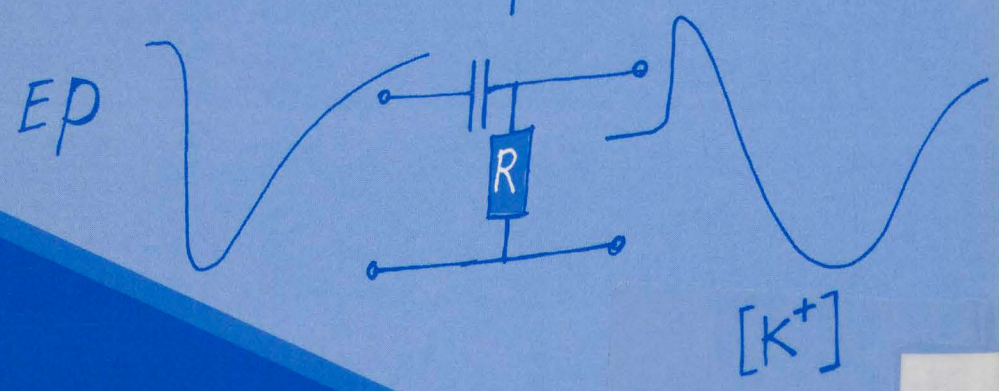
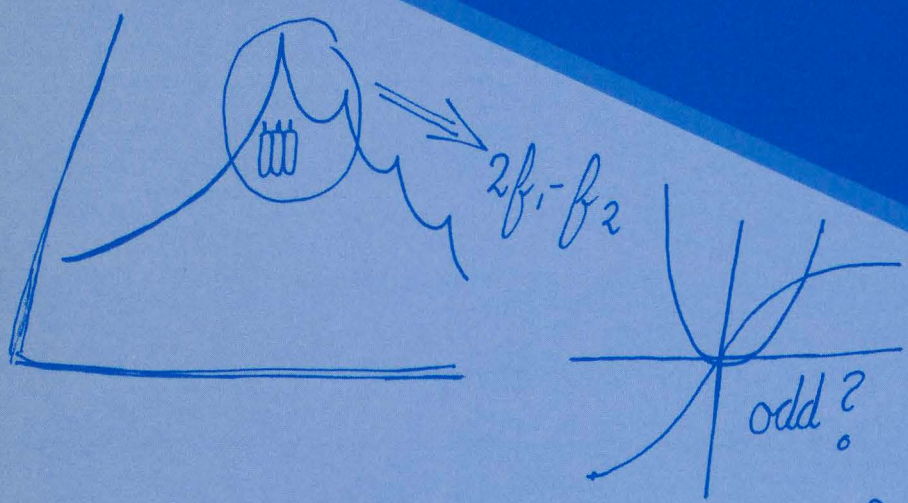
- 1) involvement of  $Ca^{++}$  regulating hormones in lateral line physiology of the catfish (*Ictalurus nebulosus*), under supervision of Prof. Dr. W.A.P.F.L. van de Grind and Dr. R.C. Peters.
- 2) feeding strategies in orang-utan (*Pongo pygmaeus*), for which he spent 9 months in the jungle of northern Sumatra, Indonesia. This study was performed under supervision of Prof. Dr. J.A.R.A.M. van Hooff.
- 3) a neuropharmacological study concerning the role of endorphins in the sexual motivation of the male rat. For this project he spent 1 year under the supervision of Prof. Dr. J.M. van Ree and Dr. N.F. Ramsey at the Rudolf Magnus Institute of Neuroscience, Utrecht. A paper on this subject has been published in Behavioural Neuroscience.

The author obtained his Drs. title in August 1992. In September of that year he started to work as a Ph.D. student on a 4-year project called "*Identification of the nonlinearities involved in the generation of stimulus-evoked DC potentials in the guinea pig cochlea*". This research was performed at the Academic Medical Centre in Utrecht under the supervision of Prof. Dr. G.F. Smoorenburg and Dr. S.F.L. Klis. Results of the research have been presented at several Inner Ear Biology meetings (1993 Budapest; 1994 Montpellier; 1996 Utrecht) and the 1996 Society for Neuroscience meeting in Washington, D.C.. Results have also been published in the form of peer-reviewed papers.

### Papers

- 1) Van Furth, W.R., Van Emst, M.G. and Van Ree, J.M. (1995) Opioids and sexual behavior of male rats: involvement of the medial preoptic area. *Behav. Neurosci.*, 109, 123-34.
- 2) Van Emst, M.G., Klis, S.F.L. and Smoorenburg, G.F. (1995) Effects of tetraethylammonium on cochlear potentials in the guinea pig. *Hear. Res.*, 88, 27-35.
- 3) Van Emst, M.G., Klis, S.F.L. and Smoorenburg, G.F. (1996) 4-Aminopyridine effects on summing potentials in the guinea pig. *Hear. Res.* In Press.





U  
A  
9